TERMINAL-AREA GUIDANCE ALGORITHMS FOR AUTOMATED AIR-TRAFFIC CONTROL

by Heinz Erzberger and Homer Q. Lee

Ames Research Center
Moffett Field, Calif. 94035

NATIONAL AERONAUTICS AND SPACE ADMINISTRATION • WASHINGTON, D. C. • APRIL 1972

TABLE OF CONTENTS

TABLE OF CONTENTS - Continued

SYMBOLS

a_1 rate of speed change in the first segment of a three-segment speed profile

a_3 rate of speed change in the third segment of a three-segment speed profile

A_a in speed profile, acceleration, numerically positive

A_d in speed profile, deceleration, numerically negative

C_o initial circle of unit radius

C_f final circle of unit radius

d_o signed distance of $\overline{P_oP_v}$; positive if the corresponding vector $\hat{n}_o$ points away from P_v

d_f signed distance of $\overline{P_vP_f}$; positive if the corresponding vector $\hat{n}_f$ points away from P_v

d_{xy} signed distance from P_v to another point P which has the same subscripts as d

g acceleration of gravity

h_c cruising altitude

h_f final altitude

$\dot{h}$ rate of altitude change; the sink rate if negative

k numerical constant for path stretching, $0 < k < 1$

ℓ normalized total path length of horizontal trajectory

ℓ_T normalized total path length between x_i and x_f in problem (d)

L as an algebraic quantity, the total horizontal path length; as a maneuver symbol, left turn

L_1 minimum distance to be traversed in time interval t when the speed is constrained to lie between V_o and V_f

L_2 maximum distance to be traversed in time interval t when the speed is constrained to lie between V_o and V_f

L_d desired path length for stretching

L_s	stretched path length
L_{min}	minimum distance to be traversed in time interval t when the speed is constrained to lie between V_{min} and V_{max}
L_{max}	maximum distance to be traversed in time interval t when the speed is constrained to lie between V_{min} and V_{max}
$\hat{n}_o$	unit vector having the same direction as the initial heading ψ_o
$\hat{n}_f$	unit vector having the same direction as the final heading ψ_f
P_o	initial horizontal position of the aircraft
P_f	final horizontal position of the aircraft
P_v	point of intersection (vertex) of the two lines containing the two unit vectors $\hat{n}_o$ and $\hat{n}_f$, respectively
P_{xy}	switching point; first subscript is either o or f, referring to points in the initial line and in the final line, respectively; the second subscript distinguishes different switching points in problem (a)
R	as an algebraic quantity, turning radius; as a maneuver symbol, right turn
R_{min}	minimum turning radius
S	as a maneuver symbol, straight flight
S_i	$i = 1, 6$; in problem (b), switching lines; defined in equations (30) through (35) and figure 12
t	time; in the controlled time-of-arrival problem, time to go before reaching the final point P_f
t_1	in the speed profile, time when constant-speed segment begins
t_2	in the speed profile, time when constant-speed segment ends
t_{min}	in the controlled time-of-arrival problem, earliest arrival time achievable with speed control alone
t_{max}	in the controlled time-of-arrival problem, latest arrival time achievable with speed control alone
Δt_2	in the speed profile, duration of time when the speed remains constant
Δt_h	in the altitude profile, duration of time when the aircraft is descending

V	ground speed
V_o	initial ground speed
V_f	final ground speed
V_ℓ	lowest achievable speed within the constraints of V_o, V_f, t, A_a, A_d
V_{max}	maximum ground speed of the aircraft in the terminal area
V_{min}	minimum ground speed of the aircraft in the terminal area
V_n	constant speed in the three-segment speed profile
V_{up}	highest achievable speed within the constraints of V_o, V_f, t, A_a, A_d
x	abscissa of P_o in a coordinate system where the final point P_f is taken as the origin, the direction of $\hat{n}_f$ as the positive x-axis, and the direction to the right of $\hat{n}_f$ as the positive y-axis
x'	normalized x, where the minimum turning radius R_{min} is taken as the unit of distance
x_i	in problem (d), the distance of the aircraft along the first segment, measuring from the point of intersection
x_f	in problem (d), the distance from the point of intersection to a desired final point in the second segment
y	ordinate of P_o, measured in the same coordinate system as x
y'	normalized ordinate of y, where the minimum turning radius R_{min} is taken as the unit of distance
ϕ	bank angle
ϕ_{max}	maximum bank angle
ψ	heading of aircraft
ψ_o	initial heading of aircraft
ψ_f	final heading of aircraft
ψ_i	total heading change in the initial turn
ψ_s	heading of the straight-line segment of the horizontal trajectory

TERMINAL-AREA GUIDANCE ALGORITHMS FOR AUTOMATED AIR-TRAFFIC CONTROL

Heinz Erzberger and Homer Q. Lee

Ames Research Center

SUMMARY

In present air-traffic control systems, certain terminal-area guidance problems are solved manually by the pilot and the controller. The solution of these problems could be automated in a new generation system with the use of ground and airborne computers and an improved navigation system (such as the proposed microwave landing system). The objectives of this study are to formulate these problems analytically, and to obtain solutions to them in the form of computer-oriented algorithms.

The principal requirement is to construct a flyable, three-dimensional trajectory that begins at the current aircraft position, heading, speed, and altitude, and that terminates at a prescribed position, heading, speed, altitude, and time. The terminal position is normally the Instrument Landing System (ILS) gate, or a waypoint, and the terminal time is the assigned landing slot. Such precise time-position control, "four-dimensional guidance," is proposed as an advanced air-traffic control technique. The algorithms developed in this report are applicable to all possible combinations of initial and final conditions, and thus can be used in a closed-loop feedback law.

The construction of the required trajectory is divided into three parts. First, the horizontal trajectory is calculated with a constraint on the turning radius. Algorithms for constructing the horizontal trajectory are given for each of four criteria: (a) to fly to a waypoint and arrive there with a specified heading, (b) to fly to a directed line in space such as a VHF Omni-Range (VOR) radial, (c) to fly to a waypoint without a constraint on the heading at the waypoint, and (d) to change smoothly from flight along one line or VOR radial to another that intersects it. For each criterion the trajectories are synthesized from straight lines and portions of circles. Assignment of the trajectories is based on minimizing the length of the path so as to reduce maneuver time and conserve airspace and is given in the form of switching diagrams.

Second, the speed profile is calculated based on the length of the horizontal trajectory and on the desired time over the waypoint or ILS gate. Constraints are the minimum and maximum airspeed, the acceleration and deceleration of the aircraft, and the desired airspeed at the terminal time. The algorithm first determines if a speed profile satisfying these constraints exists. If it does, the speed profile is synthesized; if it does not, a technique is used to stretch the path length of the horizontal trajectory by the amount required to synthesize a flyable speed profile.

Third, the altitude profile is synthesized so that the aircraft maintains the approach altitude as long as possible before descending to the specified final altitude at the waypoint. Input to this calculation is the length of the horizontal path, the desired descent rate, and the length of the final deceleration interval. The descent to the specified final altitude is timed so it does not coincide with the deceleration interval.

Finally, the completely specified flight profile is arranged into a time sequence of guidance commands that can be used as inputs to a flight director or autopilot.

INTRODUCTION

The design of aircraft navigation and flight-control systems has long followed a trend toward automation of the numerous guidance, control, and navigation functions once performed manually by the flight crew. Recently, this trend has accelerated and expanded in scope, with the momentum behind it being provided by the development of flight-worthy computers and by the increasing complexity of modern aircraft and of the air-traffic environment. Complex problems in all phases of aircraft operation indicate that such automation is not a luxury, but rather a prerequisite for safe and economic flight. Fortunately, the timely development of airborne computers has provided the means to achieve the degree of automation required to alleviate these problems.

Concepts have been proposed for flight-control systems capable of flying an aircraft automatically from takeoff to landing (refs. 1 and 2), with the pilot purely in the role of systems manager. Although such completely automatic systems are now under study, this study focuses on the problem of automating a segment of the flight during which pilot workload is particularly heavy; the segment is within the terminal area, roughly within a 50-mile radius of an airport. For a subsonic jet transport on a landing approach, it corresponds approximately to the final 15 minutes of flight.

Pilot workload in the terminal area is heavy as a result of deficiencies in the existing flight-control and air-traffic control systems. In this area, the aircraft often must be flown manually, even though an automatic landing system and an autopilot are on board. The automatic landing system can be used to fly the aircraft only along the final landing approach, after the aircraft is at the proper altitude, position, and heading to receive the Instrument Landing System (ILS) glideslope and localizer signals. Similarly, the standard autopilot has limited use in the earlier portions of terminal-area flight because it was never designed to provide precision flight-path control along the curved, decelerating, and descending flight path which is frequently required before the final approach.

The guidance of aircraft in busy terminal areas, especially in weather conditions requiring instrument flight, is conducted primarily by air-traffic control. Controllers monitor the position and movement of aircraft on radar and issue guidance instructions to the pilots, who close the guidance loop by executing them as quickly and faithfully as possible. For landings, the

controllers direct the randomly arriving aircraft into the final approach to achieve a high landing rate while maintaining a safe separation distance. The task is complicated by the differing airspeeds (and other performance characteristics) between aircraft on a common path.

The pilot and controller workload of this system of terminal-area guidance has been studied for a number of high traffic terminal areas (ref. 3). For arrivals into JFK International Airport, pilot-ATC communication requires as much as 50 percent of the last 10 minutes before touchdown. During this time, the pilot performs an average of 18 communications and navigation operations, a workload which pilots consider excessive.

To reduce the pilot-ATC workload in the terminal area, an automatic flight-control system must provide precision flight-path control along the specified trajectory. In addition, the system must also maintain synchronization of the aircraft position with a specified time schedule; this requirement is especially important for efficient air-traffic control. All methods previously studied particularly stress the importance of maintaining accurate time-position control of aircraft in the terminal area (refs. 4-6). Accurate time-position control of the aircraft should reduce landing delays due to holding and increase landing rates; however, it cannot be achieved with existing air-traffic control methods and equipment.

What techniques are available for guiding an aircraft automatically along a specified time-position trajectory? The technique suggested in reference 1 is to precompute the trajectory in a ground facility, store it on tape, and enter it into the on-board system before takeoff. The on-board equipment would consist of a means for storing the precomputed trajectory and a modified autopilot for flying the aircraft along it. Although this technique requires only relatively simple on-board equipment, it suffers from severe practical disadvantages - the dependence on a ground facility and the difficulty of making fast trajectory changes in flight. For some segments of a flight, such as climb to and descent from cruise of a supersonic transport, these disadvantages may not be significant. In terminal-area operations, however, even with precise scheduling of aircraft, unexpected trajectory changes can never be completely eliminated, making the value of a precomputed trajectory very questionable.

Few studies have addressed themselves to the synthesis of a terminal-area trajectory. Although references 1 to 7 do not address this problem specifically, they do provide insight into the terminal control process and are helpful in identifying important problems. Reference 8 deals with the construction of holding patterns and path-stretching maneuvers. Reference 9 is particularly relevant because it defines several of the problems studied here.

This study investigates a technique for calculating the trajectory on board, with provision for recalculating it in real time whenever changes are needed. The practicality of this technique hinges primarily on the solution of two problems. The first is to establish what guidance problems occur most frequently in the terminal area and can be solved by an on-board system. The second is to develop efficient computational techniques for synthesizing the required trajectories.

The guidance problems to be solved are established from an analysis of air-traffic control procedures, instrument flight maneuvers, and terminal-area route structures. They can be divided into three principal subproblems: a lateral (horizontal) maneuver, a longitudinal (vertical) maneuver, and a speed change. An important assumption made in this study is that these three problems can be treated essentially independent of each other.

A number of techniques are used to synthesize the trajectories; some are based on minimizing a specific performance function, others are derived from geometric considerations. In general, horizontal trajectories consist of connected segments of straight lines and circular arcs, while vertical trajectories consist only of connected segments of straight lines. Speed histories consist of sections of constant acceleration, constant deceleration, and constant speed flight. The choice of simple geometric shapes as basic building blocks yields trajectories that are easy to synthesize and that comply with all important aircraft maneuvering and performance constraints. There seems to be little reason to consider more complicated trajectories, at least for terminal-area operation of conventional aircraft.

The basic information required to fly the synthesized trajectories is position, altitude, ground speed, and time. It is assumed that this information is available on board the aircraft. Although the description of the guidance laws derived herein is occasionally somewhat involved, programming experience has shown that the required computations can easily be performed on currently available airborne digital computers. (The development of a control system to fly the aircraft along the synthesized trajectory is closely related to standard autopilot design, and is not considered in this report.)

DEFINITION OF GUIDANCE PROBLEMS FOR TERMINAL-AREA OPERATIONS

Before trajectories can be synthesized, the set of guidance problems that occur in terminal-area operations must be defined and formulated mathematically. Such a set can never be considered complete because there is no limit to the number of possible problems. Therefore, the objective is to choose the set as small as possible, consistent with the requirement that the most commonly encountered guidance problems are included in it or can be reformulated in terms of problems in it.

Terminal-area guidance can be viewed as the simultaneous solution of three types of problems: horizontal (lateral) guidance, airspeed management, and vertical guidance. To simplify analysis, this study assumes that each type of problem can be solved essentially independent of the other two. Although this assumption is not always justified, it is motivated by observing that in commonly encountered flight conditions pilots tend to fly aircraft in a manner that allows them to solve these three types of problems independently. Although analysis of terminal-area guidance problems is given separately for each type of problem, in practice, the three types of problems do interact. The method of dealing with these interactions is given when the problem is encountered.

Horizontal Guidance

The most complex guidance problems in terminal-area operations for conventional transport aircraft involve horizontal maneuvers. The origin and identity of these problems are most easily explained by a brief discussion of the route structure and air-traffic control procedures for an approach into a typical terminal area, that of San Francisco International Airport (SFO).

The approach routes into SFO are indicated in figure 1 by the heavy broken lines. The most important feature is that they consist chiefly of connected sections of straight lines that terminate on the final approach. Transition from one straight-line section to another is achieved by means of smoothly rounded corners. The route structure can be specified by locating the corners defining each straight-line section and arrows indicating the direction of motion along each section. Corners often coincide with the location of a VOR station (such as Woodside) or at an intersection of radials from two adjacent VOR stations (such as Altamont).

Under instrument flight conditions, air-traffic control closely monitors the movement of aircraft within the approach routes. The air-traffic controller sequences aircraft for landing, maintains separation between them within the routes, and vectors them onto the final approach with the desired spacing. In the existing ATC system, a controller normally observes aircraft on radar and issues the appropriate guidance instructions to pilots by radio telephone.

Maintaining the proper spacing between aircraft is especially critical on the final approach and at points of confluence of two or more segments. Too small a spacing is unsafe and may disrupt the smooth flow of traffic, whereas too large a spacing results in a low landing rate. Spacing distances for the final approach are typically in the range between three and seven miles, the choice depending somewhat on the individual controller as well as weather conditions. In weather conditions requiring instrument flight, controllers tend to space aircraft at greater distances than in clear weather. Spacing is achieved by controlling the speed of the aircraft or, if necessary, by vectoring to control the length of the flight path to the point of confluence with the final approach. Vectoring the aircraft onto the final approach generally has the dual purpose of aiding the aircraft to acquire the ILS localizer and of ensuring the proper spacing between aircraft. Thus the route structure in the neighborhood of the point of confluence near the final approach (point A, figure 1) is variable and not necessarily as shown; the shaded region approximates the area within which the route may vary. Having described the terminal-area route structure and the air-traffic control problem, the next step is to isolate the basic horizontal guidance problems that an automatic system would have to solve in guiding the aircraft during the approach. Five problems have been identified and are described in the following sections under the heading of problems (a), (b), (c), (d), and path stretching.

Problem (a)—Consider an aircraft that has just passed the corner at point B (fig. 1) and is cleared for an ILS approach. (Assume that no other aircraft are on the approach routes.) The aircraft must be guided so that it will be on the final approach path and headed in the landing direction at

least by the time it passes the outer marker (OM). If it follows the approach route exactly as drawn in figure 1, it achieves heading alignment at point A, a few miles before the OM. In general, an aircraft must be in close heading alignment with the final approach at or before the OM, if the approach is to continue successfully. Thus, the general problem is to guide the aircraft from any initial position and heading to a specified final position and heading, with the final position and heading achieved simultaneously. This problem is illustrated by figure 2(a).

Without some synthesis criterion there can be no unique solution to this problem, since for every combination of initial and final condition an infinite number of feasible trajectories can be found. Since a computer-oriented synthesis procedure requires unique solutions, the synthesis criterion was chosen as minimization of the path length of the trajectories connecting initial and final points. This criterion was suggested by the shape of the approach route segments (fig. 1) which show that once the trajectories have passed the last waypoint before the final approach they proceed by the most direct route to point A.

An important constraint on the trajectories is that the bank angle required to fly along them not exceed some maximum value dictated primarily by passenger comfort considerations, typically 15° to 30°. The maximum bank-angle constraint is, of course, equivalent to a constraint on the minimum turning radius; this equivalence is used in the synthesis procedure.

Problem (b)—Major portions of terminal-area routes consist of straight-line sections; if an aircraft is already flying along such a section, a standard lateral autopilot can keep it aligned. If, however, the aircraft is *not* on its assigned approach route, because the pilot or ATC have suddenly changed the route or a navigation error is discovered, then the problem arises of how to guide the aircraft onto the assigned route. This problem is the same as problem (a) when the new route must be entered at a specific point. Often, though, the only requirement is that the aircraft be flown onto the route as quickly as possible. Hence, problem (b) is defined as flying from any initial position and heading onto a straight line of specified location and heading. A solution to this problem is any trajectory that leads to the specified line without violating maneuvering constraints. As in problem (a), the selected trajectory should minimize path length without causing the aircraft to exceed a maximum bank angle. This problem is illustrated in figure 2(b), where the final line is assumed to be a VOR radial or the center line of the localizer.

Problem (c)—Another method of specifying an approach route is to choose a sequence of waypoints through which the aircraft is to fly consecutively. This method can also be used to generate holding patterns in a simple way. If trajectories connecting consecutive waypoints are chosen to minimize the path length, approach routes quite similar to those in figure 1 can be obtained by a judicious placement of waypoints.

Problem (c) is defined as flying from an arbitrary initial position and heading to a specified final position. As before, the synthesis criterion is chosen as the minimum path length, and the constraint is the maximum bank angle. This problem is similar to problem (a) except that the heading of the

aircraft when it arrives at the final position or waypoint is not specified. Figure 2(c) illustrates the problem for two waypoints.

Problem (d)—If the approach routes are specified by connected segments of straight lines as in figure 1, a procedure is needed for transitioning from one segment to another without excess overshoot or high bank angles. Problem (d) is defined as determining a control law for making a transition between two straight-line segments at any specified angle of intersection. An ideal transition between two lines is shown in figure 2(d).

Path stretching—Air-traffic control was not considered in defining problems (a) through (d), which arise in developing guidance laws for flying aircraft automatically along existing approach routes without regard to other aircraft. Air-traffic control requires knowledge of the location, heading, altitude, and speed of all aircraft operating in the terminal area. Since this knowledge is generally not available on board an aircraft, a comprehensive treatment of the air-traffic control problem from the point of view of an on-board system does not seem justified. It is reasonable, however, to consider on-board solution a portion of the air-traffic control problem that does not require explicit knowledge of other aircraft but would especially simplify the controller's job of spacing aircraft on final approach. This problem is to achieve precise arrival time of the aircraft at a designated point on the final approach or, in general, at any point on the approach route. Typically, such points might be chosen as the OM or at the junction of two or more approach routes (i.e., point A, fig. 1).

The preferred technique of achieving a specified time of arrival at a specified point on the approach route is through speed control, which does not require deviation from the assigned approach route. The use of speed control for this purpose will be discussed in the next section. However, speed control alone is often inadequate, particularly if a change in the time of arrival is required close to the final point. The inadequacy of speed control is clearly shown when a speed lower than the stall speed is needed to achieve a delay in arrival time. Since late revisions in arrival time cannot be avoided, this limitation of speed control may be overcome by stretching the approach path as required to achieve the desired delay.

Path stretching to delay arrival time is an essential element of all manual and automatic air-traffic control systems that have been studied in the literature (refs. 4-8). Although there is generally no unique trajectory that increases the path length by a specified amount, the selection of a particular technique for path stretching is of great importance, since it is closely related to the method of air-traffic control.

The effectiveness of path-stretching (and possibly also of path shortening) techniques is often evaluated in terms of the timing accuracy they achieve in delivering an aircraft at the desired point. Of those evaluated in simulations, no clearly superior technique has so far emerged. For a description and comparison of five different techniques see reference 4.

Although optimum methods of path stretching have not been developed, the method chosen should be able to increase the path length in a continuous

manner while preserving as much as possible of the approach route. Furthermore, the calculations defining the stretched trajectory should be amenable to fast, on-line computer solution. Such considerations led to the particular method of path stretching described in detail later.

To complete the definition of the problem, the path stretching is required to take place along a straight section of the approach on which a final point is specified. The path-stretching problem is then defined as selecting a trajectory that starts on the straight section, terminates on the final point, and has any specified arc length greater than the straight-line path. An example of a stretched path between two waypoints is shown in figure 2(e).

Finally, the well-known holding pattern can be considered as an example of a stretched path. Generally, a path-stretching maneuver turns into a holding pattern whenever the increase in path length specified is greater than the circumference of a holding pattern. Holding patterns are not discussed further in this report.

Speed Control

The primary purpose of speed control in the terminal area is to control time of arrival. In general terms, the problem is to calculate the speed-time or speed-position history of the aircraft so that it will arrive at a specified point on the approach route at a specified time. This calculation assumes that the horizontal trajectory has already been determined by solving one or more of the trajectory problems defined in the preceding sections, so that the path length as well as the initial time t_i and the final time t_f are known.

The speed-time history is calculated subject to the aircraft's operational constraints on cruise speed V, acceleration, and deceleration. In addition to obeying these performance constraints, the initial speed V_o of the speed-time history must equal the current aircraft speed, and the final speed V_f must equal a specified value. If the final point happens to be the OM, then V_f may equal the final approach speed with fully lowered flaps. The "simplest" speed-time history that can solve this problem consists of three segments: an acceleration or deceleration segment to the cruise speed, a cruise-speed segment, and an acceleration or deceleration segment to the final speed, as in figure 2(f).

Calculation of the speed-time history may reveal the need to apply path stretching to the horizontal trajectory. For example, the path length will need to be stretched if the calculated cruise speed is less than the minimum speed.

Vertical Guidance

For the arrival operations considered in this report, vertical guidance is restricted to descent from cruise. (For departure operations, similar

considerations are applicable to ascent to cruise.) Here it is assumed that the horizontal trajectory and the speed-time history have been obtained as solutions to previously defined problems.

A typical altitude history, illustrated in figure 2(g), consists of segments of constant altitude and of descending flight. It commences at cruise altitude h_c and terminates at a final altitude h_f approximately equal to the height above the runway of the ILS glideslope beam center at the OM.

The descent profile provides for maintaining the cruise altitude as long as possible, then descending to the final altitude at a specified descent rate and at a constant forward speed. If any speed change is needed near the final point, it should be made in level flight; the descent profile must be planned to allow for the required period of level flight after the final altitude is achieved. Thus, the speed-time history (and horizontal trajectory) must be calculated before the altitude profile.

Summary

A complete terminal-area trajectory, consisting of the position, speed, and altitude of the aircraft as a function of time, is obtained by solving sequentially the horizontal, airspeed, and vertical guidance problems that are defined in this section and summarized in table 1. Although these are not the only problems that can be defined, they are sufficient for calculating the most frequently occurring trajectories in present-day terminal-area operations. (Important additional problems could be defined if information on the locations and trajectories of other aircraft in the area were available on board the aircraft, but such problems are not discussed in this study.)

Solutions to the various problems discussed in this section are developed without explicitly considering the wind. Thus, they yield values for ground heading, ground speed, and ground acceleration time histories. If the wind speed and direction are known, as we assume in this study, these quantities can easily be converted to aircraft heading, airspeed, and acceleration with respect to the air mass.

TRAJECTORY SYNTHESIS FOR PROBLEM (a)

In reference 9, trajectories were derived for problem (a) which are of minimum path length and are constrained by the minimum turning radius. When the initial and final points are separated by less than four turning radii, such trajectories can contain up to three partial turns of minimum turning radius. When the initial and final points are separated by more than four turning radii, the trajectories need only contain a straight-line segment with a partial turn of minimum turning radius at each end. In this section, a computer-oriented algorithm for calculating the trajectory is developed based on certain simplifying assumptions and on a geometric interpretation of the guidance problem.

The trajectory patterns to be used in the development of the algorithm consist of at most two circular arcs and a straight-line segment. The three-circular-arc trajectories of reference 9 may occur in the minimum-arc-length solution of problem (a) if the distance of separation between initial and final points is less then four turning radii. However, they are excluded here since they would increase the complexity of the algorithm and are expected to occur infrequently in practice.

Another difference between reference 9 and the present development concerns the optimality of the trajectories generated by the algorithm. Reference 9 was devoted to a mathematical derivation of the minimum arc problem for problem (a). Here, for computational simplicity, the trajectories are not selected to minimize, in the strict mathematical sense, a specific performance function such as the arc length. Rather, the key criterion for selecting trajectories is geometric constructability; that is, the feasibility of constructing a particular type of trajectory for given initial and final conditions. Because the trajectories for which a feasible construction is sought are known to be optimum under some conditions, as shown in reference 9, the procedure can be expected to yield an efficient trajectory, though not necessarily the true optimum one in the minimum arc sense. The disadvantage of not always generating trajectories that minimize a performance function is outweighed by the geometric insight which the algorithm casts upon the horizontal guidance problem.

It was stated previously that the trajectories should obey a constraint on the maximum bank angle. At constant airspeed V a constraint on the minimum turning radius R_{min} is equivalent to a constraint on the maximum bank angle ϕ_{max}. The relationship between these constraints is given by the following equation:

$$R_{min} = \frac{V^2}{g \tan \phi_{max}} \tag{1}$$

where g is the acceleration of gravity. The value of V used in equation (1) should be the maximum ground speed encountered during the maneuver. An acceptable estimate would be to choose it as the sum of the maximum airspeed in the terminal area and the wind speed. In further calculations, the turning radius is treated as a parameter whose value is arbitrary and is related to the bank-angle constraint.

The trajectories in this study are chosen from the 13 basic patterns shown in the left column of table 2. (The additional patterns shown in the right column of table 2 are required for the complete minimum arc solution of problem (a), and are not used in the algorithm.) The patterns used are composed of three or fewer segments; each segment consists of a portion of either a straight line or a circle. Under the maneuver symbol column in table 2, each pattern is assigned a maneuver symbol, characterizing the consecutive maneuvers required to fly the trajectory. For instance, L S L stands for left turn, straight flight, and left turn. These symbols are used throughout the text to refer to a particular pattern.

Pattern Parameters

The assignment of a flight pattern depends on the initial and final conditions of the problem, represented by the coordinates of the initial point and the initial heading and by the coordinates of the final point and the final heading. For the purpose of pattern assignment and the calculation of pattern constants, the initial and final conditions can be reduced to three parameters or states.

The symbols P_o and P_f denote the initial and the final point and ψ_o and ψ_f the initial and the final heading, respectively. Since ψ_f is normally the runway heading, the initial heading is conveniently measured with reference to ψ_f. The initial heading thus measured is denoted by ψ and is given by $\psi = \psi_o - \psi_f$. Unit vectors $\hat{n}_o$ and $\hat{n}_f$ have directions ψ_o and ψ_f and emanate from P_o and P_f, respectively (fig. 3). If $\hat{n}_o$ and $\hat{n}_f$ are not parallel or antiparallel, lines drawn through $\hat{n}_o$ and $\hat{n}_f$, termed the "initial" and "final" lines, will intersect at a point P_v. The case where these lines do not intersect is referred to as the singular case and is considered separately elsewhere.

The pattern parameters for the nonsingular case are ψ, d_o, and d_f. A positive ψ is defined by rotating $\hat{n}_f$ clockwise into $\hat{n}_o$. The range of ψ is $-\pi < \psi \leq \pi$, with ψ in radians. The other two parameters are d_o and d_f where d_o is the signed distance $\overline{P_oP_v}$ and d_f is the signed distance $\overline{P_vP_f}$. The sign of a distance is positive if the corresponding unit vector points away from P_v. The geometric construction of these parameters and a typical trajectory are illustrated in figure 3.

The two parameters d_o and d_f are not directly measured, but must be computed from available navigation measurements. The computation is aided by relating them to a commonly used Cartesian coordinate system. As illustrated in figure 3, the origin of the coordinate system is at P_f; its x-axis points in the direction of $\hat{n}_f$, and its y-axis points to the right of the reference direction. This coordinate system is often used in aircraft guidance and control studies. Let (x,y) be the coordinate vector of P_o in this system, normalized by using the turning radius R as the unit of distance: $(x',y') = (x/R, y/R)$. Then $d_o = y'/\sin\psi$, and $d_f = -x' + y'/\tan\psi$, or

$$d_o = \frac{y}{R \sin\psi} \tag{2}$$

$$d_f = -\frac{x}{R} + \frac{y}{R \tan\psi} \tag{3}$$

The quantities d_o and d_f are also normalized distances. Equations (2) and (3) are valid for all ψ except $\psi = 0$ or $\psi = \pi$, corresponding to the singular cases. In an actual computer mechanization, ψ will be considered zero or π when it lies in the neighborhood of these values.

Switching Points

Our objective in the next several sections is to describe how flight patterns are assigned as a function of the three parameters ψ, d_o, and d_f and to determine those combinations of parameters, called the switching points, at which changes from one type of pattern to another occur. Although the switching points can be functions of all three parameters, the pattern assignment problem is simplified by choosing many of the switching points as dependent only on ψ, and the others as simple functions of ψ and d_o. The pattern assignment problems are different for nonsingular and for singular values of ψ; the assignment problem for the nonsingular case is considered first.

All switching points are defined by points of tangency involving the initial or the final line and certain circles which arise in the geometric construction of flight patterns. The six switching points on the initial line are $P_{o\bar{\alpha}}$, $P_{o\delta}$, $P_{o\bar{\sigma}}$, $P_{o\beta}$, $P_{o\sigma}^{+}$, and $P_{o\alpha}^{+}$, and the six switching points on the final line are $P_{f\bar{\gamma}}$, $P_{f\bar{\sigma}}$, $P_{f\bar{\delta}}$, $P_{f\delta}^{+}$, $P_{f\sigma}^{+}$, $P_{f\gamma}^{+}$. The directed distances measured from the origin at P_v to these switching points are $d_{o\bar{\alpha}}$, $d_{o\delta}$, $d_{o\bar{\sigma}}$, $d_{o\beta}$, $d_{o\sigma}^{+}$, $d_{o\alpha}^{+}$ for those lying on the initial line and $d_{f\bar{\gamma}}$, $d_{f\bar{\sigma}}$, $d_{f\bar{\delta}}$, $d_{f\delta}^{+}$, $d_{f\sigma}^{+}$, $d_{f\gamma}^{+}$ for those lying on the final line. The "initial" circle is the circle tangent to the initial line at P_o, and the "final" circle is the circle tangent to the final line at P_f.

Flight Patterns for Normal Maneuvers

The "normal" flight patterns apply, and the derivation of switching points is simplest, if the initial and final points are far apart compared to the turning radius. Figure 4 illustrates the trajectories for this case with an acute and an obtuse value of ψ for $0 \leq \psi \leq \pi$. Each part of the figure shows four trajectories corresponding to four pairs of initial and final conditions, with designations corresponding to those in table 2. (Circles involved in the construction of the trajectories are completed by broken lines.) The region of large separation between initial and final points can now be defined more precisely as the set of initial and final conditions for which neither of the two initial circles intersects either of the two final circles. In this region, the four trajectories shown in figures 4(a) and 4(b) can always be drawn. The boundaries of these regions can be defined by studying the figures as either the initial or final point moves along its line.

The trajectory starting at P_{o1} and ending at P_{f1} is of the LSL type. As P_{f1} moves down, the trajectory changes to the RSL type when the left initial circle becomes tangent to d_o at switching point $P_{f\sigma}^{+}$. The distance of $P_{f\sigma}^{+}$ from P_v is $d_{f\sigma}^{+} = \tan \psi/2$.

The same trajectory, as P_{o1} moves to the right, changes from LSL to LSR when the left initial circle is tangent to the line d_f at $P_{o\bar{\sigma}}$; $P_{o\bar{\sigma}}$

and $P_{f\sigma}^{+}$ are both on the same circle. The distance of $P_{o\bar{\sigma}}$ from P_v is $d_{o\bar{\sigma}} = -\tan \psi/2$.

The final two switching points are defined from geometric convenience in contrast to the first two, where the switching must take place at the defined points. A trajectory starting at P_{o1} and ending at P_{f2} is of type RSL. As P_{o1} moves to the right, the right initial circle first becomes tangent to the final lines at $P_{o\beta}$, at $d_{o\beta} = -1/\tan(\psi/2)$.

The last switching point, $P_{f\gamma}^{+}$, modifies the trajectory connecting P_{o2} and P_{f1}. As P_{f1} moves toward P_{f2}, the switch from type LSR to type RSR occurs at $P_{f\gamma}^{+}$. As with $P_{o\beta}$, this switching point is not a geometrical necessity, since both LSR and RSR trajectories are usable for all points on d_f. However, the switch from LSR to RSR at some point near P_v yields trajectories of shorter path length. Since $P_{f\gamma}^{+}$ is a geometrically significant point for near-distance maneuvers, it was chosen for this purpose also for minimizing the total number of switching points. Its location on d_f is established by locating P_{o2} so that the left initial circle of P_{o2} and the right final circle of P_{f1} are tangent at only one point as P_{f1} moves toward P_{f2}. P_{o2} is then at $P_{o\alpha}^{+}$, and P_{f1} is at $P_{f\gamma}^{+}$ (fig. 4). To construct the circles establishing these points, draw a circle with center at the intersection of two lines, one line three units to the right of d_f and the other line one unit above d_o, tangent to d_o at $P_{o\alpha}^{+}$. The second circle can now be drawn tangent to this circle, and also tangent to d_f at $P_{f\gamma}^{+}$. Thus, $d_{f\gamma}^{+} = 3/\tan \psi + 1/\sin \psi$ and $d_{o\alpha}^{+} = 3/\sin \psi + 1/\tan \psi$.

From symmetry, trajectories for the negative ψ range, $-\pi < \psi < 0$, can be taken as the mirror images of trajectories for the positive ψ range reflected about the d_o axis. The reflection of trajectories for negative ψ values is essentially equivalent to the introduction of another switching point at $\psi = 0$. This reflection procedure for negative ψ is also valid for near-distance maneuvers.

Flight Patterns for Near-Distance Maneuvers

If the initial and the final points are so close that at least one pair of initial and final circles intersect, the flight patterns given in the preceding section may become invalid. Flight patterns for this condition are referred to as near-distance maneuvers. Near-distance maneuvers rarely occur in terminal-area operation of aircraft and should always be avoided since the resulting disruption of aircraft on landing approach can cause landing delays. Nevertheless, events that generally require near-distance maneuvers, such as go-arounds and emergencies, do occur in a small but not negligible percentage of takeoffs and approaches. Therefore, no automatic terminal guidance system is complete unless it can also handle such events.

Pattern selection rules for near-distance maneuvers are somewhat involved. Readers not interested in following these details may go directly to the next section, on switching diagrams, where the selection rules are summarized.

When P_o is to the left of $P_{o\bar{\sigma}}$, two groups of switching points are needed to define the trajectories. The first group contains the points $P_{f\bar{\gamma}}$, $P_{f\delta}^{+}$, and $P_{o\bar{\alpha}}$. If in figure 4(a) or 4(b) the points P_{o1} and P_{f2} move simultaneously toward the origin, they will reach positions where the straight-line segment of the RSL trajectory vanishes and the right initial circle becomes tangent to the left final circle. There are generally two possible final circles tangent to the line d_f and to the initial circle; in figure 5(a), points of tangency of the final circles with d_f are denoted by $P_{f\bar{\gamma}}$ for the further of the two points and by $P_{f\delta}^{+}$ for the nearer of the two from the origin. The positions of these two points are functions of the position of P_{o1}; as P_{o1} moves back to the left to $P_{o\bar{\alpha}}$, the points of tangency $P_{f\bar{\gamma}}$ and $P_{f\delta}^{+}$ merge into a single point. For initial points to the left of $P_{o\bar{\alpha}}$, initial and final circles do not intersect, and the region is as discussed in the preceding section. The upper limit of $P_{f\delta}^{+}$ is $P_{f\sigma}^{+}$, reached when P_{o1} is at $P_{o\bar{\sigma}}$.

The second group contains the points $P_{f\bar{\sigma}}$ and $P_{o\delta}$. Point $P_{f\bar{\sigma}}$ is defined by a circle tangent to the negative d_f axis and the positive d_o axis, as illustrated in figure 5(a). The definition of $P_{o\delta}$ depends on the value of ψ. For $0 < \psi \leq \pi/2$, $P_{o\delta}$ is obtained by moving P_{o1} toward $P_{o\bar{\sigma}}$ until $P_{f\delta}^{+}$ coincides with $P_{f\bar{\sigma}}$, in figure 5(c). For $\pi/2 \leq \psi < \pi$, $P_{o\delta}$ is obtained similarly by moving P_{o1} toward $P_{o\bar{\sigma}}$ until $P_{f\bar{\gamma}}$ (instead of $P_{f\delta}^{+}$) coincides with $P_{f\bar{\sigma}}$, in figure 5(d). This definition of $P_{o\delta}$ is continuous at $\psi = \pi/2$, the angle common to both definitions. Thus, for small ψ, $P_{o\delta}$ lies near $P_{o\bar{\sigma}}$. As ψ increases $P_{o\delta}$ moves toward $P_{o\bar{\alpha}}$, coinciding with $P_{o\bar{\alpha}}$ at $\psi = \pi/2$. For $\psi > \pi/2$, $P_{o\delta}$ reverses its direction and moves in the positive d_o direction.

For final points in $[P_{f\bar{\gamma}}, P_{f\delta}^{+}]$, the trajectory assignment depends on values of ψ and on the initial point. If $0 < \psi \leq \pi/2$, and the initial point is in $[P_{o\bar{\alpha}}, P_{o\delta}]$, an RSR trajectory is used as shown in figure 5(a). For initial points in $[P_{o\delta}, P_{o\bar{\sigma}}]$, an RSR trajectory is used for final points below $P_{f\bar{\sigma}}$ as in figure 5(a), and an LSR trajectory is used for final points above $P_{f\bar{\sigma}}$, as in figure 6(a). If $\pi/2 < \psi < \pi$, an LSR trajectory is assigned for P_o in $[P_{o\bar{\alpha}}, P_{o\delta}]$, either an LSR or an RSR type for P_o in $[P_{o\delta}, P_{o\bar{\sigma}}]$, an LSR

trajectory is used for final points above $P_{f\bar{\sigma}}$, and an RSR type for final points below $P_{f\bar{\sigma}}$.

The effect of $P_{o\beta}$ on pattern assignment is to modify the definition of $P_{f\bar{\gamma}}$. Whenever P_o is at or to the right of $P_{o\beta}$, the corresponding $P_{f\bar{\gamma}}$ is at negative infinity on the d_f axis. If P_o is to the left of $P_{o\beta}$, $P_{f\bar{\gamma}}$ is located by the procedure illustrated in figure 5(a).

For initial points in $[P_{o\bar{\alpha}},P_{o\bar{\sigma}}]$ and final points not in $[P_{f\bar{\gamma}},P_{f\delta}^{+}]$, trajectories are assigned so as to be compatible with those in the preceding section. Thus, if P_f is in $[P_{f\delta}^{+},P_{f\sigma}^{+}]$ an RSL type is used; if P_f is above $P_{f\sigma}^{+}$, an LSL type is used. Final points can be below $P_{f\bar{\gamma}}$ only if P_o is in $[P_{o\bar{\alpha}},P_{o\beta}]$, since otherwise $P_{f\bar{\gamma}}$ is at negative infinity. In addition, $P_{o\beta}$ and $P_{o\bar{\sigma}}$ interchange the order of their positions on the d_o axis as ψ passes through $\pi/2$ radians. However, for all values of ψ, the RSL type is used if P_o is in $[P_{o\bar{\alpha}},P_{o\beta}]$ and P_f is below $P_{f\bar{\gamma}}$. This completes the trajectory assignment for the set of initial points to the left of $P_{o\bar{\sigma}}$ and all points on d_f.

Trajectories for points to the right of $P_{o\bar{\sigma}}$ involve switching points $P_{f\gamma}^{+}$, $P_{o\alpha}^{+}$, $P_{o\sigma}^{+}$, and arise as a point on d_o, far to the right of the origin, is moved toward $P_{o\bar{\sigma}}$. In figure 4, as P_{o2} and P_{f1} move simultaneously toward the origin, they reach positions where the initial and the final circles become tangent. As discussed previously, past this point there are two final circles tangent to the initial circle. However, unlike the case discussed earlier, only the tangent point farthest from the origin is of interest. This point ($P_{f\gamma}^{+}$) and the trajectory that defines it are illustrated in figure 5(b). The position of P_{o2}, which yields only a single tangent point between initial and final circles, as P_{f2} and its right final circle are moved along d_f, is defined (fig. 4) as $P_{o\alpha}^{+}$. For P_{o2} to the left of $P_{o\alpha}^{+}$, $P_{f\gamma}^{+}$ is a function of both ψ and P_{o2}; whereas to the right of $P_{o\alpha}^{+}$, $P_{f\gamma}^{+}$ is arbitrarily assigned the value corresponding to P_{o2} at $P_{o\bar{\sigma}}$. For all initial points to the right of $P_{o\bar{\sigma}}$ and final points above $P_{f\gamma}^{+}$, an LSR type is chosen, which is simply the continuation of the type used in figure 4 between P_{o2} and P_{f1}. Similarly, an RSR type is used for all initial points to the right of $P_{o\sigma}^{+}$ and final points below $P_{f\gamma}^{+}$. This type is shown in figure 5(b) as the trajectory connecting points P_{o2} and P_{f2}. (The switching point $P_{o\sigma}^{+}$, which is the companion point to $P_{f\bar{\sigma}}$ and is illustrated in figure 5(b), will be discussed in

the next paragraph.) The RSR type is also used for final points below $P_{f\bar{\sigma}}$ if the initial points are in $[P_{o\bar{\sigma}},P_{o\sigma}^{+}]$.

The trajectory assignment problem is concluded by specifying the trajectories for P_o in $[P_{o\bar{\sigma}},P_{o\sigma}^{+}]$ and P_f in $[P_{f\bar{\sigma}},P_{f\gamma}^{+}]$. The need for a switching point at $P_{o\sigma}^{+}$ is shown when P_{o2} in figure 5(b) is moved into coincidence with $P_{o\sigma}^{+}$ while maintaining P_{f2} between $P_{f\bar{\sigma}}$ and $P_{f\gamma}^{+}$. At the point of coincidence, the RSR trajectory assigned to points to the right of $P_{o\sigma}^{+}$ degenerates into a RS trajectory, thus establishing $P_{o\sigma}^{+}$ as a limiting point of the RSR type. Similarly, $P_{f\bar{\sigma}}$, the companion point to $P_{o\sigma}^{+}$, is a limiting point of the RSR type. If, in figure 5(b), P_{o2} is in $[P_{o\bar{\sigma}},P_{o\sigma}^{+}]$ and P_{f2} is below $P_{f\bar{\sigma}}$, the RSR trajectory assigned in the preceding paragraph to this combination of initial and final points degenerates into an SR type as P_{f2} moves into coincidence with $P_{f\bar{\sigma}}$. If P_{f2} moves slightly above $P_{f\bar{\sigma}}$, and the left initial circle and the right final circle do not intersect, an LSR type is used, shown in figure 6(b) between P_o and P_f. The final switching point, denoted by $P_{f\bar{\delta}}$, then occurs as P_f is moved up until the left initial circle and the right final circle become tangent. For final points above $P_{f\bar{\delta}}$, the LSL type in figure 6(c) is used. The range of $P_{f\bar{\delta}}$ is $[P_{f\bar{\sigma}},P_{f\gamma}^{+}]$, the lower limit being reached as P_o approaches $P_{o\sigma}^{+}$ and the upper limit as P_o approaches $P_{o\bar{\sigma}}$.

As before, these rules must be slightly qualified to take into account the effect of $P_{o\beta}$, which moves to the right of $P_{o\bar{\sigma}}$ for $\psi > \pi/2$. If P_o lies to the right of $P_{o\beta}$, no changes in the rules are needed. For P_o in $[P_{o\bar{\sigma}},P_{o\beta}]$, $P_{f\bar{\gamma}}$ is located with respect to P_f. If P_f is above $P_{f\bar{\gamma}}$, $P_{f\bar{\gamma}}$ is disregarded and the established assignment rules are used. If P_f is below $P_{f\bar{\gamma}}$, the previously established RSL trajectory is used. This concludes the assignment of trajectories for all combinations of the pattern parameters.

Derivation of Switching Functions

The next step is to derive the analytical expressions not yet given for some switching points. An essential step in the derivation is to solve for various parts of the right triangle P_v, C_o, P_n, shown in figure 7. Since all circles in the construction have unit radius, $\overline{P_vC_o} = \sqrt{1 + d_o^2}$ and $\psi_2 = \psi + \tan^{-1} 1/d_o$ where d_o is negative in this example. Now

$$\overline{C_oP_n} = \sqrt{1 + d_o^2} \sin \psi_2 ,$$

$$\overline{P_n P_v} = \sqrt{1 + d_o^2} \cos \psi_2$$

$$\overline{P_{f\gamma^-} P_n} = \overline{P_n P_{f\delta^+}} = \sqrt{4 - (\sqrt{1 + d_o^2} \sin \psi_2 - 1)^2}$$

These expressions suffice to calculate $d_{f\delta^+}$ and $d_{f\gamma^-}$:

$$d_{f\delta^+} = d_o \cos \psi - \sin \psi + \sqrt{4 - (d_o \sin \psi + \cos \psi + 1)^2} \tag{4}$$

$$d_{f\gamma^-} = d_o \cos \psi - \sin \psi - \sqrt{4 - (d_o \sin \psi + \cos \psi + 1)^2} \tag{5}$$

The expression for $d_{o\alpha^-}$ can be obtained by equating to zero the expression for $\overline{P_n P_{f\delta^+}}$, solving the resulting equation for d_o, and substituting $d_{o\alpha^-}$ for d_o:

$$d_{o\alpha^-} = -\frac{3}{\sin \psi} + \frac{1}{\tan \psi} \tag{6}$$

The expressions for $d_{o\sigma^+}$ and $d_{f\sigma^-}$ are:

$$d_{o\sigma^+} = \tan \frac{\psi}{2} \tag{7}$$

$$d_{f\sigma^-} = -\tan \frac{\psi}{2} \tag{8}$$

If $0 < \psi < \pi/2$, $d_{o\delta}$ is obtained by equating expressions for $d_{f\delta^+}$ and $d_{f\sigma^-}$ and solving the resulting equation for d_o, which is then interpreted as $d_{o\delta}$:

$$d_{o\delta} = -\tan \frac{\psi}{2} \cos \psi - \sin \psi - \sqrt{4 - \left(1 + \cos \psi - \tan \frac{\psi}{2} \sin \psi\right)^2} \tag{9}$$

Similarly, for $\pi/2 < \psi < \pi$, $d_{o\delta}$ is obtained by equating $d_{f\gamma^-}$ and $d_{f\sigma^-}$. However, after the proper sign is chosen in front of the square root expression occurring in the solution of the quadratic equation, the equation obtained is the same as equation (9).

The expressions for $d_{f\gamma^+}$ and $d_{f\delta^-}$ can be derived in the same way as $d_{f\gamma^-}$ and $d_{f\delta^+}$. They may also be deduced directly from $d_{f\delta^+}$ and $d_{f\gamma^-}$ by symmetry:

$$d_{f\gamma^+} = d_o \cos \psi + \sin \psi + \sqrt{4 - (-d_o \sin \psi + \cos \psi + 1)^2} \tag{10}$$

$$d_{f\bar{\delta}} = d_o \cos\psi + \sin\psi - \sqrt{4 - (-d_o \sin\psi + \cos\psi + 1)^2} \qquad (11)$$

A complete collection of all switching functions, along with their domains of definition, is given in table 3.

Switching Diagrams

The various regions of trajectory patterns in the three-dimensional parameter space (ψ, d_o, d_f) can be illustrated with switching diagrams which consist of planar cuts through this space obtained by holding one of the three parameters constant. When ψ is constant, the switching diagrams are as shown in figures 8(a), (b), and (c) for three values of ψ: $\pi/4$, $\pi/2$, and $3\pi/4$. Each region is labeled with the pattern type established for it in the preceding sections. On the region boundaries, the four types of three-segment patterns often degenerate to one- or two-segment patterns, as indicated by the coded lines. In addition to giving a compact representation of pattern regions, the switching diagrams find use in developing decision logic for pattern type selection.

The switching diagrams show that for $\psi = \pi/4$ and $3\pi/4$, $d_{o\beta} = d_{o\delta}$. The line segment $d_{f\bar{\sigma}}$ is terminated on the left by $d_{f\bar{\gamma}}$ for $\psi < 3\pi/4$ and by $d_{o\beta}$ for $\psi \geq 3\pi/4$, as shown by the two inserts in figure 8(c). No other changes in the structure of the switching diagrams occur as ψ is varied in the range $0 < \psi < \pi$.

Flight Patterns for $\psi = 0$ and $\psi = \pi$ Radians

For the two singular values of ψ, $\psi = 0$ and $\psi = \pi$ radians, the parameters d_o and d_f are not defined. Instead, the parameters used are the rectangular coordinates of the initial point, P_o, expressed in the X,Y coordinate system of figure 3. This coordinate system is centered at P_f and has its x-axis pointing in the direction of the final heading. Unlike the parameter space (d_o, d_f), the parameter space (X, Y) preserves the geometric shapes of figures under mappings; therefore pattern assignment and switching diagrams can be combined in one figure.

Switching diagrams, as well as example trajectories, are given for $\psi = 0$ in figure 9(a) and for $\psi = \pi$ radians in figure 9(b). For both values of ψ, the switching curves which separate the parameter space into regions of different patterns are either straight lines or portions of circles with radius 2. For $\psi = 0$, one circle is centered at (0,-2), the other at (0,2). For $\psi = \pi$, the one circle is centered at the origin. These circles define the locus of initial points for which an initial circle is tangent to a final circle. The switching diagrams are symmetric about the x-axis. This symmetry is also present in the pattern assignment; for a given value of X, trajectories in the negative Y plane are the mirror images of trajectories in

the positive Y plane. Several sample trajectories are superimposed on the switching diagrams to illustrate the pattern assignment.

Derivation of Path-Length Equation

In preceding sections, rules were derived for choosing a particular trajectory for each initial position and heading of an aircraft. The next step is to derive equations for calculating the path length and the heading changes in the first and final turns for each trajectory. For the RSR trajectory between P_o and P_f in figure 10(a), P_o is at (x,y), the initial heading is ψ, and the turning radius is R. Then:

$$\overrightarrow{P_f C_{or}} = \overrightarrow{P_f P_o} + \overrightarrow{P_o C_{or}} = \left[X + R\cos\left(\psi + \frac{\pi}{2}\right),\ Y + R\sin\left(\psi + \frac{\pi}{2}\right)\right] \tag{12}$$

Further, the vector $\overrightarrow{C_{or}C_{fr}}$ is the difference between $\overrightarrow{P_f C_{fr}}$ and $\overrightarrow{P_f C_{or}}$:

$$\overrightarrow{C_{or}C_{fr}} = \left[-X - R\cos\left(\psi + \frac{\pi}{2}\right),\ R - R\sin\left(\psi + \frac{\pi}{2}\right) - Y\right] \tag{13}$$

The heading of the vector $\overrightarrow{C_{or}C_{fr}}$, denoted by ψ_1, equals the heading of the straight-line segment, ψ_s, whereas the length of this vector equals the length of the straight-line segment:

$$\psi_s \equiv \begin{matrix}\text{heading of straight-}\\ \text{line segment}\end{matrix} = \tan^{-1}\frac{R - R\sin[\psi + (\pi/2)] - Y}{-X - R\cos[\psi + (\pi/2)]} \tag{14}$$

$$\overline{P_1P_2} \equiv \begin{matrix}\text{length of straight-}\\ \text{line segment}\end{matrix} = \sqrt{\{X+R\cos[\psi+(\pi/2)]\}^2+\{R-R\sin[\psi+(\pi/2)]-Y\}^2} \tag{15}$$

The arctangent is evaluated in the conventional manner as an angle ψ in the range $0 \le \psi < 2\pi$. The heading change ψ_i in the first turn is seen to be

$$\psi_i = \psi_s - \psi \quad \text{if} \quad \psi_s \ge \psi \tag{16}$$

$$\psi_i = 2\pi + \psi_s - \psi \quad \text{if} \quad \psi_s < \psi \tag{17}$$

The path length in the first turn is then $\overline{P_oP_1} = \psi_i R$. Finally, the angle ψ_f and the path length of the final turn are

$$\psi_f = 2\pi - \psi_s \quad \text{if} \quad \psi_s > 0 \qquad \overline{P_2P_f} = R\psi_f \tag{18}$$

$$\psi_f = 0 \quad \text{if} \quad \psi_s = 0 \qquad \overline{P_2P_f} = 0 \tag{19}$$

The trajectory constants for an RSL trajectory, as in figure 10(b), begin with vector $\overrightarrow{C_{or}C_{fe}}$:

$$\overrightarrow{C_{or}C_{fe}} = \overrightarrow{P_fC_{fe}} - \overrightarrow{P_fC_{or}} \tag{20}$$

which can be written in Cartesian coordinates:

$$\overrightarrow{C_{or}C_{fe}} = \left[-X - R\cos\left(\psi + \frac{\pi}{2}\right), -R - R\sin\left(\psi + \frac{\pi}{2}\right) - Y\right] \tag{21}$$

For the trajectory to exist we must have $\| C_{or}C_{fe}\| \geq 2R$. The existence of the trajectory is guaranteed if the pattern selection rules established in the preceding section are applied. The next step is to calculate ψ', the angle between the vectors $\overrightarrow{P_1P_2}$ and $\overrightarrow{C_{or}C_{fe}}$; since $\overline{C_{or}P_c} = (1/2)\|\overrightarrow{C_{or}C_{fe}}\|$,

$$\psi' = \arcsin\frac{R}{\frac{1}{2}\|\overrightarrow{C_{or}C_{fe}}\|} \tag{22}$$

The length of the straight-line segment and its heading are therefore

$$\overline{P_1P_2} \equiv \begin{matrix}\text{length of straight-}\\ \text{line segment}\end{matrix} = \frac{2R}{\tan\psi'} \tag{23}$$

$$\psi_s \equiv \begin{matrix}\text{heading of straight-}\\ \text{line segment}\end{matrix} \begin{matrix} = \psi_1 + \psi' & \text{if} \quad \psi_1 + \psi' < 2\pi \\ = \psi_1 + \psi' - 2\pi & \text{if} \quad \psi_1 + \psi' \geq 2\pi \end{matrix} \tag{24}$$

where ψ_1 is the heading of the vector $\overrightarrow{C_{or}C_{fe}}$:

$$\psi_1 = \arctan\frac{-R - R\sin[\psi + (\pi/2)] - Y}{-X - R\cos[\psi + (\pi/2)]} \tag{25}$$

Finally, the heading changes and arc length of the initial and the final turns are:

$$\psi_i = \begin{cases}\psi_s - \psi & \psi_s \geq \psi \\ \psi_s + 2\pi - \psi\,, & \psi_s < \psi\end{cases} \qquad \overline{P_oP_1} = \psi_i R \tag{26}$$

$$\psi_f = \psi_s\,, \qquad \overline{P_2P_f} = \psi_s R \tag{27}$$

For the LSL and LSR patterns, the same techniques used for the RSR pattern above are applicable. Table 4 summarizes path-length and heading change equations for the four major pattern types. When possible, the equations are simplified by application of trigonometric identities. Patterns with fewer than three segments are special cases of the three-segment patterns and are not included in the table.

The major computational units in the horizontal guidance algorithm are summarized in the flow chart given in figure 11. Reference in the chart to a figure or table in the text identifies a major unit and implies that logic must be developed to perform the indicated function. For example, entering a switching diagram to select a pattern requires the development of a flow chart of inequality tests performed on the switching functions given in table 3 to locate the correct pattern region. Examples of such flow charts for the switching diagrams of problems (b) and (c) are in the next section.

TRAJECTORY SYNTHESIS FOR PROBLEMS (b), (c), (d)

Optimum control laws for the minimum-path-length trajectories of problems (b) and (c) are derived in reference 9. To complete the solution of these horizontal trajectory problems, equations are required for the path length and the turning angles of the optimum trajectories. In addition, computer algorithms are needed for the implementation of the control laws. Further, a solution to problem (d) is necessary. As in the previous section, distances are normalized to units of turning radius.

Trajectory Synthesis for Problem (b)

Problem (b) was to fly from any initial position and heading to intercept and fly along a line of specified heading. The minimum-arc-length control law for this problem, from reference 9, is shown as the switching diagram in figure 12. Coordinates are d and ψ; d is the perpendicular distance in units of turning radii from the final line, and ψ is the heading measured with respect to the heading of the final line. The coordinate d is positive for initial points to the right of the final line if one faces in the direction of the final heading. The heading ψ is positive for a clockwise rotation from the direction of the final line, and its range is $-\pi < \psi \leq \pi$. Solid switching lines with arrows indicate the direction a phase point travels toward the origin. The switching lines and the dashed lines separate the phase plane into various regions. Each switching line and region is labeled with its respective pattern type. Reference 9 shows that the optimum trajectories for this problem consist at most of three segments, with the middle segment a straight line and the first and last segments portions of minimum-radius circles.

In the phase plane, right and left turns with unity turning radius are parameterized by the equations

$$d_r(\psi) = d_o + \cos \psi_o - \cos \psi \quad \text{(right turn)} \tag{28}$$

$$d_\ell(\psi) = d_o - \cos \psi_o + \cos \psi \quad \text{(left turn)} \tag{29}$$

where d_o and ψ_o are the phase points where the turns are initiated. Straight-line flight generates a line parallel to the d axis. The switching lines are special cases of these phase plane trajectories and are labeled S_1 through S_6 in the switching diagram. The equations for the switching lines, along with their domain of definition, are required by the computer algorithm to select the correct pattern type for a given initial condition:

$$S_1(\psi) = 1 - \cos \psi \qquad \psi \notin [0, \pi/2] \tag{30}$$

$$S_2(\psi) = 1 + \cos \psi \qquad -\pi/2 \leq \psi \leq \pi \tag{31}$$

$$S_3(\psi) = -1 + \cos \psi \qquad \psi \notin [0, -\pi/2] \tag{32}$$

$$S_4(d) = -\pi/2 \qquad d \geq 1 \tag{33}$$

$$S_5(d) = \pi/2 \qquad d \leq -1 \tag{34}$$

$$S_6(\psi) = -1 - \cos \psi \qquad -\pi < \psi \leq \pi/2 \tag{35}$$

The dashed lines which also form portions of the boundaries between pattern regions do not represent phase-plane trajectories. Instead, they define the set of initial points for which two trajectory types yield equal path length. For example, the RSR trajectory and the LSR trajectory yield the same value for the path length for initial conditions on the dashed line segment $\psi = \pi/2$, $d \geq 1$. For definiteness, one of the minimum-path-length trajectories is arbitrarily assigned to such points of ambiguity. The phase trajectories for eight initial conditions (P_a - P_h) are traced out in figure 12, and their corresponding geometric patterns are shown in figure 13.

Parametric equations (28) and (29) for the phase-plane trajectories, together with the switching diagram, are used to derive equations for turning angles and for the length of the straight-line portion of the various patterns. Table 5 lists these equations and their region of validity for all trajectory types beginning with a left turn. Equations for the mirror-image trajectories are obtained by reversing the signs of ψ and d. For example, if d and ψ are such that the switching diagram specifies an RSR trajectory, the signs of d and ψ are reversed, then entered into the equations for the LSL trajectory given in table 5.

Finally, the switching diagram (fig. 12), equations (30) through (35), and the equations in table 5 can be used to construct a flow chart for trajectory synthesis (fig. 14). The input to the flow chart is d and ψ, and its output is the trajectory type and parameters. The first part of the flow chart consists of a sequence of inequality tests on d and ψ to determine the pattern type, and the second part consists of the calculation of the trajectory parameters. The flow chart logic was simplified by making use of the odd symmetry of the switching diagram. If the given d and ψ require a pattern beginning with a right turn, the algorithm reverses their signs, identifying

the situation by setting index $i_r = 2$. After the pattern parameters are computed, i_r is checked; if it is 2, the pattern is reversed to its mirror image.

Trajectory Synthesis for Problem (c)

Problem (c) is to fly from a given initial position and heading to a specified final point with an unspecified final heading. The control law that minimizes arc length, derived in reference 9, is shown in figure 15(a), with distances normalized to the unit turning radius. The location of the final point is expressed in a coordinate system which has its origin at the initial position, P_o, its x-axis pointing in the direction of the initial heading, and its y-axis pointing to the right. The switching lines in this control law are the x-axis and two circles with unit radii and centers at (0,-1) and (0,1). Trajectories for points on the negative x-axis can be taken as either LS or RS with no change in path length; they are arbitrarily made RS. Example trajectories for four final points are shown in figure 15(b).

Equations for the path length and turning angles, and the flow chart for trajectory synthesis, are determined next. Symmetry in the control law reduces the complexity of the trajectory constants and algorithm. Only the positive y-plane need be considered, since trajectories for the negative y-plane can be obtained by reflection about the x-axis. Then the switching logic need only determine whether a final point is inside or outside the unit circle at (0,1), and the path length and turning angle equations are easily derived by simple trigonometry. Table 6 summarizes the equations and their region of validity; ψ_i denotes the angle in the initial turn, ψ_f the angle in the final turn, and ℓ the length of the straight-line segment. (The arctangent is an angle ψ in the range $-\pi < \psi < \pi$.) The flow chart for trajectory synthesis, shown in figure 16, is an implementation of figure 15(a) and table 6. It has as inputs the x,y coordinates of the final point, and as outputs the trajectory pattern, turning angles, and path length. For purposes of developing this flow chart, each pattern was assigned an integer, which is represented in the chart by the index i_p. The correspondence between the pattern types and this index is given in the chart.

Trajectory Synthesis for Problem (d)

Problem (d) is to make a smooth transition from flight along one straight-line segment to flight along a second, intersecting straight-line segment. The distance from the aircraft to the point of intersection along the first segment is x_i, and the distance from the point of intersection to a desired final point on the second segment is x_f. Angle ψ is the heading difference between the two segments; since the segments intersect, ψ is neither zero nor π. To make the transition without overshoot, the aircraft should begin a circular turn of radius R at a distance before the intersection point given by

$$x_T = R \tan \frac{|\psi|}{2} \quad \begin{cases} 0 < \psi < \pi, \text{ or} \\ -\pi < \psi < 0 \end{cases} \tag{36}$$

When proper account is taken of the circular segment, the total path length between x_i and x_f is

$$\ell_T = x_i + x_f - 2R \tan \frac{|\psi|}{2} + \frac{|\psi|}{R} \tag{37}$$

CONTROLLED TIME OF ARRIVAL AND VERTICAL GUIDANCE

The problem of achieving precise arrival time of an aircraft at some point on the final approach or any other specified point of the approach route generally consists of selecting both a speed profile and a horizontal trajectory of appropriate length such that the aircraft, starting with initial speed V_o arrives at the end point with speed V_f in the time interval t. As explained earlier, we first attempt to achieve the desired arrival time with speed control alone, assuming that the horizontal trajectory, and therefore the path length, is fixed. If it is found that speed control cannot achieve the desired arrival time because the aircraft's performance capabilities are exceeded, the path length will be modified as required to control the arrival time. Solution of the controlled time of arrival problem therefore involves two algorithms, one to select the speed profile, assuming a fixed length of trajectory to the final point, the other to change the length of the trajectory by an appropriate amount.

Speed Control

The problem of speed profile selection is considered first. The time to the final point and the length of the path are denoted by t and L, respectively. In addition to beginning with V_o and ending with V_f, the speed V along the profile must at all times obey the constraint $V_{min} \le V \le V_{max}$. Speed changes are made by constant acceleration A_a (numerically positive) or constant deceleration A_d (numerically negative). These six quantities, t, L, V_{min}, V_{max}, A_a, and A_d, are treated as parameters in developing logic for speed profile selection. The speed profile consists of a maximum of three segments: an acceleration or deceleration segment starting at V_o, a constant speed segment, and another acceleration or deceleration segment ending at V_f. Unless one or more of the segments has zero time duration, the three segments can be arranged to yield four possible speed profiles. The profile to be used is selected by comparing the path length L with two distances, L_1 and L_2:

$$L_1 = \begin{cases} V_o t + \dfrac{(V_f - V_o)^2}{2A_a} & V_o \le V_f \qquad (38) \\ V_f t - \dfrac{(V_f - V_o)^2}{2A_d} & V_o \ge V_f \qquad (39) \end{cases}$$

$$L_2 = \begin{cases} V_o t + \dfrac{(V_f - V_o)^2}{2A_d} & V_o \geq V_f \quad (40) \\ V_f t - \dfrac{(V_f - V_o)^2}{2A_a} & V_o \leq V_f \quad (41) \end{cases}$$

where L_1 is the minimum, and L_2 the maximum distance to fly in interval t when speed is between V_o and V_f. The relation between the required speed profile and the distances L_1 and L_2 is shown in figure 17, where V_n is the aircraft speed in the constant-speed segment. The distances L_1 and L_2 are represented by the shaded areas of the speed profiles in the left-hand column of figure 17. The profiles to be used are in the right-hand column. The required profiles are selected by comparing the shaded areas of left-hand column profiles with those of the right. If $L < L_1$, the required profile consists of deceleration, constant speed, and acceleration; if $L > L_2$, the required profile consists of acceleration, constant speed, and deceleration. For $L_1 \leq L \leq L_2$, the required profile consists of deceleration, constant speed, and deceleration segments if $V_o > V_f$, or of acceleration, constant speed, and acceleration segments if $V_o < V_f$.

The "profile constants" are the second-segment speed V_n, starting time t_1 and ending time t_2. With permissible acceleration (or deceleration) of a_1 in the first segment and a_3 in the third segment, V_n is computed by equating L with the area under the speed-history curve:

$$L = V_n t - \frac{(V_n - V_o)^2}{2a_1} + \frac{(V_n - V_f)^2}{2a_3} \quad (42)$$

Equation (42) is quadratic in V_n and can be expressed as

$$V_n^2\left(\frac{1}{2a_3} - \frac{1}{2a_1}\right) + V_n\left(t + \frac{V_o}{a_1} - \frac{V_f}{a_3}\right) + \left(\frac{V_f^2}{2a_3} - \frac{V_o^2}{2a_1} - L\right) = 0 \quad (43)$$

After solving for V_n, the remaining profile constants t_1 and t_2 are

$$t_1 = \frac{V_n - V_o}{a_1} \quad (44)$$

$$t_2 = t - \frac{V_f - V_n}{a_3} \quad (45)$$

The profile is physically meaningful only if $t_1 \leq t_2$; if $t_1 > t_2$, the final time must be changed. The profile degenerates to two segments if $V_n = V_o$ or $V_n = V_f$, or to one segment if $V_o = V_f$.

The final step is to compare V_n with V_{min} and V_{max}. If $V_{min} \leq V_n \leq V_{max}$, the profile is valid. If $V_n > V_{max}$, the time permitted to the final point must be increased. If $V_n < V_{min}$, the path length must be increased.

Path Stretching

This section considers a technique for increasing the path length. Path stretching is applied only to the straight-line portions of the trajectory. Any technique for path stretching must provide for continuous increases in path length, so that the difference between the length of the stretched path and that of the unstretched path can range from zero to any desirable number. The proposed technique provides for this type of continuity when the distance between the initial and final point is greater than four turning radii. When this distance is less than four turning radii, a continuous range of stretched path length is not always possible.

The patterns for the stretched path consist of circular arcs and line segments. Although different radii may be used for different arcs without introducing any complexity into the path-stretching algorithm, the radii of all arcs in a pattern are assumed to be the same to simplify presentation of the technique.

Path-stretching patterns are generated by three circles connected by tangent lines as shown in figure 18(a), to form a path confluent with the unstretched path at the initial and final points. Two of the circles, C_1 and C_2, are fixed and tangent to the unstretched path at P_o and P_f, respectively. The third circle, C_3, moves to generate different path lengths. The center of the third circle is restricted to move along a curve consisting first of a 90° arc with a two-unit radius and then of a half line, as shown in figure 19. The pattern is completed by connecting the three circles with the appropriate tangent lines.

If the center of C_3 lies on the half-line portion of the curve, the pattern consists of five segments and is "nondegenerate." Otherwise, the pattern contains fewer segments and is "degenerate." The nondegenerate pattern is used most often because it provides a large range of path length. Figure 18 shows the four patterns generated by placing the center of C_3 at points P_A, P_B, P_C, and P_D of figure 19. As the center of C_3 moves along the locus of centers from P_A, the difference between the stretched and the unstretched path length increases monotonically from zero to any positive number. Since the distance between P_o and P_f is not less than four radii, circles C_1, C_2, and C_3 cannot intersect. At worst, C_3 is tangent to C_1 and C_2; thus the tangents required to complete the pattern can always be constructed.

The relationship between the direct path length L_d (the distance between P_o and P_f) and the stretched-path length L_s is plotted in figure 20. The location of the center of circle C_3 on the locus of centers (fig. 19) is a parameter. Between P_A and P_C, the parameter is θ_s; beyond P_C, the parameter is the perpendicular distance Y_{C_3} between the center of C_3 and the line

connecting C_1 and C_2 in units of turning radii. For any fixed value of L_d in the interval of $[4, \infty)$, the value of L_s increases continuously as C_3 moves along the locus of centers starting from point P_A. Moreover, it can be concluded from the characteristics of these curves that for any given combination of values of (L_d, L_s), where $L_d \notin [4, \infty)$ and $L_s \geq L_d$, a unique curve intersects point (L_d, L_s). The parameter value that generates that intersecting curve defines the solution of the path-stretching problem. The equation for the unknown value of the parameter is nonlinear in the parameter and can be solved by known techniques; it is derived in the appendix.

Algorithm for Controlled Time of Arrival

The algorithm for synthesizing controlled time-of-arrival profile consists of speed-control, path-stretching, and decision logic (fig. 21). The profile is synthesized in three steps:

(1) Determine L_{min} and L_{max}, the minimum and maximum distances the aircraft is capable of traversing, for the given V_o, V_f, A_a, A_d, V_{max}, V_{min}, and t.

(2) Determine if L is within the range of $[L_{min}, L_{max}]$, (a) if $L < L_{min}$, stretch the path length to L_s so that $L_{min} < L_s < L_{max}$ and proceed to step 3, (b) if $L > L_{max}$, return message stating that the given time t is too short for the aircraft to traverse the given distance L, (c) if $L_{min} \leq L \leq L_{max}$, proceed to step 3.

(3) Determine the profile pattern and compute profile constants V_n, t_1, and t_2.

The distances L_{max} and L_{min} correspond to the areas under speed-profile curves whose constant-speed segments are flown at V_{max} and V_{min}, and are computed by substituting the speed and acceleration limits into equation (42):

$$L_{max} = V_{max}t - \frac{(V_{max} - V_o)^2}{2A_a} + \frac{(V_{max} - V_f)^2}{2A_d}$$

$$= V_{max}t - \frac{(V_{max} - V_o)^2}{2A_a} - \frac{(V_{max} - V_f)^2}{2|A_d|} \tag{46}$$

$$L_{min} = V_{min}t - \frac{(V_{min} - V_o)^2}{2A_d} + \frac{(V_{min} - V_f)^2}{2A_a}$$

$$= V_{min}t + \frac{(V_o - V_{min})^2}{2|A_d|} + \frac{(V_f - V_{min})^2}{2A_a} \tag{47}$$

When t is too short for the aircraft to accelerate to V_{max} at A_a, the corresponding maximum-distance profile consists of two segments: an acceleration segment from V_o to V_{up} ($<V_{max}$), and a deceleration segment from V_{up} to V_f. The upper speed, V_{up}, is computed by equating the sum of the time duration of the two segments to t:

$$t_1 + (t - t_1) = \frac{V_{up} - V_o}{A_a} + \frac{V_{up} - V_f}{|A_d|} = t$$

Upon rearranging terms,

$$V_{up} = \frac{t + \frac{V_o}{A_a} + \frac{V_f}{|A_d|}}{\frac{1}{A_a} + \frac{1}{|A_d|}} \tag{48}$$

The area under the curve is

$$L_{max} = V_o t_1 + \frac{V_{up} - V_o}{2} t_1 + V_f(t - t_1) + \frac{V_{up} - V_f}{2}(t - t_1) \tag{49}$$

$$= \frac{V_{up}^2 - V_o^2}{2A_a} + \frac{V_{up}^2 - V_f^2}{2|A_d|} \tag{50}$$

Similarly, the minimum-distance profile for small t consists of two segments: a deceleration segment from V_o to V_ℓ (a speed greater than V_{min}), and an acceleration segment from V_ℓ to V_f. For V_ℓ,

$$t_1 + (t - t_1) = \frac{V_o - V_\ell}{|A_d|} + \frac{V_f - V_\ell}{A_a} = t$$

Upon rearranging terms,

$$V_\ell = \frac{\frac{V_o}{|A_d|} + \frac{V_f}{A_a} - t}{\frac{1}{|A_d|} + \frac{1}{A_a}} \tag{51}$$

The area under the curve is

$$L_{min} = V_\ell t + \frac{V_o - V_\ell}{2} t_1 + \frac{V_f - V_\ell}{2}(t - t_1) \tag{52}$$

$$= V_\ell t + \frac{(V_o - V_\ell)^2}{2|A_d|} + \frac{(V_\ell - V_f)^2}{2A_a} \tag{53}$$

Second, a comparison is performed to ascertain that the controlled time of arrival can be accomplished by speed control alone. If not, then the given nominal path length L is increased to L_s by path stretching as specified by k:

$$L_s = kL_{max} + (1 - k)L_{min} \tag{54}$$

where $0 < k < 1$. Third, the path length L (or L_s) is compared with L_1 and L_2 to determine the pattern for the speed profile, and the trajectory constants are computed by equations (43), (44), and (45).

Time Reference

In the controlled-time-of-arrival problem, time-to-go is an important variable to pilot and air-traffic controller. As arrival time approaches, air traffic control must know by how much this time can still be changed. The earliest arrival time t_{min} and the latest arrival time t_{max} achievable by speed control alone are

$$t_{min} = \frac{L + \dfrac{(V_{max} - V_o)^2}{2A_a} + \dfrac{(V_{max} - V_f)^2}{2|A_d|}}{V_{max}} \tag{55}$$

$$t_{max} = \frac{L - \dfrac{(V_o - V_{min})^2}{2|A_d|} - \dfrac{(V_f - V_{min})^2}{2A_a}}{V_{min}} \tag{56}$$

These times could be used as decision variables instead of L_{max} and L_{min} in the algorithm. If $t < t_{min}$, the trajectory is beyond the aircraft's capability. If $t_{min} \leq t \leq t_{max}$, the controlled time of arrival can be accomplished by speed control alone, but if $t > t_{max}$, path stretching is also required.

Vertical Guidance

Criteria for generating the vertical profile were described earlier. The vertical profile is defined by the time to begin descent to the desired final altitude. This time is calculated by subtracting from the specified arrival time, t, the time intervals required to change the approach speed to the specified final speed in level flight, and to change the cruise altitude to the final altitude. The first time interval is profile constant t_2, available from the already calculated speed-time history, and the second interval is given by $(h_c - h_f)/\dot{h}$.

Summary

This section has developed procedures for synthesizing speed profiles to achieve specified arrival times at specified points on the approach path, and for modifying the length of the approach path if the speed profile required for a specified arrival time is outside the aircraft's performance envelope. A simple technique for vertical guidance was also described. The simplicity of the technique resulted from the use of parameters already calculated in the synthesis of horizontal and airspeed profiles. The synthesis algorithms discussed in this and the previous sections are illustrated in the next section by an example.

OVERALL FLIGHT PROFILE SYNTHESIS - AN EXAMPLE

A numerical example will be used to illustrate how a complete, three-dimensional trajectory with time constraints may be synthesized by applying the techniques developed for horizontal guidance, controlled time of arrival, and vertical guidance. It is assumed that an aircraft has reached the last waypoint before the outer marker. Wind velocity is assumed to be zero. If it is not, the trajectory to be synthesized must be modified somewhat to account for the wind velocity.

Problem Description

Consider an aircraft whose current position is 21.8 km (13.56 miles) from the OM at an azimuth of 292°. It has a heading of 216°, an altitude of 1520 m (5000 ft), and a speed of 149.6 m/sec (290 knots). The flight profile to be synthesized must guide the aircraft to arrive at the OM six minutes later, aligned with the runway at a final altitude of 456 m (1500 ft) and a final speed of 67 m/sec (130 knots). The acceleration and deceleration capability of the aircraft is 0.61 m/sec^2 (2 ft/sec^2), and the maximum and minimum speeds of the aircraft are 154.5 m/sec (300 knots) and 67 m/sec (130 knots). The sink rate (rate of change of altitude) is 305 m/min (1000 ft/min). The aircraft must maintain cruise altitude (1520 m in this case) as long as possible, descend at constant speed, and hold altitude during speed changes. A minimum turning radius of 6.45 km (4 miles) is used during horizontal maneuvers. The conditions and constraints for this example are summarized in figure 22.

As outlined earlier, the complete profile of the aircraft's time-position relationship is synthesized in three sequential steps: horizontal guidance, controlled time of arrival, and vertical guidance. Each subproblem and its methods of solution are discussed separately. After the complete profile is solved, it is summarized as a command sequence, which gives the order, initiation times, and termination times of commands required to fly the profile.

Horizontal Guidance

From the description of the example, the horizontal guidance problem is classed as problem (a), and steps for synthesis are: (1) compute pattern parameters, (2) determine the flight pattern, and (3) compute turning angles, linear path length, and total path length.

First, the pattern parameters d_o and d_f are computed using equations (2) and (3):

$$d_o = \frac{y_o}{R \sin \psi} = 5.32$$

$$d_f = -\frac{x_o}{R} + \frac{y_o}{R \tan \psi} = -5.6$$

The heading of 216°, converted to modulus 180°, is -144°. Since it is negative, a reflection about the d_o axis is required for pattern determination: $\psi^r = -\psi = 144°$.

Second, the flight pattern is determined by comparing d_o and d_f with the appropriate switching points in the switching diagram (fig. 8(c)). Comparing d_o with $d_{o\alpha}^+$, where the value of $d_{o\alpha}^+$ is computed by equations listed in table 3:

$$d_{o\alpha}^+ = \frac{3}{\sin \psi^r} + \frac{1}{\tan \psi^r} = 3.73$$

so $d_o > d_{o\alpha}^+$. The value of d_f is then compared with $d_{f\gamma}^+$ where

$$d_{f\gamma}^+ = \frac{3}{\tan \psi_r} + \frac{1}{\sin \psi_r} = -2.43$$

so that $d_f < d_{f\gamma}^+$. These inequalities establish that the flight pattern is RSR and that the reflected flight pattern is therefore LSL.

Third, the turning angles, curved path length, linear path length, and total path length are computed by the equations for the LSL pattern in table 4:

$$\overline{P_1P_2} = \sqrt{(x_o + R \sin \psi)^2 + (R - R \cos \psi + y_o)^2} = 9.65 \text{ km (6 miles)}$$

$$\psi_s = \tan^{-1}\left(\frac{-R + R \cos \psi - y_o}{-x_o - R \sin \psi}\right) = 118°$$

$$\psi_i = \psi - \psi_s + 360° = 98°$$

$$\overset{\frown}{P_oP_1} = \frac{98^\circ \times 6.45 \times \pi}{180} = 11 \text{ km } (6.84 \text{ miles})$$

$$\psi_f = \psi_s = 118^\circ$$

$$\overset{\frown}{P_2P_f} = \frac{118 \times 6.45 \times \pi}{180} = 13.25 \text{ km } (8.24 \text{ miles})$$

$$L = \overset{\frown}{P_oP_1} + \overline{P_1P_2} + \overset{\frown}{P_2P_f} = 34 \text{ km } (21.1 \text{ miles})$$

This concludes the computation of the horizontal trajectory.

Controlled Time of Arrival

The numerical inputs for this problem are those specified in figure 22, with the addition of the path length, 34 km (21.1 miles), obtained in the preceding section.

The logical path traced in synthesizing the speed profile is shown with heavy lines in figure 23. At node ⚠1, the time interval, Δt_2, for the maximum distance profile is computed to be 208.1 seconds. Since Δt_2 is positive, the maximum distance profile consists of three segments. Next, L_{max}, the distance corresponding to this profile, is computed before node ⚠2 :

$$L_{max} = V_{max}t - \frac{(V_{max} - V_o)^2}{2A_a} - \frac{(V_{max} - V_f)^2}{2|A_d|}$$

$$= 49.1 \text{ km } (30.5 \text{ miles})$$

Since the given distance L for this problem (34 km) is less than L_{max}, the profile synthesized is within the aircraft's capability.

Similarly, at node ⚠3 , Δt_2 for the minimum distance profile is computed to be 225 seconds. The positive value for Δt_2 implies that the minimum distance profile contains a constant speed segment. Before node ⚠4 , the distance corresponding to this profile is computed and then compared with L:

$$L_{min} = V_{min}t + \frac{(V_o - V_{min})^2}{2|A_d|} + \frac{(V_f - V_{min})^2}{2A_a}$$

$$= 29.6 \text{ km } (18.4 \text{ miles})$$

Since L is greater than L_{min}, path stretching is not necessary.

Two further comparison tests establish a three-segment profile pattern of deceleration/constant speed/deceleration. At node ⚠5 , the speed for the

constant-speed segment is computed by solving for V_n in equation (43):

$$V_n = 86 \text{ m/sec (167 knots)}$$

Finally, the values of t_1 and t_2, the time instants corresponding to a change from deceleration to constant speed and from constant speed back to deceleration, are computed by substituting numerical values into equations (44) and (45):

$$t_1 = \left| \frac{V_o - V_n}{A_d} \right| = 103.6 \text{ sec}$$

$$t_2 = t - \left| \frac{V_n - V_f}{A_d} \right| = 360 - 31.4 = 328.6 \text{ sec}$$

This concludes the synthesis of the speed profile.

Vertical Guidance

The time duration, Δt_h, required to descend from a cruising altitude of 1520 m (5000 ft) to a final altitude of 456 m (1500 ft) at a sink rate of 305 m/min (1000 ft/min) is

$$\Delta t_h \frac{1520 - 456}{305} = 3.5 \text{ min} = 210 \text{ sec}$$

Since the aircraft is permitted to descend only when the speed is constant, it must descend within the time interval

$$[t_1, t_2] = [103.6, 328.6]$$

Since this time interval (226.3 sec) is greater than Δt_h, the aircraft can descend at constant speed. Since the aircraft is also required to maintain cruise altitude as long as possible, the altitude change will take place during the last portion of the constant-speed time interval, from $t_1 = t_2 - \Delta t_h = 118.6$ sec to t_2.

Overall Command Profile

The overall command profile expresses the horizontal guidance, controlled time of arrival, and altitude profile in a time sequence. The time for termination of the first left turn, t_{P1}, determined by the time required to traverse the arc length $\overset{\frown}{P_o P_1}$:

$$\overset{\frown}{P_o P_1} = \int_o^{t_{P1}} (V_o + A_d t)dt = V_o t_{P1} + \frac{A_d}{2} t_{P1}^2$$

(An additional equation is required if A_d is zero over a segment of the turn.) Substituting the known numerical values into this equation gives the value of 90.53 seconds for t_{P_1}.

The time for initiation of the second left turn, t_{P_2}, is computed next. The distance traversed while the aircraft is decelerating from V_n to V_f, ℓ_{s_2}, is the area under the last segment of the speed profile curve:

$$\ell_{s_2} = V_f(t_f - t_2) + \frac{1}{2}(t_f - t_2)(V_n - V_f)$$

Substituting the known constants gives a value of 2.4 km (1.49 miles) for ℓ_{s_2}. Comparing the numerical value of ℓ_{s_2} with the arc length $\overset{\frown}{P_2P_f}$ = 13.25 km (8.24 miles) shows that t_{P_2} occurs in the arc $\overset{\frown}{P_2P_f}$. Then t_{P_2} is computed by subtracting the time to fly the constant-speed segment of the arc $\overset{\frown}{P_2P_f}$ from t_2:

$$t_{P_2} = t_2 - \frac{\overset{\frown}{P_2P_f} - \ell_{s_2}}{V_n}$$

$$= 202.23 \text{ seconds}$$

A complete command profile can now be constructed from a time history of the three profiles. Figure 24 is a complete profile of the overall trajectory. Figure 25 is the corresponding horizontal trajectory with points P_o, P_1, P_2, P_3, P_4, P_5, and P_f marked to indicate the beginning or termination of commands and the times at which they occur. Table 7 summarizes the entire command sequence. If a ground-based computer performs the trajectory synthesis, table 7 gives the essential information the on-board guidance system must receive to fly the trajectory.

CONCLUSIONS

The technique developed in this report for automating terminal-area guidance, when properly implemented, enables an aircraft to fly from a given initial position, altitude, heading, and airspeed to a specified final position, altitude, heading, and airspeed in a prescribed time. The technique is based on the formulation of a class of principal subproblems in terms of which any flight profile can be expressed from takeoff to landing. The required subproblems are established by a study of air-traffic control procedures, instrument-flight maneuvers, and terminal-area route structures. They are:

(1) Horizontal guidance: (a) Guiding an aircraft from any initial position and heading to a specified final position and heading, (b) guiding an aircraft from any initial position and heading onto a straight line of specified location and heading, (c) guiding an aircraft from any initial position

and heading to a specified final position, and (d) guiding an aircraft smoothly from one straight line onto another intersecting straight line.

(2) Controlled time of arrival: Guiding an aircraft (along the preselected horizontal trajectory) from an initial airspeed to a specified final speed in a specified time interval.

(3) Vertical guidance: Guiding an aircraft (along the preselected horizontal trajectory and speed profile) from an initial altitude to a specified final altitude.

The criterion used for selection of the horizontal trajectory is to minimize the total path length subject to the constraint imposed by a minimum turning radius. The horizontal trajectory consists of arcs of circles and segments of straight lines which form a confluent path connecting the initial and final points. It is synthesized in two steps: First, a flight pattern is assigned, then arc lengths and straight-line distances are computed to specify the horizontal trajectory completely.

For the speed-profile synthesis, the horizontal distance determined already is compared with the maximum and minimum distances the aircraft can traverse (for the specified initial speed, final speed, time of arrival, maximum and minimum allowable speed, and acceleration and deceleration capability). If the horizontal path length is greater than the maximum distance, no speed profile is possible. If it is between the minimum and maximum distance, speed variation alone can control time of arrival. If it is below the minimum distance, path stretching of the horizontal trajectory is necessary, and the controlled time of arrival is achieved by a combination of speed control and path stretching.

When the horizontal trajectory and the speed profile are determined, the vertical guidance trajectory is synthesized. The criterion for this synthesis is maintaining cruise altitude as long as possible consistent with the specified descent rate and with the required final altitude.

A composite command profile is generated by superimposing the already determined horizontal, speed, and vertical profiles. Essentially, this command profile is a time history of commands (such as decelerate, turn left, and descend) to be issued at the proper time. This profile can provide automatic guidance of an aircraft for transitioning from any initial state to any specified final state, where a state is specified by the aircraft coordinates, altitude, speed, heading, and the clock time.

In general, the overall flight profile of an aircraft, starting from takeoff to landing, may be decomposed into a sequence of waypoints. The flight profile for each pair of adjacent waypoints can readily be synthesized by applying the various guidance problems discussed. Therefore, the overall flight profile, starting from takeoff to landing, may be synthesized by concatenation of flight profiles for consecutive pairs of waypoints.

The advantage of this technique lies in its versatility and efficiency. It requires no precomputation of trajectories, and can provide fast, in-flight changes in trajectory as required. Since the only aircraft parameters used in synthesizing the trajectories are performance limitations, the technique is applicable to any aircraft. Finally, by synthesizing trajectories subject only to aircraft performance limitations and ATC constraints, the technique uses airspace efficiently and therefore makes possible reduction of separation requirements and thus achieves higher landing rates.

Ames Research Center
National Aeronautics and Space Administration
Moffett Field, Calif., 94035, February 11, 1972

APPENDIX

COMPUTATION OF PATH LENGTH FOR STRETCHED PATH

For the coordinate system used to compute the stretched-path length, the origin is at the center of circle C_1 and the positive x-axis is in the direction of $\vec{n}_o$; the unit of distance is the turning radius. For the nondegenerate pattern in figure 26, the parameter is y_{C_3} and the total length of the stretched path is

$$L_s = \overset{\frown}{P_oP_1} + \overline{P_1P_2} + \overset{\frown}{P_2P_3} + \overline{P_3P_4} + \overset{\frown}{P_4P_f} \tag{A1}$$

where

$$\overset{\frown}{P_oP_1} = \frac{\pi}{2} \tag{A2}$$

$$\overline{P_1P_2} = y_{C_3} \tag{A3}$$

$$\overset{\frown}{P_2P_3} = \frac{\pi}{2} + \lambda \tag{A4}$$

$$\overline{P_3P_4} = \sqrt{y_{C_3}^2 + (L_o - 2)^2 - 4} \tag{A5}$$

$$\overset{\frown}{P_4P_f} = \lambda \tag{A6}$$

The angle λ is given by

$$\lambda = \pi - \tan^{-1}\frac{L_o - 2}{y_{C_3}} - \cos^{-1}\frac{2}{\sqrt{y_{C_3}^2 + (L_o - 2)^2}} \tag{A7}$$

Equations (A5) and (A7) are derived by solving for parts of right triangles $P_5C_3C_2$ and $C_3P_3P_c$. By adding expressions (A2) through (A6) we obtain the expression for the total path length.

$$L_s = 3\pi + y_{C_3} - 2\tan^{-1}\frac{L_o-2}{y_{C_3}} - 2\cos^{-1}\frac{2}{\sqrt{y_{C_3}^2 + (L_o-2)^2}} + \sqrt{y_{C_3}^2 + (L_o-2)^2 - 4} \tag{A8}$$

For the degenerate pattern in figure 27, the parameter is θ_s and the total path length is

$$L_s = \overset{\frown}{P_oP_1} + \overset{\frown}{P_1P_3} + \overset{\frown}{P_3P_4} + \overset{\frown}{P_4P_f} \tag{A9}$$

where

$$\overset{\frown}{P_oP_1} = \theta_s \tag{A10}$$

$$\overset{\frown}{P_1P_3} = \theta_s + \lambda \tag{A11}$$

$$\overset{\frown}{P_3P_4} = \sqrt{4 \cos^2 \theta_s + (L_o - 2 \sin \theta_s)^2 - 4} \tag{A12}$$

$$\overset{\frown}{P_4P_f} = \lambda \tag{A13}$$

Solving for parts of right triangles $C_3P_5C_2$ and $C_3P_3P_c$,

$$\lambda = \tan^{-1} \frac{L_o - 2 \sin \theta_s}{2 \cos \theta_s} - \cos^{-1} \frac{2}{\sqrt{(L_o - 2 \sin \theta_s)^2 + \psi \cos \theta_s^2}} \tag{A14}$$

The total path length can then be written in terms of λ by adding (A10) through (A13):

$$L_s = 2\theta_s + 2\lambda + \sqrt{4 \cos^2 \theta_s + (L_o - 2 \sin \theta_s)^2 - 4} \tag{A15}$$

REFERENCES

1. Petrie, David M.: Automatic Flight Management of Future High-Performance Aircraft. J. Aircraft, vol. 5, no. 4, July-Aug. 1968, pp. 335-343.

2. Cook, W. H.; and Clifford, D. R.: Evolution of Automatic Flight Control. AIAA Aircraft Design for 1980 Operations Meeting, Washington, D. C., Feb. 12-14, 1968.

3. Sawyer, R. H.; McLaughlin, M. D.; and Silsby, N. S.: Simulation Studies of the Supersonic Transport in the Present-Day Air Traffic Control System. NASA TN D-4638, 1968.

4. Jackson, A. S.: A Computer Simulation Study of Five Automatic Air Traffic Control Concepts. Milgo Electronics Corp., Miami, Florida.

5. Simpson, R. W.: Analytical Methods of Research into Terminal Area Air Traffic Operations. J. Aircraft, vol. 2, no. 3, May-June 1965, pp. 185-193.

6. O'Brien, J. P.: Automating Terminal Air Traffic Control. J. ATC, Jan. 1970, pp. 15-21.

7. Ottoson, H. I.: Sensitivity of a Terminal Area Control Concept to Uncertainties in Control Information. Report of Department of Transportation Air Traffic Control Advisory Committee, vol. 2, Dec. 1969, pp. 95-104.

8. Porter, L. W.: On Optimal Scheduling and Holding Strategies for the Air Traffic Control Problem. M.S. Thesis, Massachusetts Institute of Technology, Sept. 1969.

9. Erzberger, H.; and Lee, H. Q.: Optimum Horizontal Guidance Techniques for Aircraft. J. Aircraft, vol. 8, no. 2, Feb. 1971, pp. 95-101.

TABLE 1.- SUMMARY OF TERMINAL-AREA GUIDANCE PROBLEMS

Class	Brief title	Description	Operational constraints	Preferred synthesis criterion
Horizontal guidance	Problem (a)	Fly from any initial position & heading to a specified final position & heading	Maximum bank angle	Minimum path length to achieve final position & heading
	Problem (b)	Fly from any initial position & heading onto a line of specified location & direction	Maximum bank angle	Minimum path length to achieve final line
	Problem (c)	Fly from any initial position & heading to a specified final position with arbitrary final heading	Maximum bank angle	Minimum path length to achieve final point
	Problem (d)	Transition between intersecting straight lines	Maximum bank angle	Smooth transition, minimum overshoot
	Path stretching	Increase length of flight path by a specified amount	Maximum bank angle	Unknown
Speed control	Controlled time of arrival	Determine speed profile to achieve specified arrival time at a specified location with specified final speed	Minimum & maximum speed & maximum acceleration & deceleration	Simplicity of speed profile
Vertical guidance	Descent from cruise	Determine flight path in vertical plane to achieve a specified final altitude at a specified position	Maximum descent rate	Maintain cruise altitude as long as possible & descend at constant $\dot{h}$

TABLE 2.- OPTIMAL FLIGHT PATTERNS FOR MINIMUM-ARC-LENGTH HORIZONTAL GUIDANCE

Patterns used in simplified solution		Additional patterns required for optimum solution (ref. 9) (not used)	
Maneuvers*	Geometric shape	Maneuvers*	Geometric shape
L S L	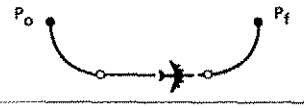	L R L	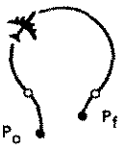
R S R		R L R	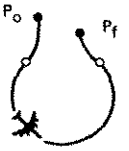
L S R	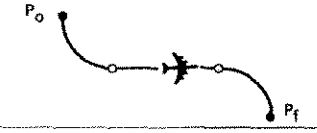		
R S L			
L S	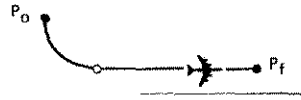		
R S			
S L	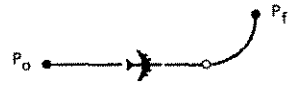		
S R			
L R			
R L			
L			
R	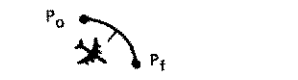		
S			
	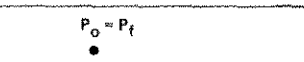		

*Significance of symbols in column as follows:

L – left turn
S – straight flight
R – right turn
P_o – initial position
P_f – final position

TABLE 3.- ANALYTICAL EQUATIONS FOR COMPUTING SWITCHING POINTS

Type of switching points	Equation	Domain
Switching point on d_o axis	$d_{o\bar{\sigma}} = -\tan(\psi/2)$	$0 < \psi < \pi$
	$d_{o\sigma}^{+} = \tan(\psi/2)$	$0 < \psi < \pi$
	$d_{o\beta} = -\dfrac{1}{\tan(\psi/2)}$	$0 < \psi < \pi$
	$d_{o\bar{\alpha}} = -\left(\dfrac{3}{\sin\psi} + \dfrac{1}{\tan\psi}\right)$	$0 < \psi < \pi$
	$d_{o\alpha}^{+} = \left(\dfrac{3}{\sin\psi} + \dfrac{1}{\tan\psi}\right)$	$0 < \psi < \pi$
	$d_{o\delta} = -\tan(\psi/2)\cos\psi - \sin\psi - \sqrt{4-(1+\cos\psi-\tan(\psi/2)\sin\psi)^2}$	$0 < \psi < \pi$
Switching point on d_f axis	$d_{f\bar{\sigma}} = -\tan(\psi/2)$	$0 < \psi < \pi$
	$d_{f\sigma}^{+} = \tan(\psi/2)$	$0 < \psi < \pi$
	$d_{f\bar{\gamma}} = d_o\cos\psi - \sin\psi - \sqrt{4-(d_o\sin\psi+\cos\psi+1)^2}$	$0 < \psi < \pi,\ d_{o\bar{\alpha}} \le d_o \le d_{o\beta}$
	$d_{f\gamma}^{+} = \begin{cases} d_o\cos\psi+\sin\psi+\sqrt{4-(-d_o\sin\psi+\cos\psi+1)^2} \\ \dfrac{3}{\tan\psi}+\dfrac{1}{\sin\psi} \end{cases}$	$\begin{cases} 0 < \psi < \pi,\ d_{o\bar{\sigma}} \le d_o \le d_{o\alpha}^{+} \\ 0 < \psi < \pi,\ d_o > d_{o\alpha}^{+} \end{cases}$
	$d_{f\bar{\delta}} = d_o\cos\psi+\sin\psi - \sqrt{4-(-d_o\sin\psi+\cos\psi+1)^2}$	$0 < \psi < \pi,\ d_{o\bar{\sigma}} \le d_o \le d_{o\sigma}^{+}$
	$d_{f\delta}^{+} = d_o\cos\psi-\sin\psi + \sqrt{4-(d_o\sin\psi+\cos\psi+1)^2}$	$0 < \psi < \pi,\ d_{o\bar{\alpha}} \le d_o \le d_{o\bar{\sigma}}$

TABLE 4.- TRAJECTORY PARAMETER FORMULAS FOR PROBLEM (a)

Pattern type	$\overline{P_1P_2}$, Length of straight-line segment	ψ_s, Heading of straight-line segment	ψ_i, Heading change in initial turn	ψ_f, Heading change in final turn
RSR	$\sqrt{(x-R\sin\psi)^2+(R-R\cos\psi-y)^2}$	$\arctan\dfrac{R-R\cos\psi-v}{-x+R\sin\psi}$	$\psi_i=\begin{cases}\psi_s-\psi;\psi_s>\psi\\ \psi_s+2\pi-\psi;\psi_s<\psi\end{cases}$	$\psi_f=\begin{cases}2\pi-\psi_s;\psi_s>0\\ 0;\psi_s=0\end{cases}$
RSL	$\dfrac{2R}{\tan\psi'}$ where $\psi'=\arcsin\dfrac{2R}{\sqrt{(-x+R\sin\psi)^2+(R+R\cos\psi+y)^2}}$	$\psi_s=\begin{cases}\psi_1+\psi';\psi_1+\psi'<2\pi\\ \psi_1+\psi'-2\pi;\psi_1+\psi'\geq 2\pi\end{cases}$ where $\psi_1=\arctan\dfrac{-R-R\cos\psi-y}{-x+R\sin\psi}$	$\psi_i=\begin{cases}\psi_s-\psi;\ \psi_s\geq\psi\\ \psi_s+2\pi-\psi;\psi_s<\psi\end{cases}$	$\psi_f=\psi_s$
LSL	$\sqrt{(x+R\sin\psi)^2+(R-R\cos\psi+y)^2}$	$\arctan\dfrac{-R+R\cos\psi-y}{-x-R\sin\psi}$	$\psi_i=\begin{cases}\psi-\psi_s;\ \psi\geq\psi_s\\ \psi-\psi_s+2\pi;\psi<\psi_3\end{cases}$	$\psi_f=\psi_s$
LSR	$\dfrac{2R}{\tan\psi'}$ where $\psi'=\arcsin\dfrac{2R}{\sqrt{(x+R\sin\psi)^2+(R+R\cos\psi-y)^2}}$	$\psi_s=\begin{cases}\psi_1-\psi';\ \psi_1-\psi'>0\\ \psi_1-\psi+2\pi;\psi_1-\psi'<0\end{cases}$ where $\psi_1=\arctan\dfrac{R+R\cos\psi-y}{-x-R\sin\psi}$	$\psi_i=\begin{cases}\psi-\psi_s;\ \psi\geq\psi_s\\ \psi-\psi_s+2\pi;\psi<\psi_s\end{cases}$	$\psi_f=\begin{cases}2\pi-\psi_s;\psi_s>0\\ 0;\ \psi_s=0\end{cases}$

TABLE 5.- TRAJECTORY CONSTANTS FOR PROBLEM (b)

Pattern type	Specification of region	Trajectory constants	Range of turning angles
LSL	$-\pi < \psi < -\pi/2$ $d \le S_3(\psi)$	$\psi_i = 3\pi/2 + \psi$ $\psi_f = \pi/2$ $\ell = -d - 1 + \cos\psi$	$0 \le \psi_i \le \pi$ $\psi_f = \pi/2$
	$\pi/2 \le \psi \le \pi$ $d \le S_3(\psi)$	$\psi_i = \psi - \pi/2$ $\psi_f = \pi/2$ $\ell = -d - 1 + \cos\psi$	
LSR	$-\pi/2 \le \psi \le \pi/2$ $d \ge S_2(\psi)$	$\psi_i = \psi + \pi/2$ $\psi_f = \pi/2$ $\ell = d - 1 - \cos\psi$	$0 \le \psi_i \le \pi$ $\psi_f = \pi/2$
LR	$\pi/2 < \psi \le \pi; S_2(\psi) < d \le S_1(\psi)$	$\psi_i = -\cos^{-1}\left(\frac{1 + \cos\psi - d}{2}\right) + \psi$	$0 \le \psi_i \le \pi/2$
		$\psi_f = -\cos^{-1}\left(\frac{1 + \cos\psi - d}{2}\right) + 2\pi$	$\pi \le \psi_f < 3\pi/2$
	$0 \le \psi \le \pi; S_3(\psi) \le d \le S_2(\psi)$ or $-\pi/2 \le \psi \le 0; S_1(\psi) \le d \le S_2(\psi)$	$\psi_i = \cos^{-1}\left(\frac{1 + \cos\psi - d}{2}\right) + \psi$	$0 \le \psi_i \le 3\pi/2$
		$\psi_f = \cos^{-1}\left(\frac{1 + \cos\psi - d}{2}\right)$	$0 \le \psi_f \le \pi/2$

TABLE 6.- TRAJECTORY CONSTANTS FOR PROBLEM (c)

Pattern type	Specification of region	Trajectory constants
RS	$y > 0$ and $x^2 + (y-1)^2 \geq 1$	$\psi_i = \pi - \tan^{-1}\frac{x}{y-1} - \cos^{-1}\frac{1}{\sqrt{x^2 + (y-1)^2}}$ $\ell = \sqrt{x^2 + (y-1)^2 - 1}$
LR	$y > 0$ and $x^2 + (y-1)^2 < 1$	$\psi_i = \tan^{-1}\frac{x}{y+1} + \cos^{-1}\frac{3 + x^2 + (y+1)^2}{4\sqrt{x^2 + (y+1)^2}}$ $\psi_f = 2\pi - \cos^{-1}\frac{5 - x^2 - (y+1)^2}{4}$

TABLE 7.- OVERALL COMMAND PROFILE

Point	Time, second	Polar coordinates*	Commands
P_o	0	21.8 (13.56), 292	Begin left turn and begin deceleration
P_1	90.5	18 (11.18), 266	Fly straight
P_2	103.6	17.2 (10.58), 263	Hold speed
P_3	118.6	15.95 (9.9), 261	Begin descent
P_4	202.2	11.3 (6.85), 239	Begin left turn
P_5	328.6	2.38 (1.48), 191	Hold altitude and begin deceleration
P_f	360	0 0 0	Fly straight and hold speed

*Distances in km (miles), angles in degrees

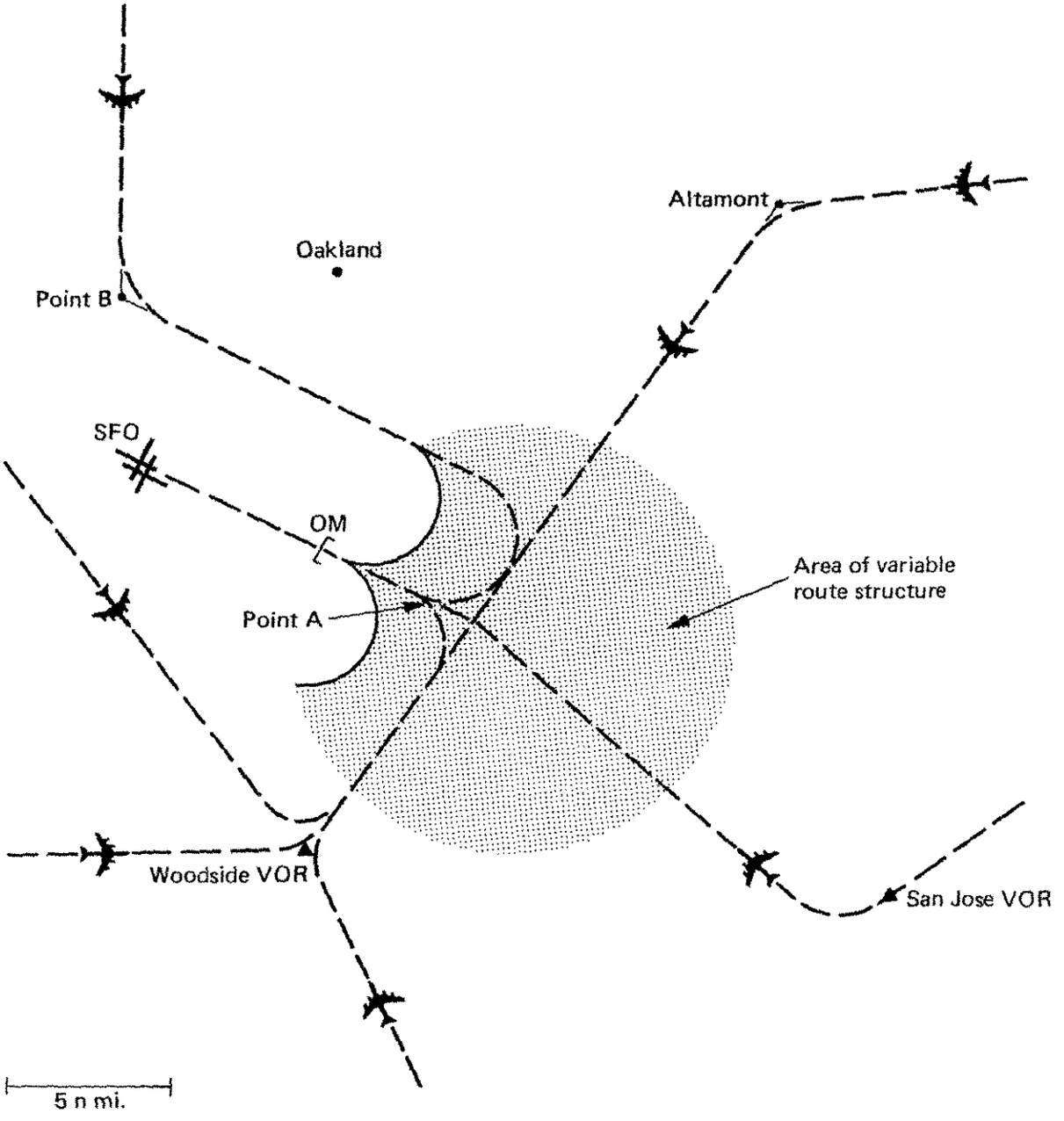

Figure 1.- SFO terminal-area approach routes.

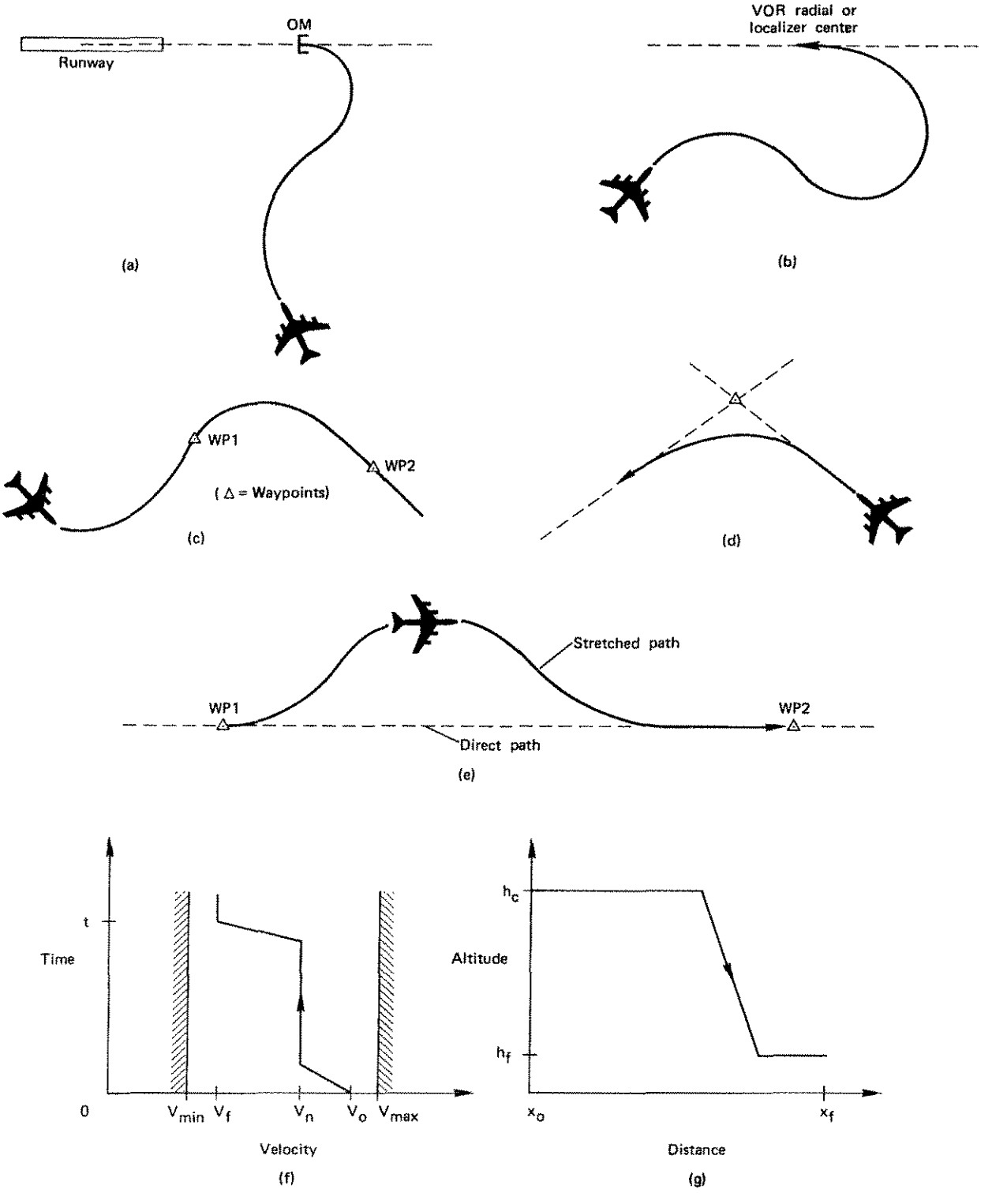

Figure 2.- Terminal-area guidance problems.

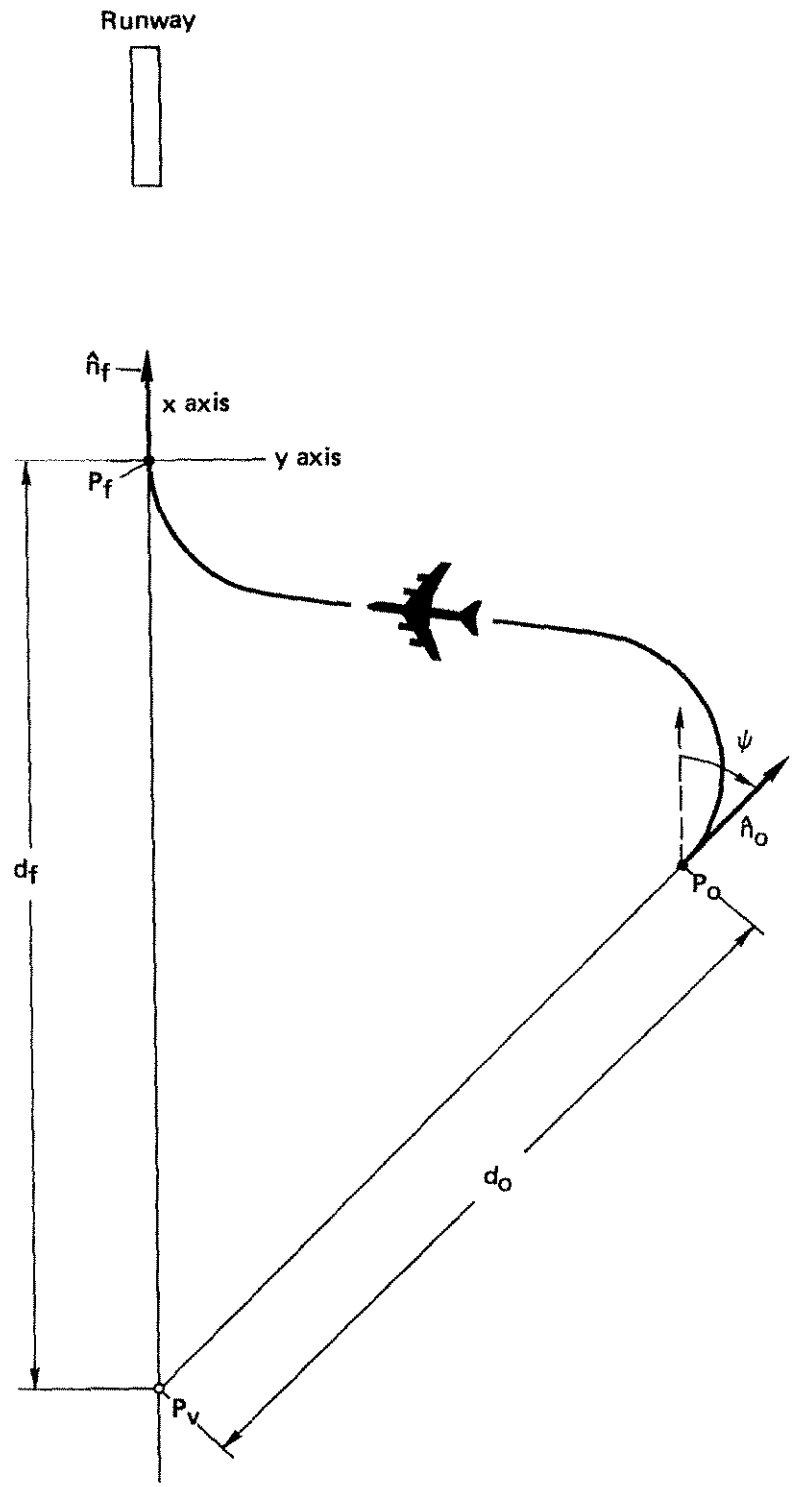

Figure 3.- Pattern parameters and coordinate system for problem (a).

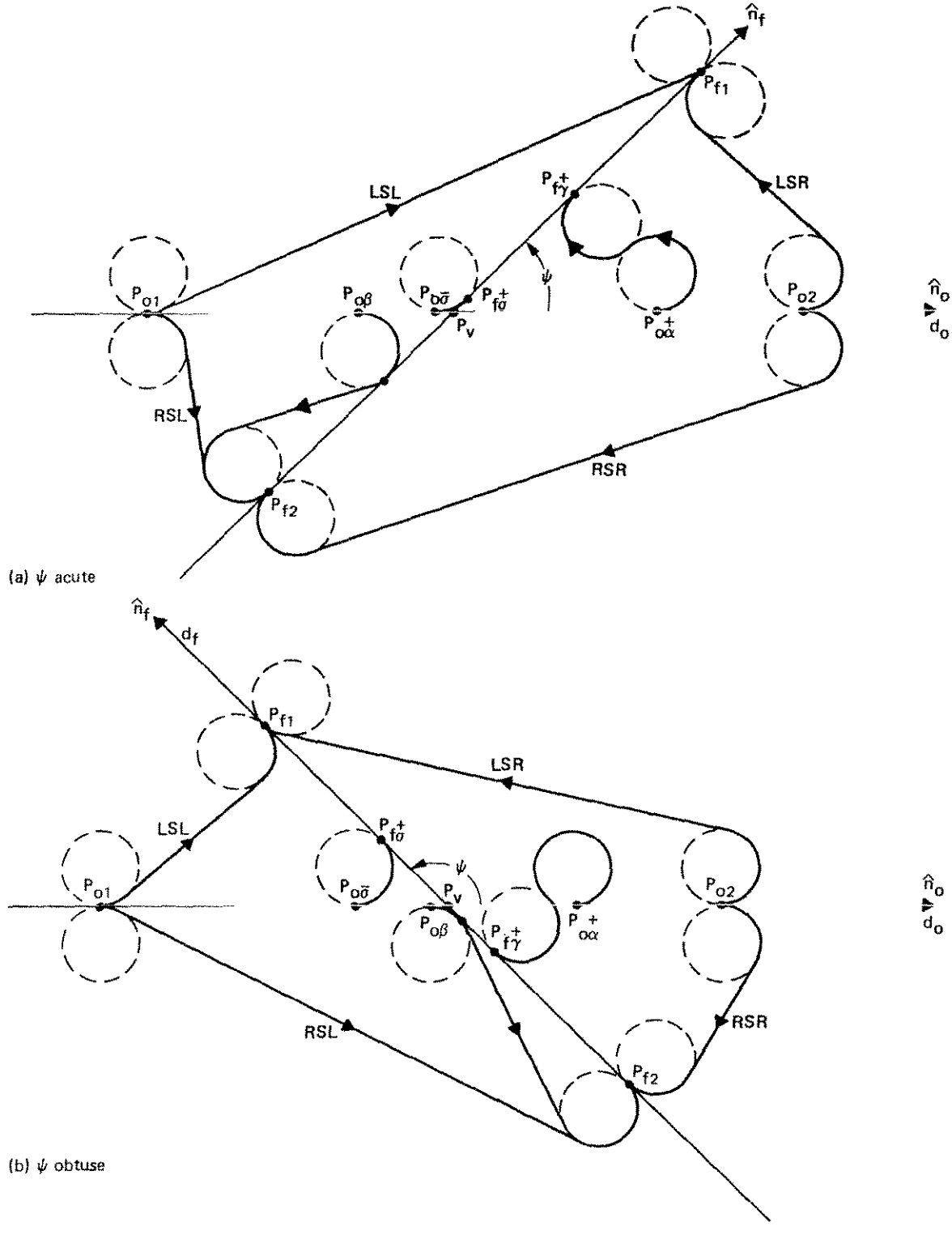

Figure 4.- Trajectories and switching points for normal maneuvers.

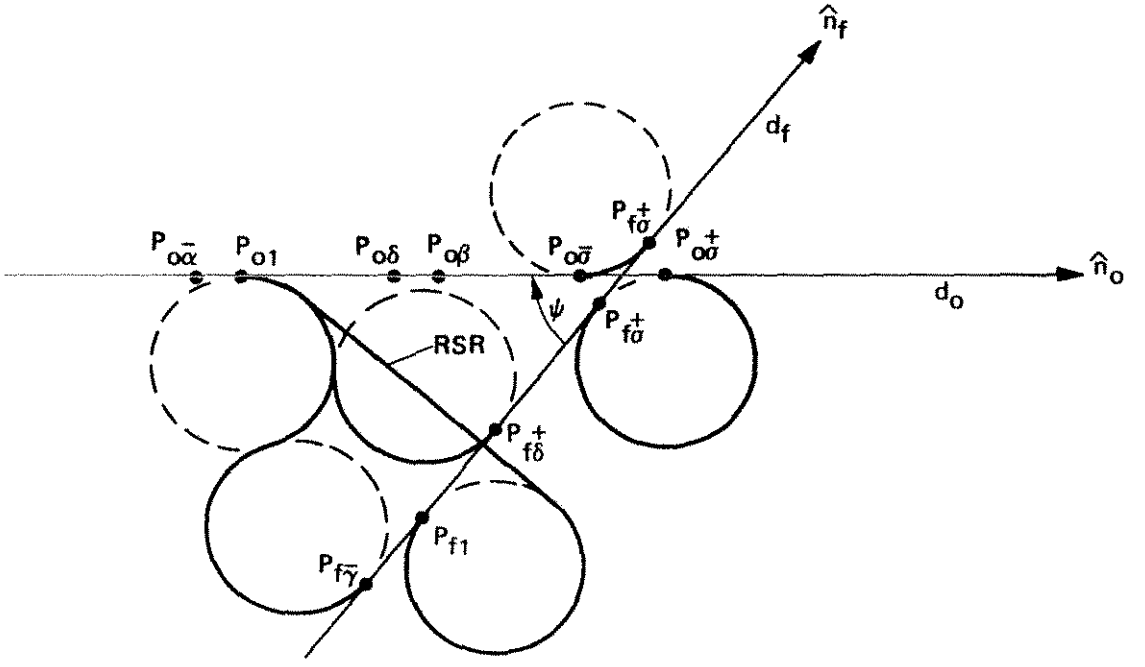

(a)

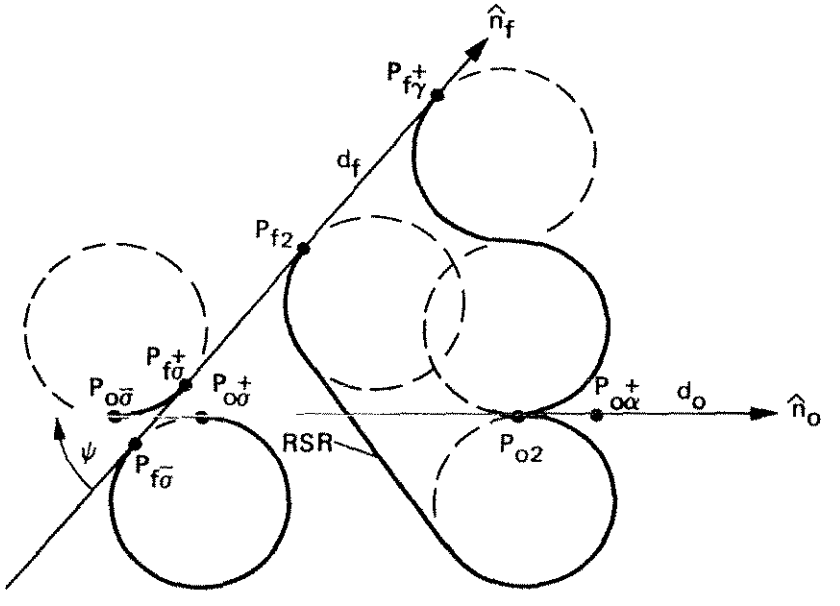

(b)

Figure 5.- Switching points for near distance maneuvers if P_o is not between $P_{o\bar{\sigma}}$ and $P_{o\sigma}^+$ and $P_{f\delta}^+$ lies below $P_{f\sigma}^+$.

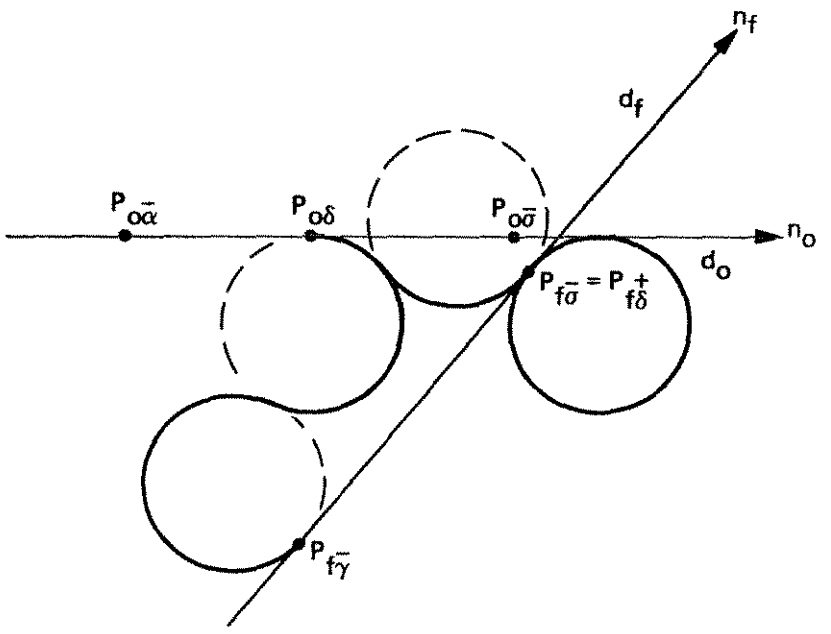

(c) Definition of $P_{o\delta}$ for $\psi \leq \pi/2$

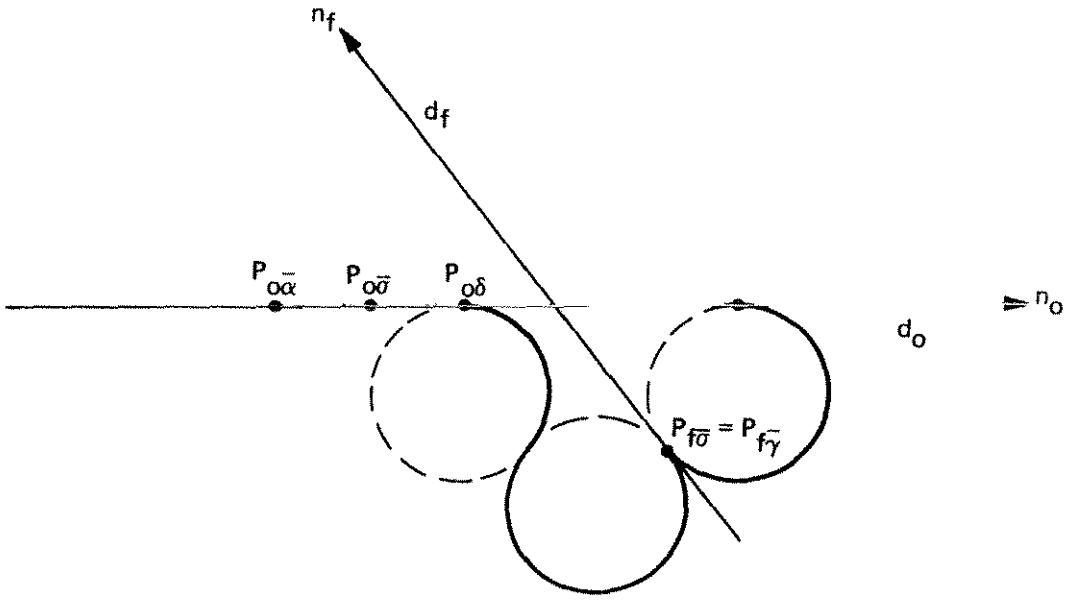

(d) Definition of $P_{o\delta}$ for $\psi \geq \pi/2$

Figure 5.- Concluded.

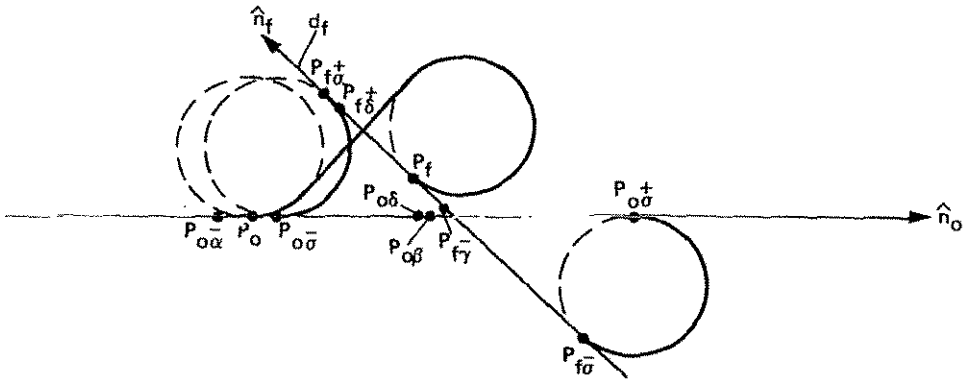

(a) P_o between $P_{o\bar{\alpha}}^{-}$ and $P_{o\bar{\sigma}}^{-}$; P_f between $P_{f\bar{\delta}}^{+}$ and $P_{f\bar{\gamma}}^{-}$ and above $P_{f\bar{\sigma}}^{-}$

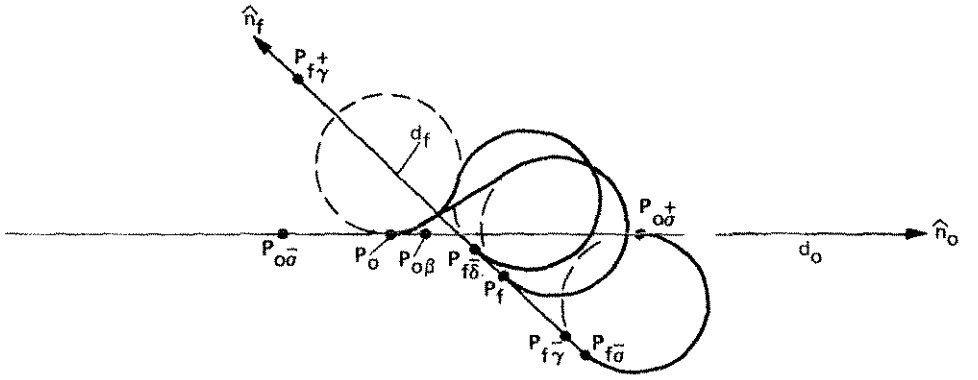

(b) P_o between $P_{o\bar{\sigma}}^{-}$ and $P_{o\bar{\sigma}}^{+}$; P_f between $P_{f\bar{\delta}}^{-}$ and $P_{f\bar{\gamma}}^{-}$ and above $P_{f\bar{\sigma}}^{-}$

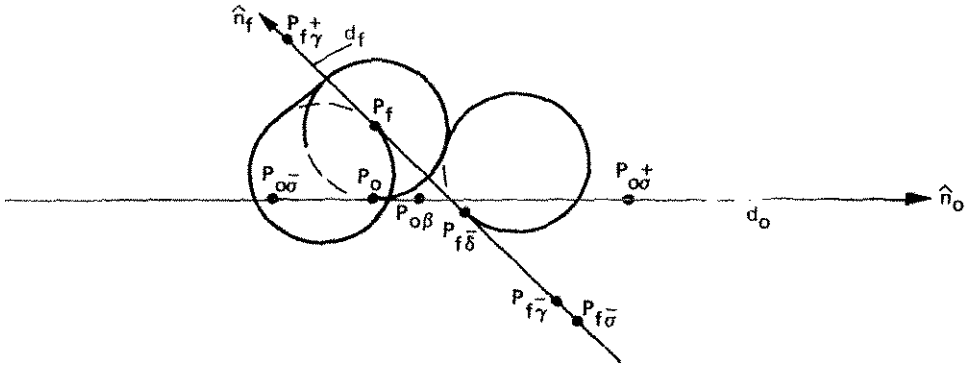

(c) P_o between $P_{o\bar{\sigma}}^{-}$ and $P_{o\bar{\sigma}}^{+}$; P_f between $P_{f\bar{\gamma}}^{+}$ and $P_{f\bar{\delta}}$

Figure 6.- Switching points and near distance trajectories if $P_{f\bar{\delta}}^{+}$ lies above $P_{f\bar{\sigma}}^{-}$ and P_f lies between $P_{f\bar{\sigma}}^{-}$ and $P_{f\bar{\gamma}}^{+}$.

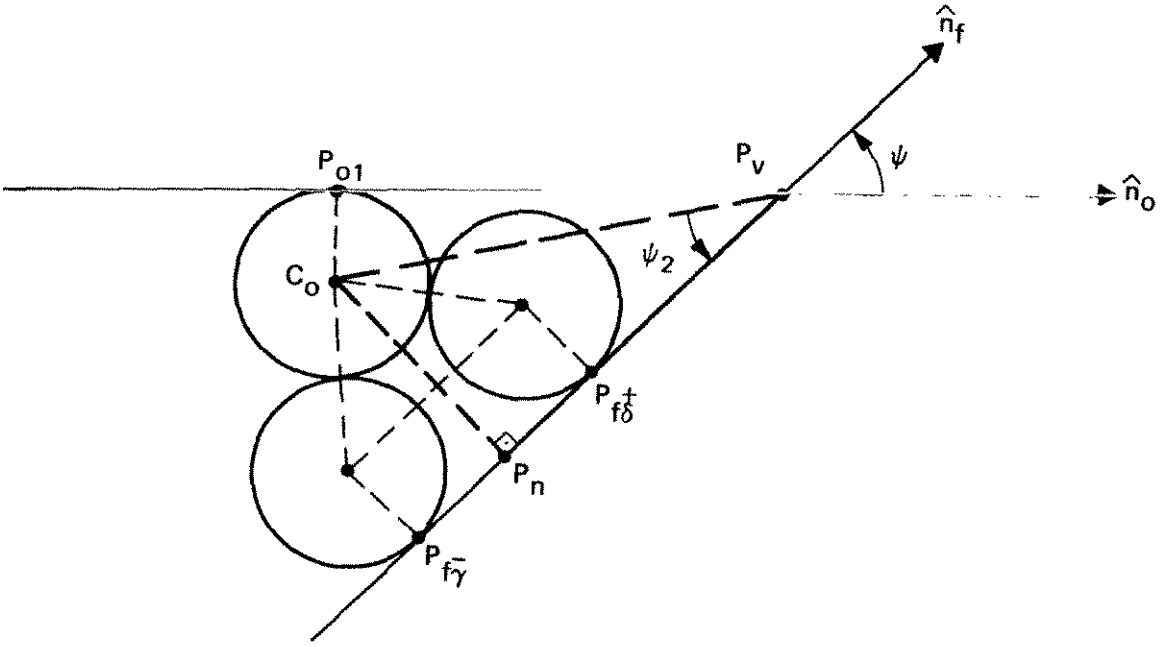

Figure 7.- Construction details for defining the locations of $P_{f\delta}^{+}$ and $P_{f\bar{\gamma}}$.

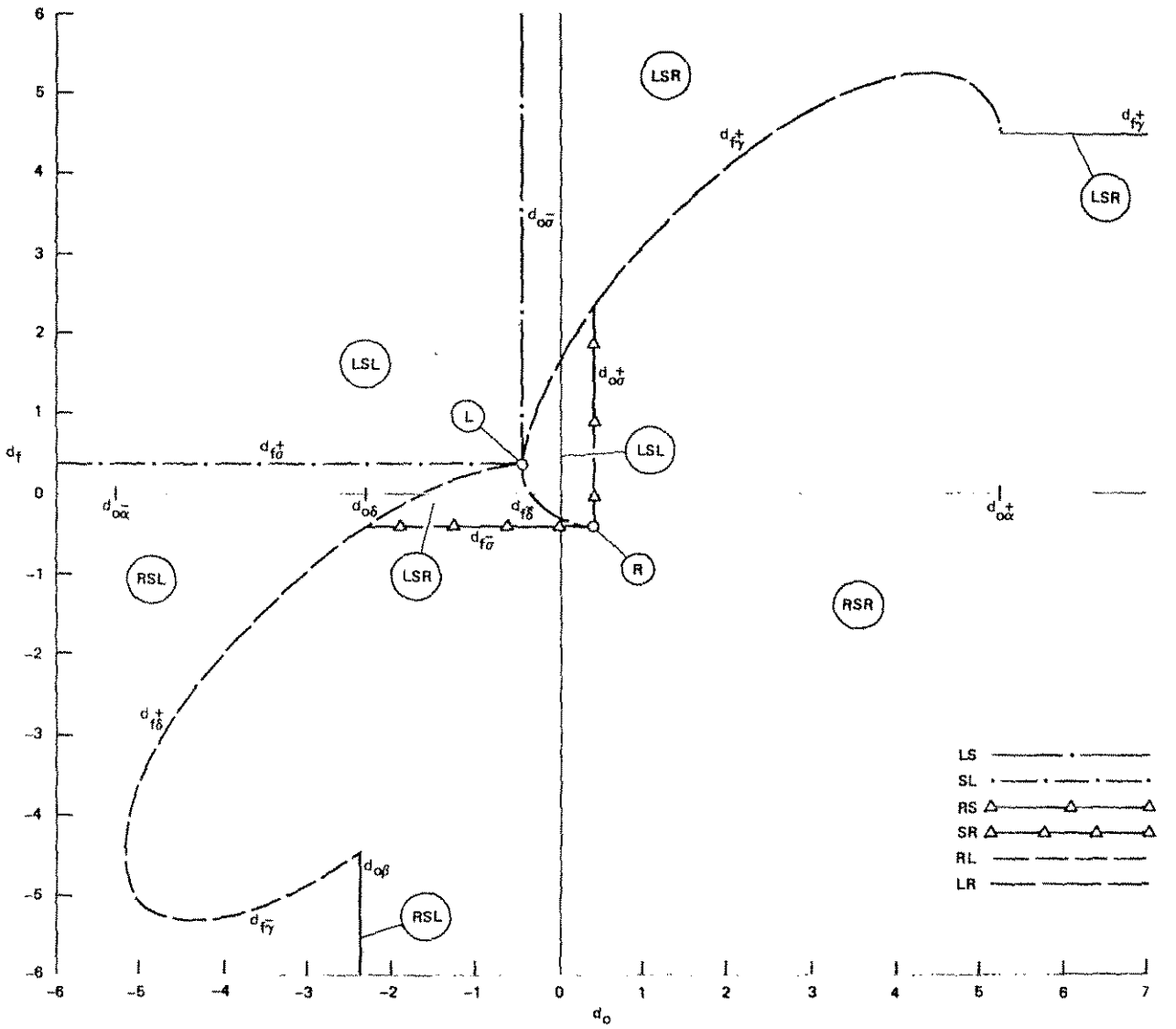

(a) $\psi = \pi/4$

Figure 8.- Switching diagram for $\psi = \pi/4$, $\psi = \pi/2$, and $\psi = 3\pi/4$ radians.

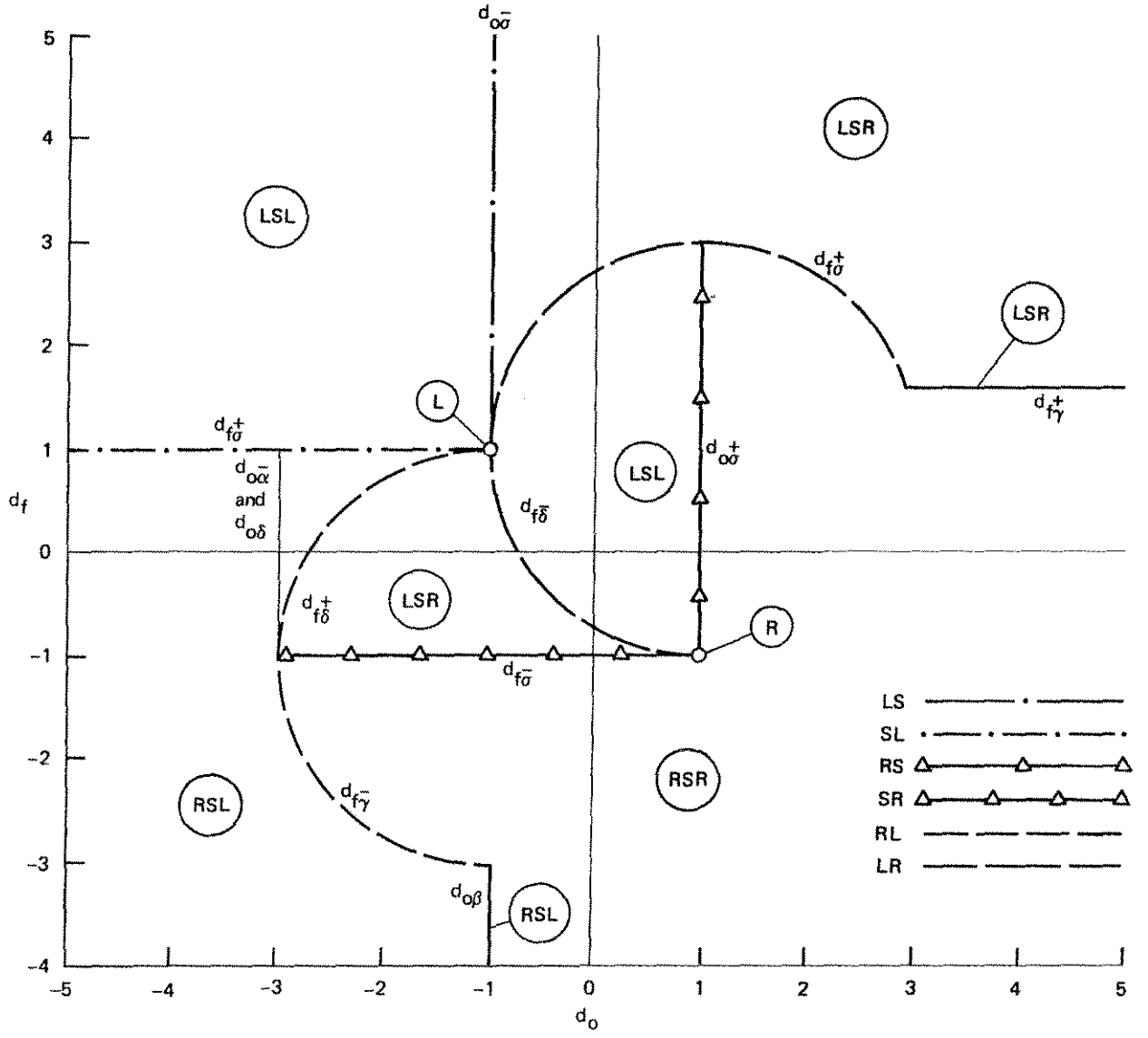

(b) $\psi = \pi/2$

Figure 8.- Continued.

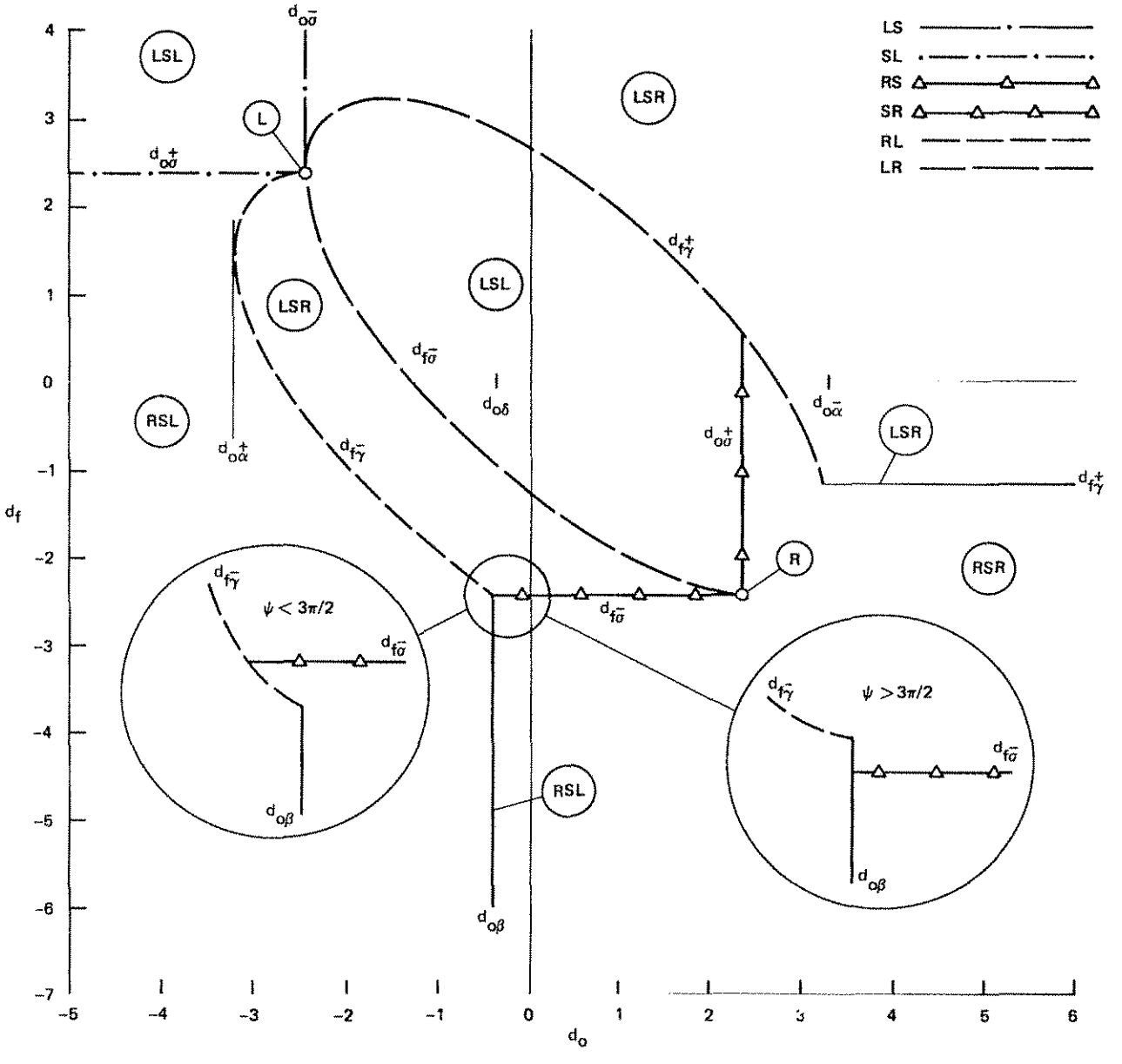

(c) $\psi = 3\pi/4$

Figure 8.- Concluded.

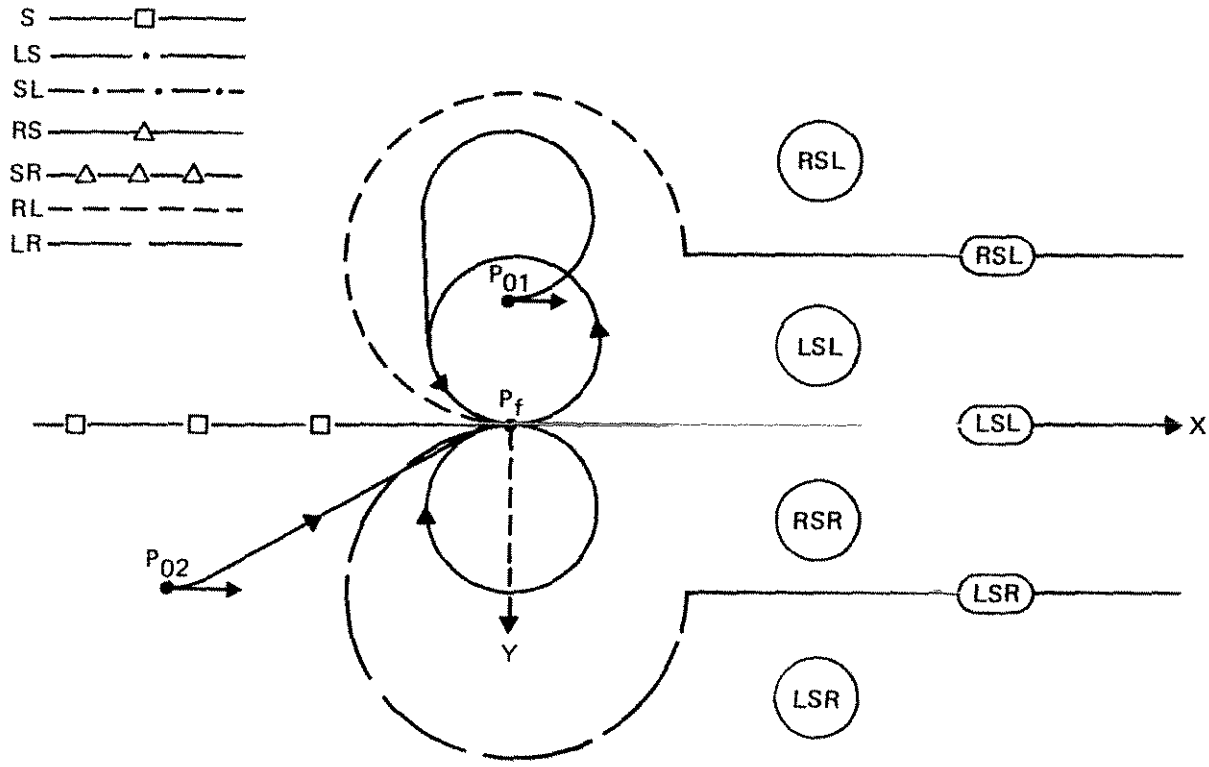

(a) $\psi = 0°$

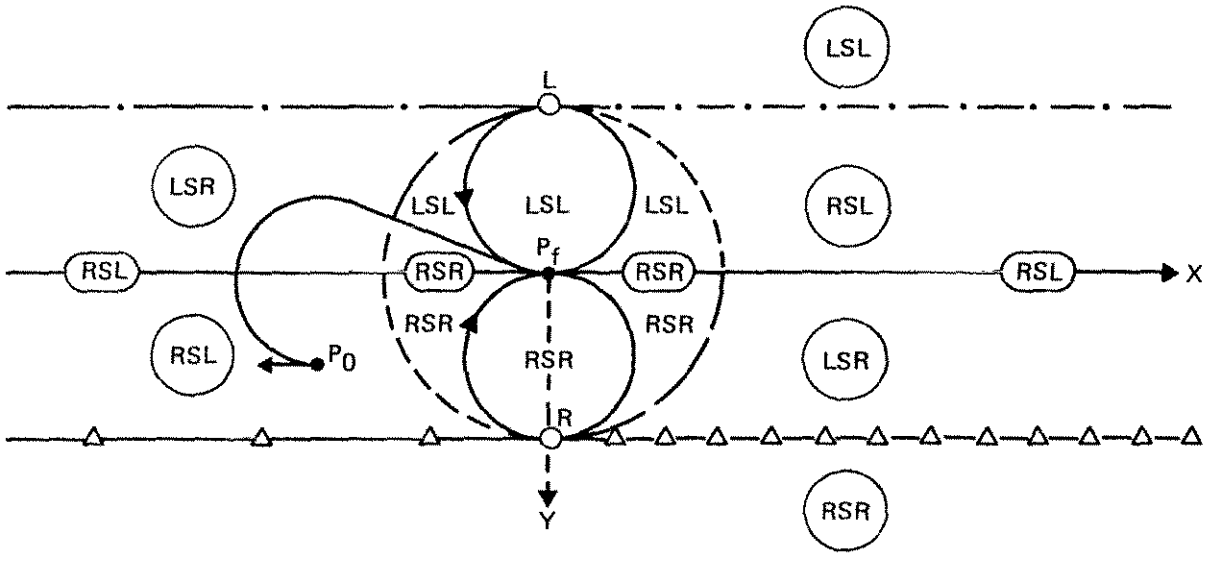

(b) $\psi = \pi$

Figure 9.- Switching diagrams for $\psi = 0°$ and $\psi = \pi$ radians.

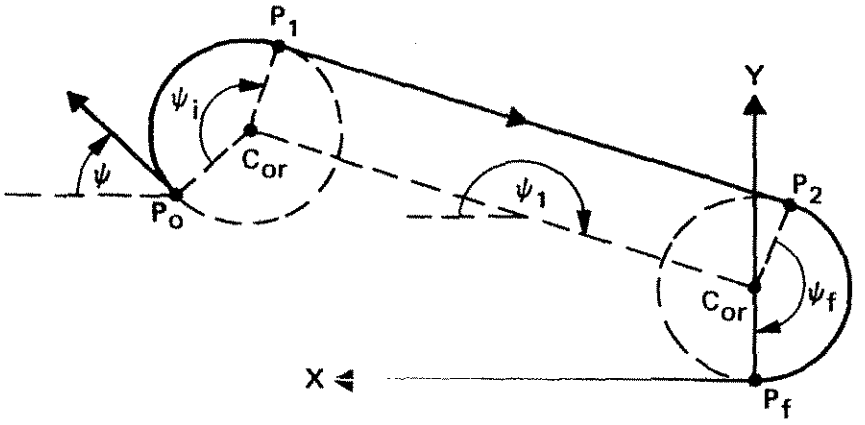

(a) RSR trajectory

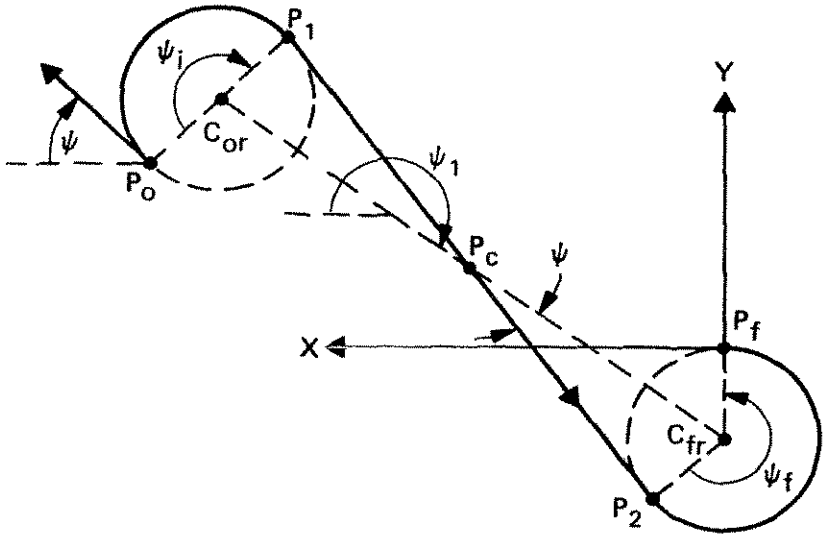

(b) RSL trajectory

Figure 10.- Construction for calculating path length and heading changes of trajectories.

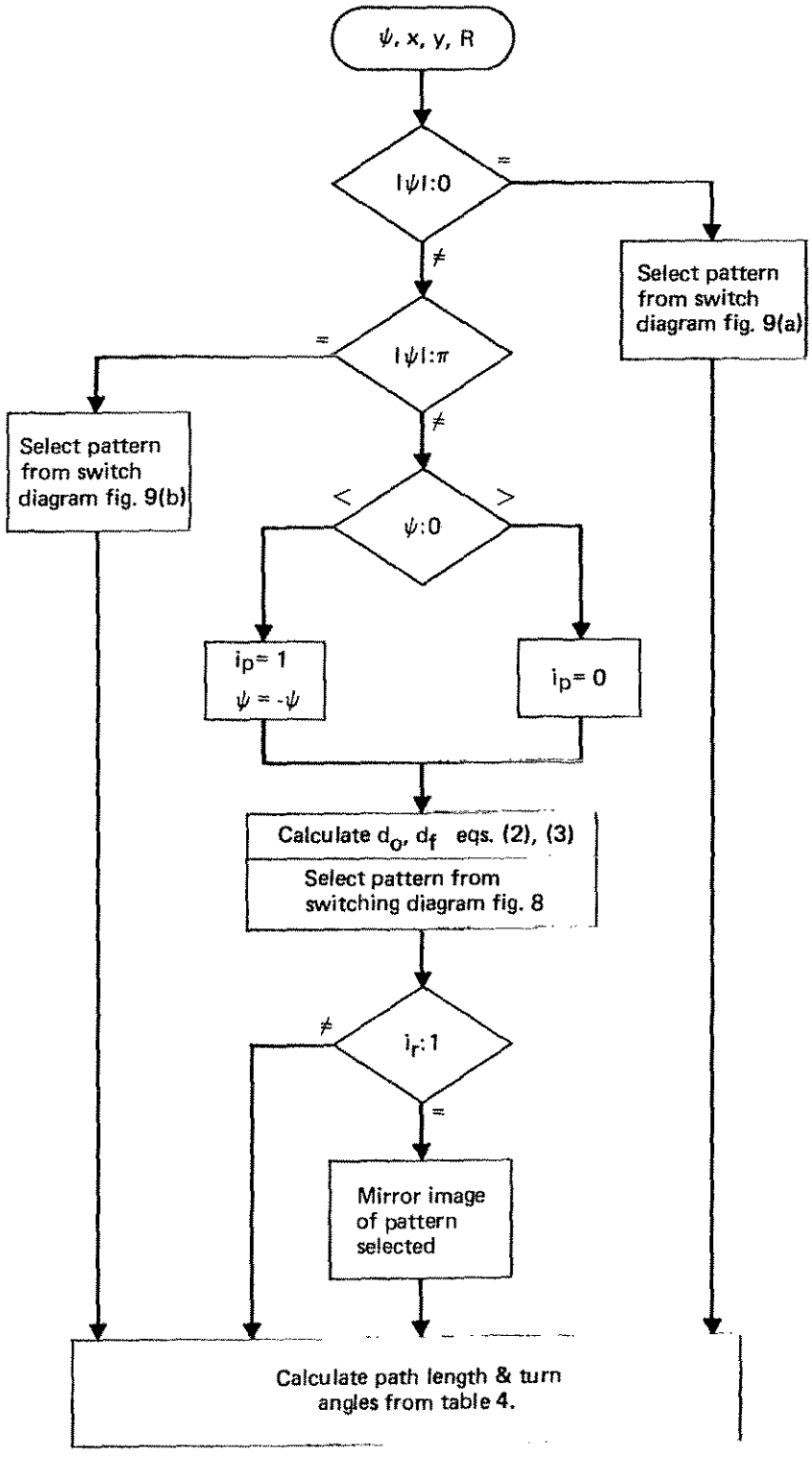

Figure 11.- Trajectory algorithm for problem (a).

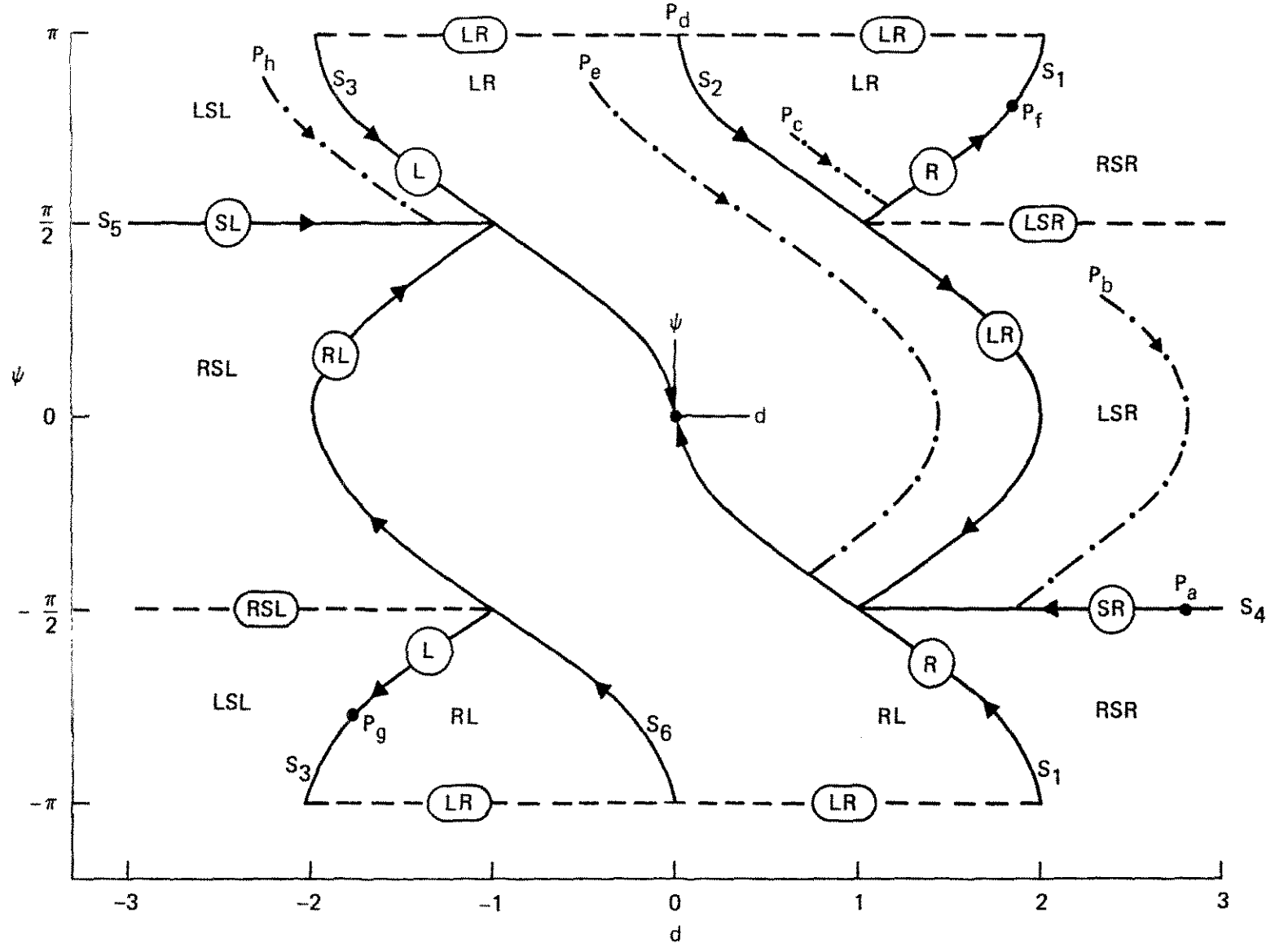

Figure 12.- Switching diagram for problem (b).

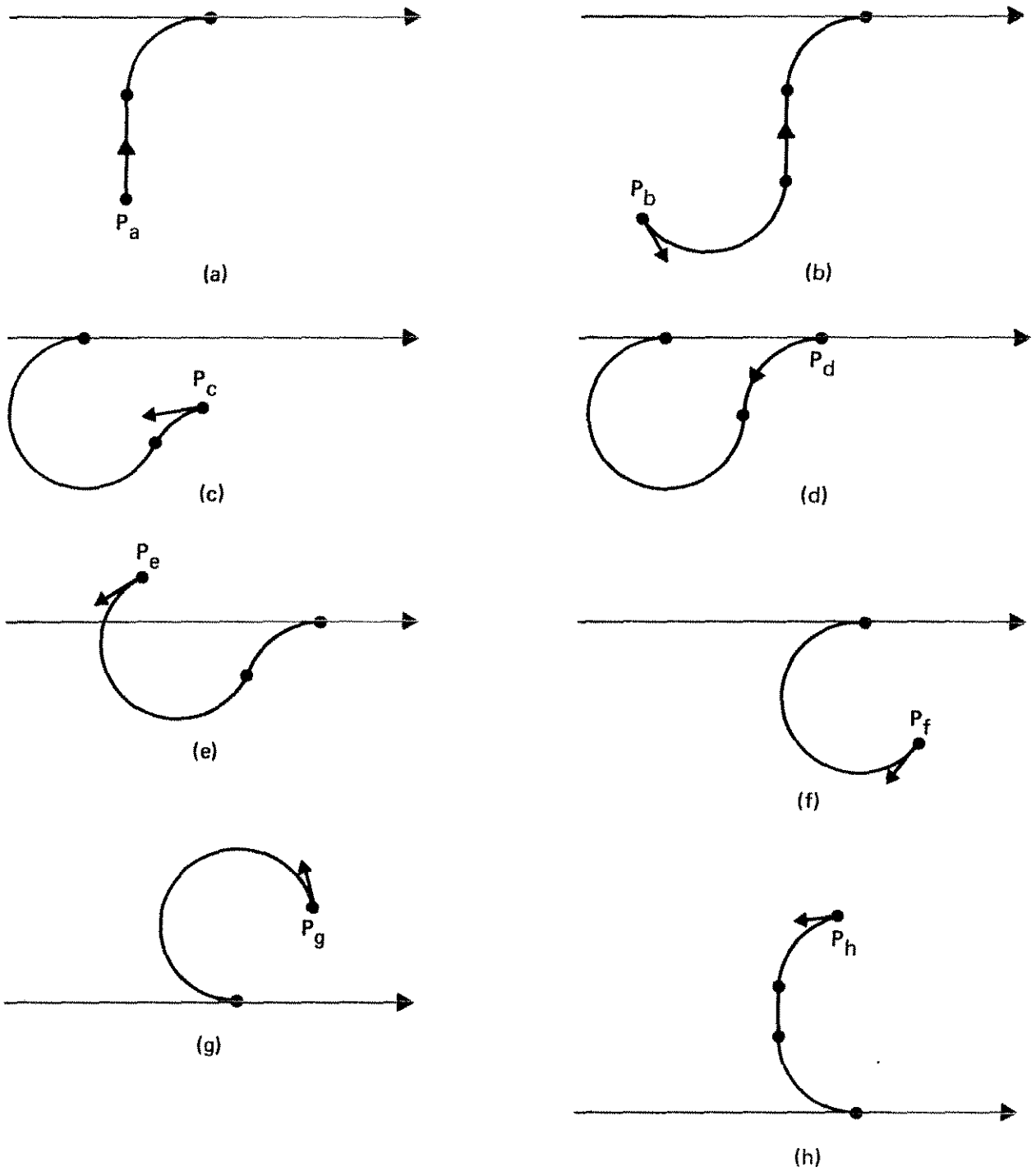

Figure 13.- Flight patterns for problem (b).

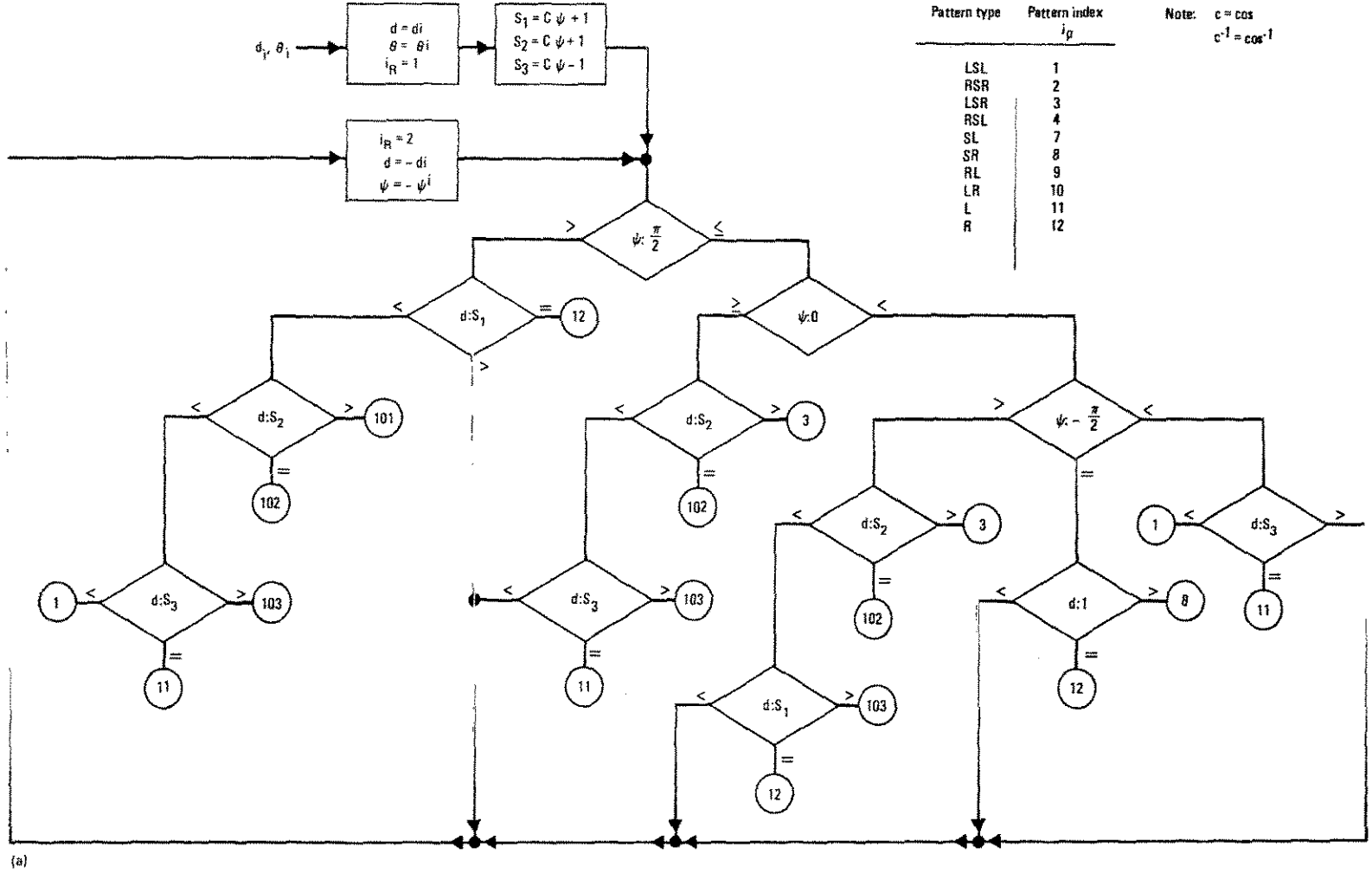

Figure 14.- Trajectory algorithm for problem (b).

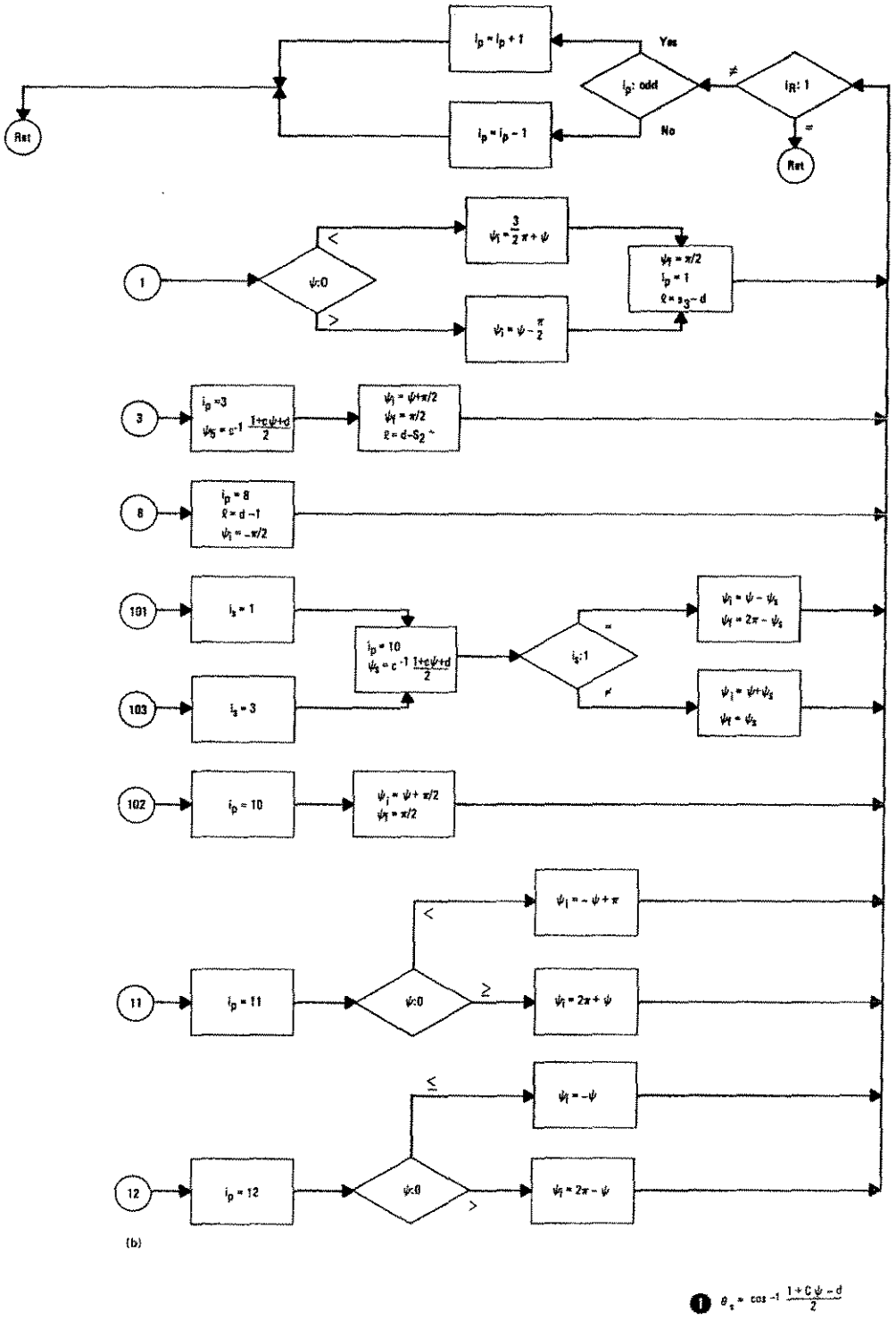

Figure 14.- Concluded.

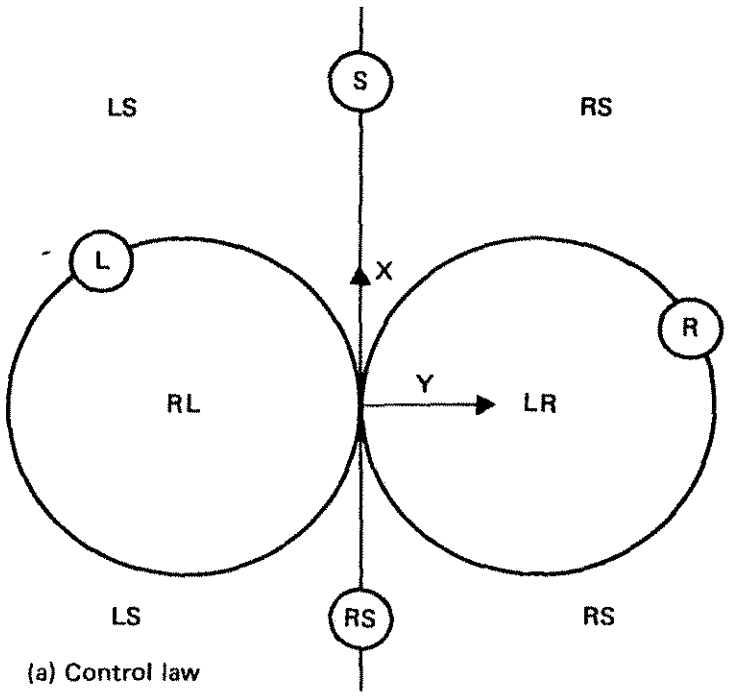

(a) Control law

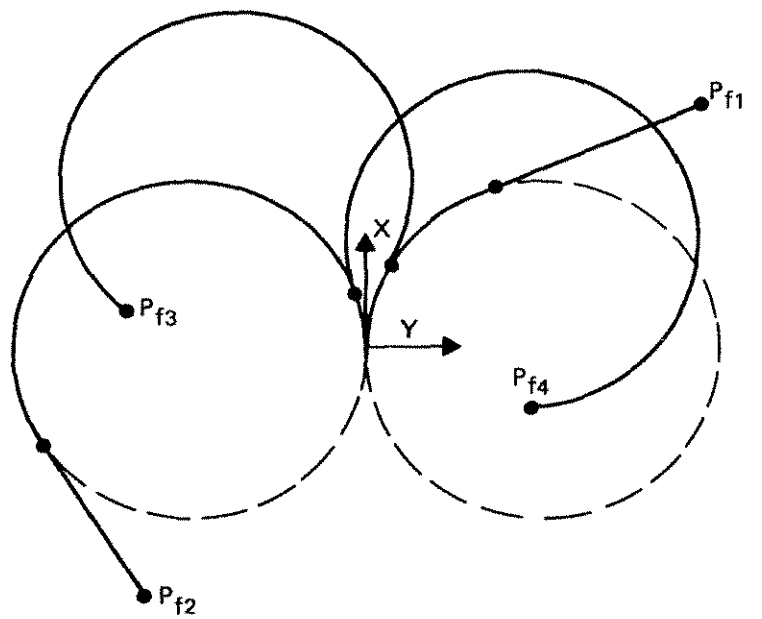

(b) Example trajectories

Figure 15.- Control law and examples for problem (c).

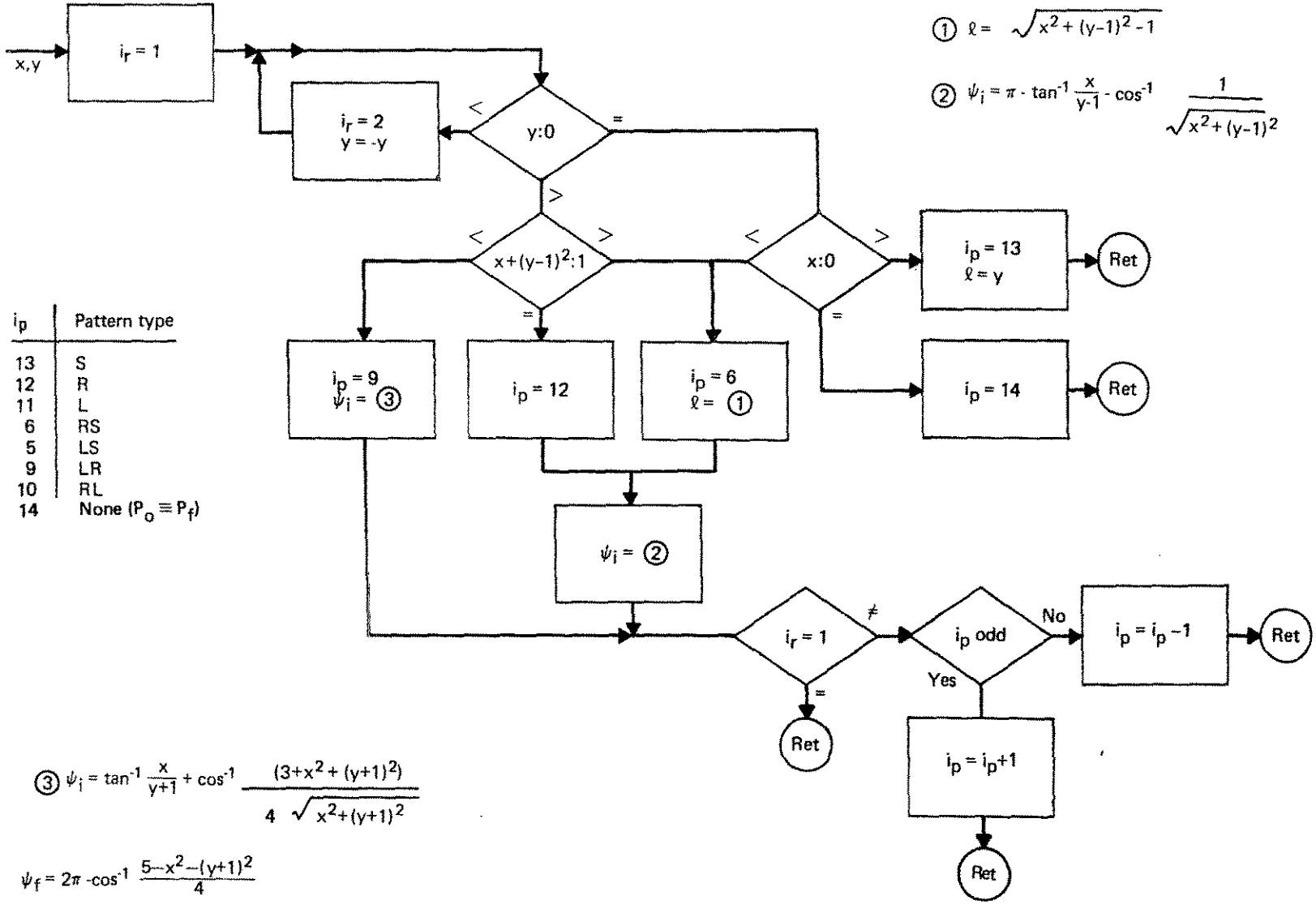

i_p	Pattern type
13	S
12	R
11	L
6	RS
5	LS
9	LR
10	RL
14	None ($P_o \equiv P_f$)

Figure 16.- Trajectory algorithm for problem (c).

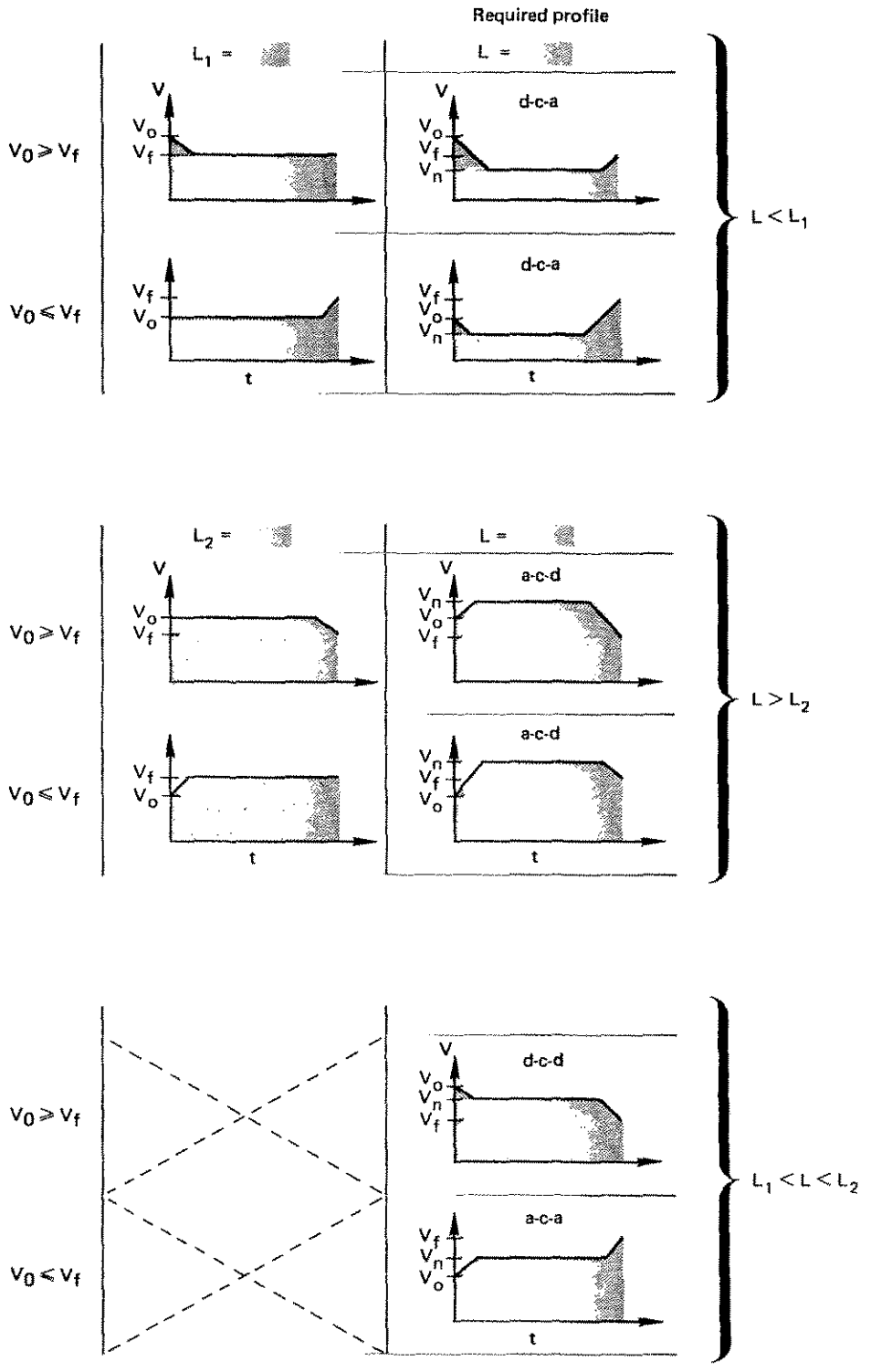

Figure 17.- Speed profiles for speed control.

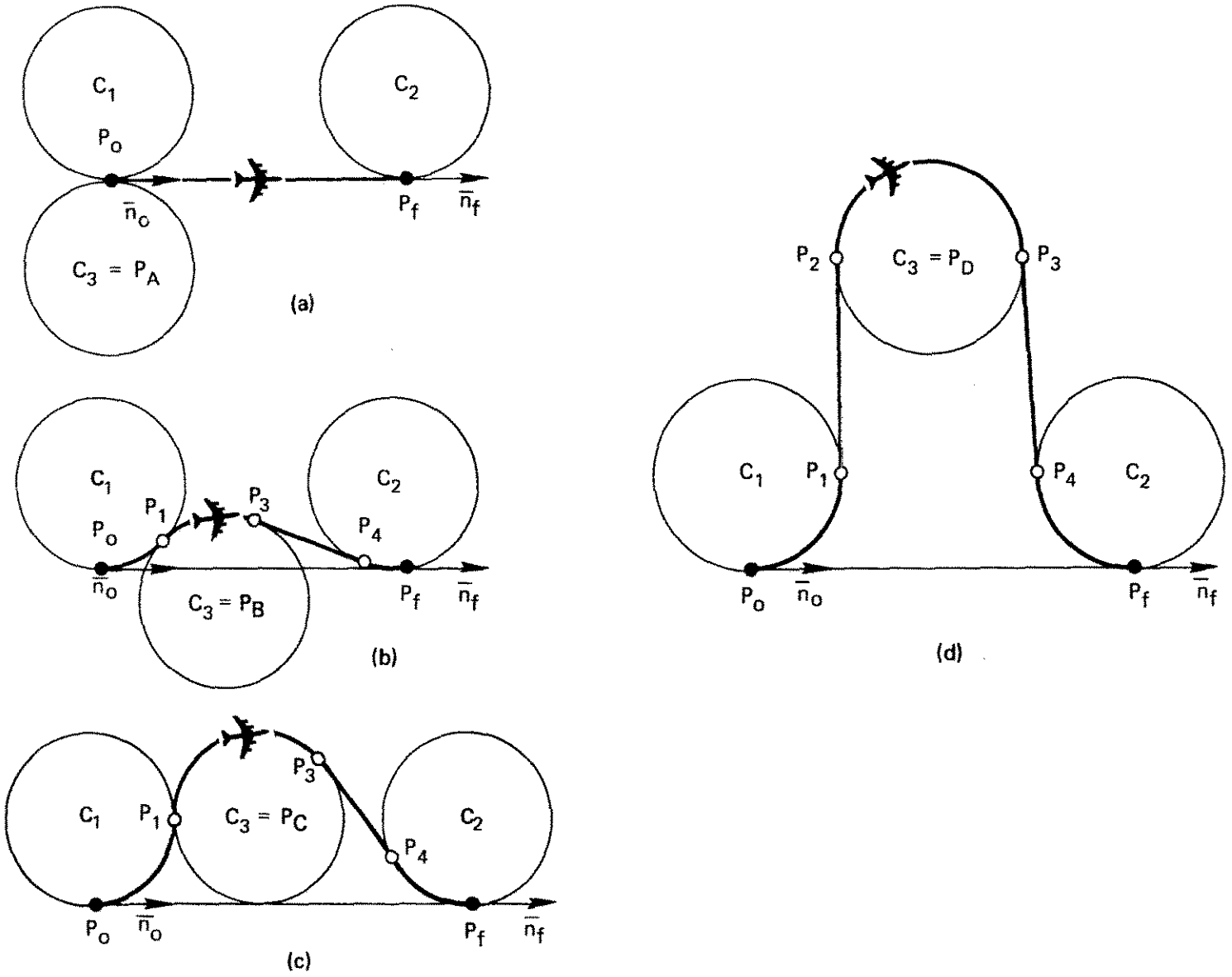

Figure 18.- Patterns of stretched paths.

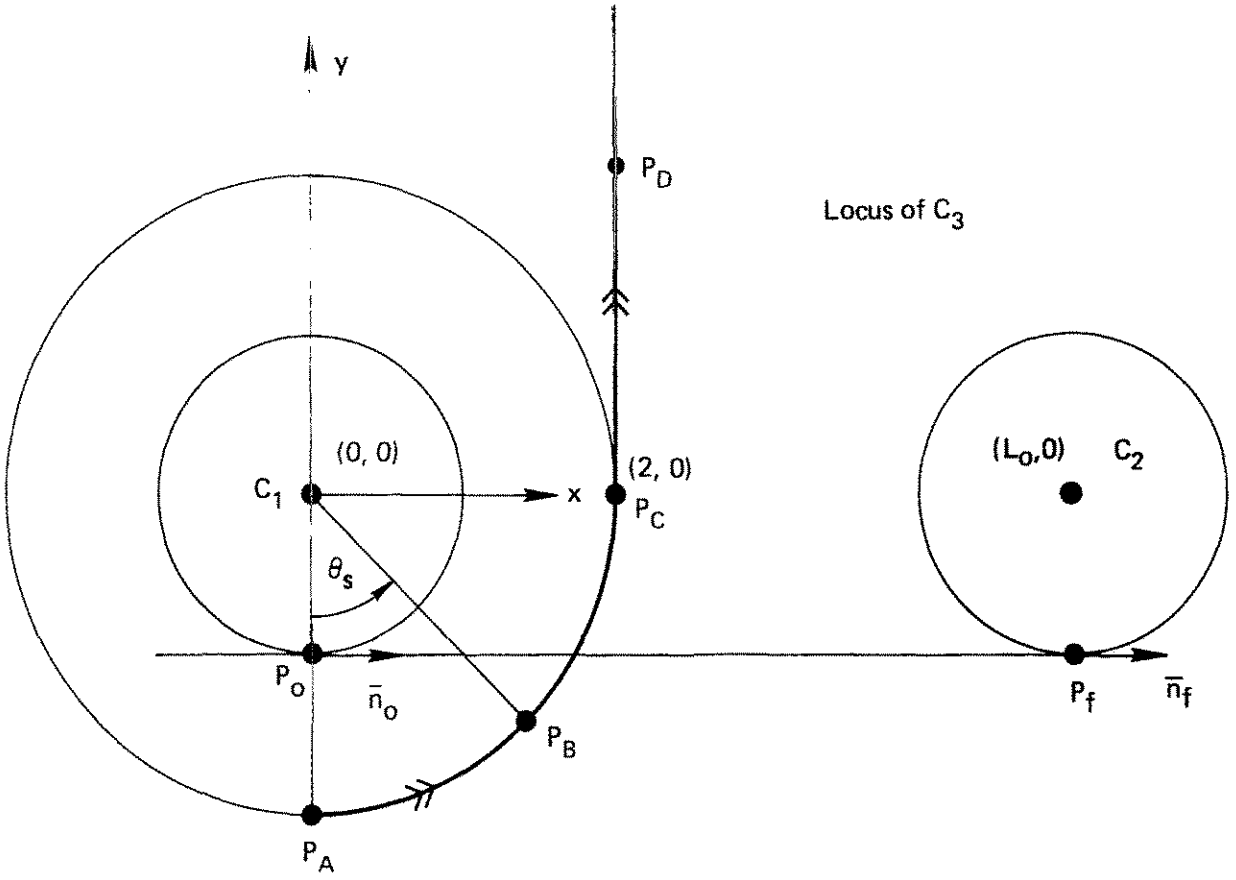

Figure 19.- Locus of centers for circle C_3.

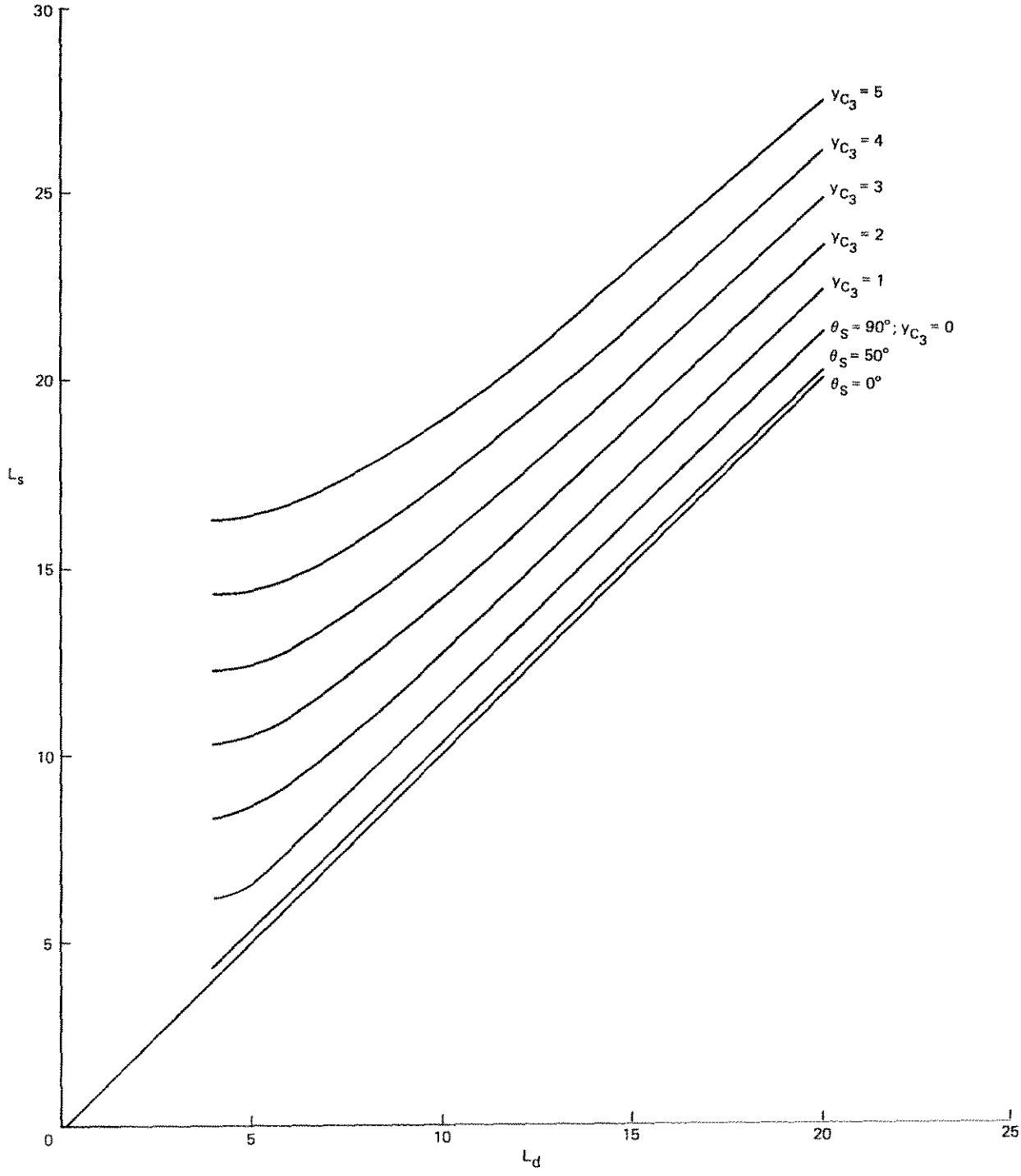

Figure 20.- Unstretched versus stretched path length.

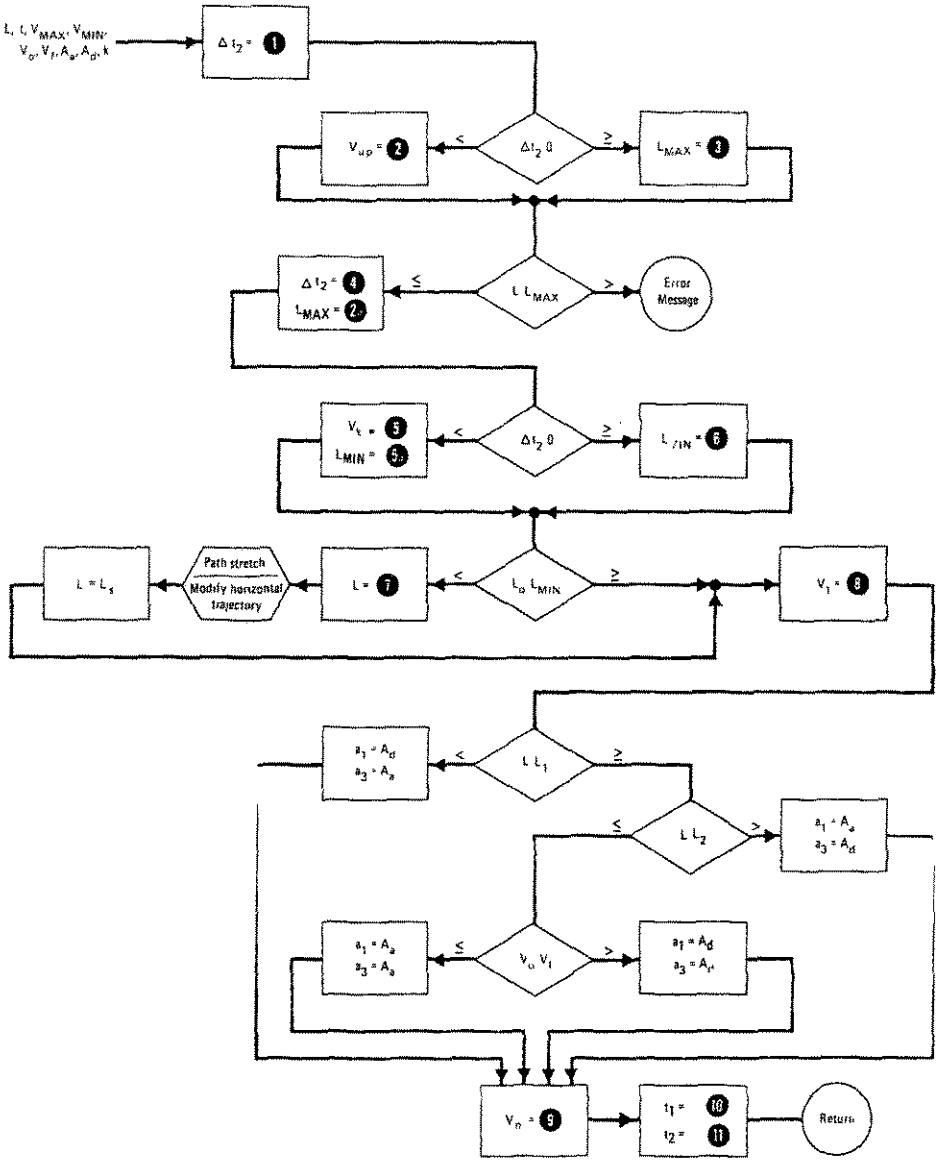

1. $\Delta t_2 = t - \frac{V_{MAX} - V_o}{A_a} - \frac{V_{MAX} - V_f}{|A_d|}$

2. $V_{up} = \frac{t + \frac{V_o}{A_a} + \frac{V_f}{|A_d|}}{\frac{1}{A_a} + \frac{1}{|A_d|}}$,

2a. $L_{MAX} = \frac{V_{up}^2 - V_o^2}{2A_a} + \frac{V_{up}^2 - V_f^2}{2|A_d|}$

3. $L_{MAX} = V_{MAX}\, t - \frac{(V_{MAX} - V_o)^2}{2A_a} - \frac{(V_{MAX} - V_f)^2}{2|A_d|}$

4. $\Delta t_2 = t - \frac{V_o - V_{MIN}}{|A_d|} - \frac{V_f - V_{MIN}}{A_a}$

5. $V_t = \frac{\frac{V_o}{|A_d|} + \frac{V_f}{A_a} - t}{\frac{1}{|A_d|} + \frac{1}{A_a}}$,

5a. $L_{MIN} = V_t\, t + \frac{(V_o - V_t)^2}{2|A_d|} + \frac{(V_t - V_f)^2}{2A_a}$

6. $L_{MIN} = V_{MIN}\, t + \frac{(V_o - V_{MIN})^2}{2|A_d|} + \frac{(V_{MIN} - V_f)^2}{2A_a}$

7. $L_S = k\, L_{MAX} + (1 - k)\, L_{MIN}$

8. $V_1 = \text{MIN}\,(V_o, V_f)$,
$V_2 = \text{MAX}\,(V_o, V_f)$,
$L_1 = V_1\, t + \frac{1}{2}\frac{(V_2 - V_1)^2}{A_a}$,
$L_2 = (V_1 + V_2)\, t - L_1$

9. $V_n^2 \left(\frac{1}{2a_3} - \frac{1}{2a_1}\right) + V_n \left(t + \frac{V_o}{a_1} - \frac{V_f}{a_3}\right) + \left(\frac{V_f^2}{2a_3} - \frac{V_o^2}{2a_1} - L\right) = 0$.

10. $t_1 = \left|\frac{V_o - V_n}{a_1}\right|$.

11. $t_2 = t - \left|\frac{V_n - V_f}{a_3}\right|$

Figure 21.- Algorithm for controlled time of arrival.

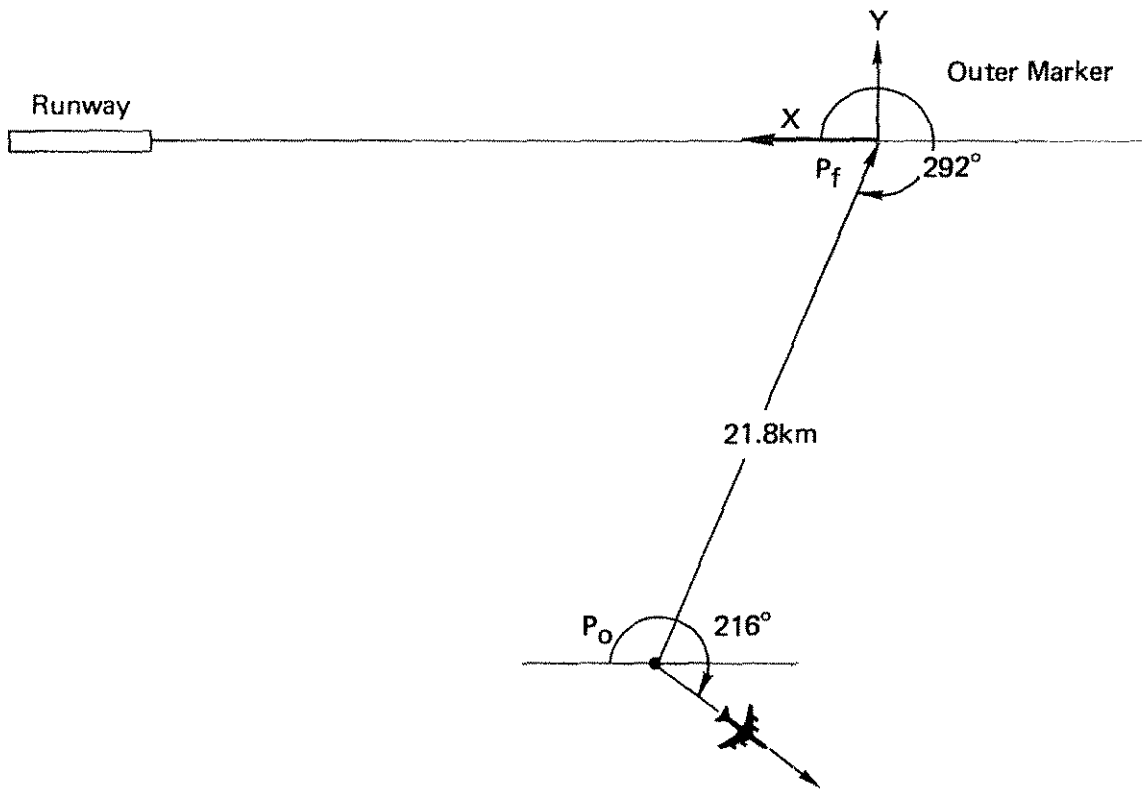

Conditions	Initial	Final	Constraints	
x coordinate of P_o, km	5.2	0	Turning radius	6.45 km
y coordinate of P_o, km	-12.5	0	Acc., dec.	0.61 m/sec^2
Aircraft heading, degrees	216	0	Max. speed	154.5 m/sec
Speed, m/sec	149.6	67	Min. speed	67 m/sec
Altitude, m	1520	456	Sink rate	305 m/min
Time, sec	0	360		

Figure 22.- Parameters for example problem.

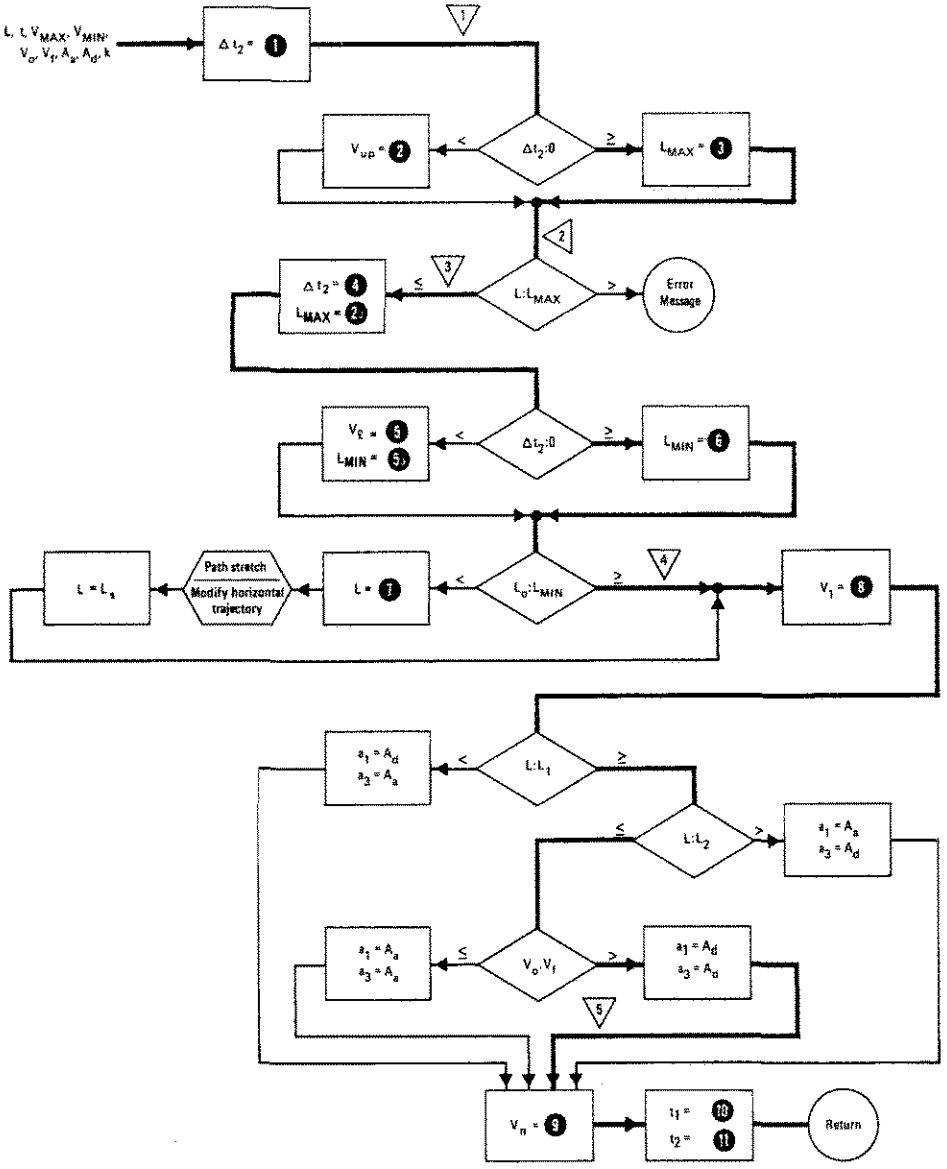

1. $\Delta t_2 = t - \frac{V_{MAX} - V_o}{A_a} - \frac{V_{MAX} - V_f}{|A_d|}$

2. $V_{up} = \frac{t + \frac{V_o}{A_a} + \frac{V_f}{|A_d|}}{\frac{1}{A_a} + \frac{1}{|A_d|}}$,

2'. $L_{MAX} = \frac{V_{up}^2 - V_o^2}{2A_a} + \frac{V_{up}^2 - V_f^2}{2|A_d|}$

3. $L_{MAX} = V_{MAX}\, t - \frac{(V_{MAX} - V_o)^2}{2A_a} - \frac{(V_{MAX} - V_f)^2}{2|A_d|}$

4. $\Delta t_2 = t - \frac{V_o - V_{MIN}}{|A_d|} - \frac{V_f - V_{MIN}}{A_a}$

5. $V_\ell = \frac{\frac{V_o}{|A_d|} + \frac{V_f}{A_a} - t}{\frac{1}{|A_d|} + \frac{1}{A_a}}$,

5'. $L_{MIN} = V_\ell\, t + \frac{(V_o - V_\ell)^2}{2|A_d|} + \frac{(V_\ell - V_f)^2}{2A_a}$

6. $L_{MIN} = V_{MIN}\, t + \frac{(V_o - V_{MIN})^2}{2|A_d|} + \frac{(V_{MIN} - V_f)^2}{2A_a}$

7. $L_S = k\, L_{MAX} + (1 - k)\, L_{MIN}$

8. $V_1 = MIN\,(V_o, V_f)$,
$V_2 = MAX\,(V_o, V_f)$,
$L_1 = V_1\, t + \frac{1}{2}\frac{(V_2 - V_1)^2}{A_a}$,
$L_2 = (V_1 + V_2)\, t - L_1$

9. $V_n^2 \left(\frac{1}{2a_3} - \frac{1}{2a_1}\right) + V_n \left(t + \frac{V_o}{a_1} - \frac{V_f}{a_3}\right) + \left(\frac{V_f^2}{2a_3} - \frac{V_o^2}{2a_1} - L\right) = 0$,

10. $t_1 = \left|\frac{V_o - V_n}{a_1}\right|$,

11. $t_2 = t - \left|\frac{V_n - V_f}{a_3}\right|$

Figure 23.- Speed profile calculation for example.

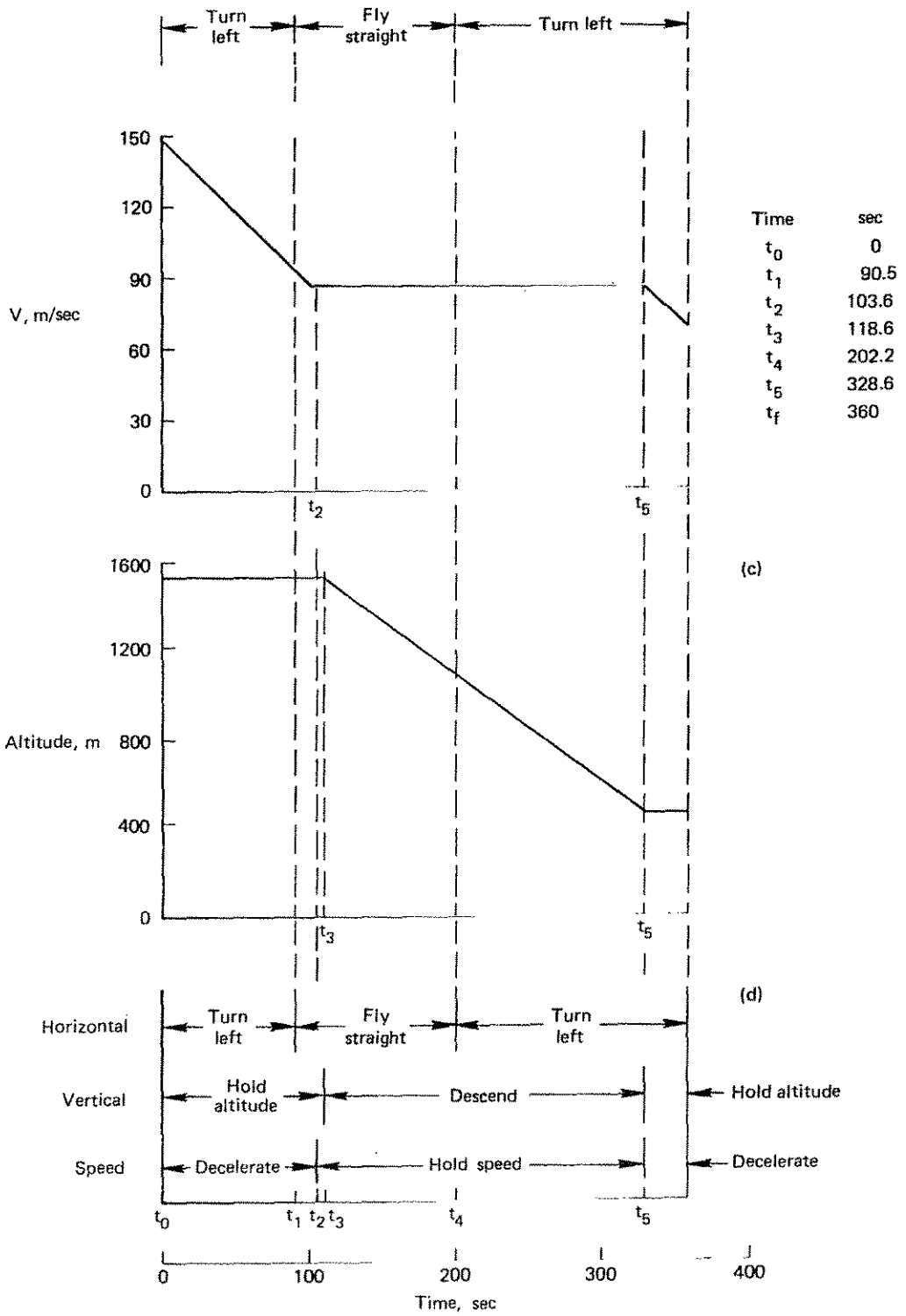

Figure 24.- Synthesized overall profile on time reference.

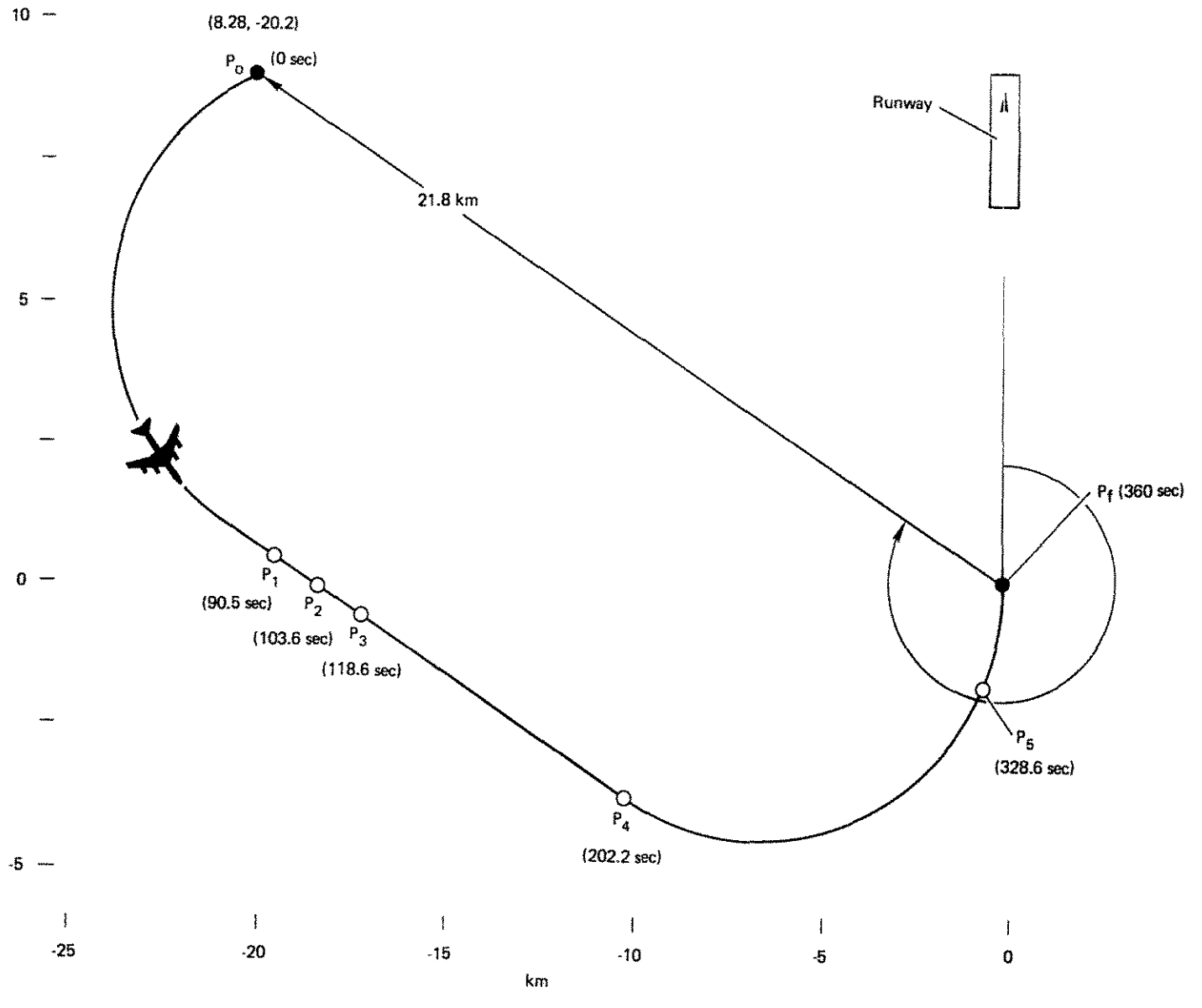

Figure 25.- Synthesized horizontal flight profile.

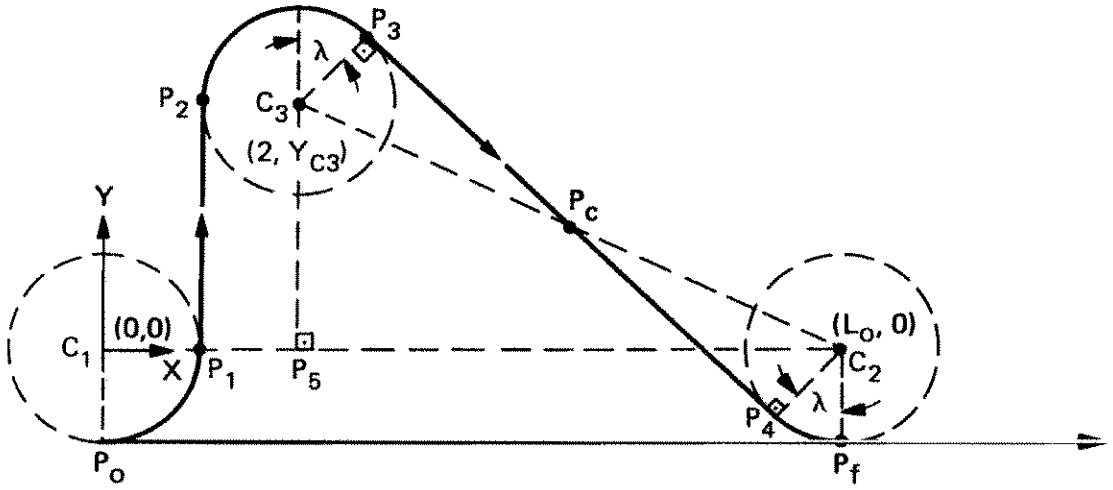

Figure 26.- Path length calculation for nondegenerate case.

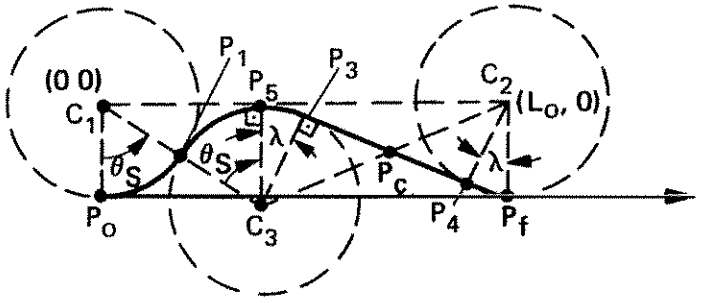

Figure 27.- Path length calculation for degenerate case.

NASA-Langley, 1972 —— 2 A-3741

1. Report No.	2. Government Accession No.	3. Recipient's Catalog No.
NASA TN D-6773		

4. Title and Subtitle
TERMINAL-AREA GUIDANCE ALGORITHMS FOR AUTOMATED AIR-TRAFFIC CONTROL

5. Report Date
April 1972

6. Performing Organization Code

7. Author(s)
Heinz Erzberger and Homer Q. Lee

8. Performing Organization Report No
A-3741

9. Performing Organization Name and Address
NASA Ames Research Center
Moffett Field, Calif., 94035

10. Work Unit No.
135-19-02-08

11. Contract or Grant No.

12. Sponsoring Agency Name and Address
National Aeronautics and Space Administration
Washington, D.C. 20546

13. Type of Report and Period Covered
Technical Note

14. Sponsoring Agency Code

15. Supplementary Notes

16. Abstract

Terminal-area guidance problems are solved in the form of computer-oriented algorithms. A flyable, three-dimensional trajectory is constructed that begins at the current aircraft position, heading, speed, and altitude, and that terminates at a prescribed position, heading, speed, altitude, and time. The terminal position is a waypoint and the terminal time is the assigned landing slot. The algorithms developed are applicable to all possible combinations of initial and final conditions, and thus can be used in a closed-loop feedback law.

The construction of the required trajectory is divided into three problems solved in sequence. First, the horizontal trajectory is calculated with a constraint on the turning radius. Algorithms for constructing the horizontal trajectory are given for trajectories synthesized from straight lines and portions of circles. Assignment of the trajectories is based on minimizing the length of the path so as to reduce maneuver time and conserve airspace and is given in the form of switching diagrams. Second, the speed profile is calculated based on the length of the horizontal trajectory and on the desired time over the waypoint. Constraints are the minimum and maximum airspeed, the acceleration and deceleration of the aircraft, and the desired airspeed at the terminal time. The algorithm first determines if a speed profile satisfying these constraints exists. If it does, the speed profile is synthesized; if it does not, a technique is used to stretch the path length of the horizontal trajectory by the amount required to synthesize a flyable speed profile. Third, the altitude profile is synthesized so that the aircraft maintains the approach altitude as long as possible before descending to the specified final altitude at the waypoint. Input to this calculation is the length of the horizontal path, the desired descent rate, and the length of the final deceleration interval. The descent to the specified final altitude is timed so it does not coincide with the deceleration interval. Finally, the completely specified flight profile is arranged into a time sequence of guidance commands that can be used as inputs to a flight director or autopilot.

17. Key Words (Suggested by Author(s))	18. Distribution Statement
Air-traffic control Automatic guidance of aircraft	Unclassified - Unlimited

19. Security Classif. (of this report)	20. Security Classif. (of this page)	21. No. of Pages	22. Price*
Unclassified	Unclassified	83	$3.00

*For sale by the National Technical Information Service, Springfield, Virginia 22151